Chapter 1: Introduction

1.1 Abstract

This chapter provides an introduction to a class of inorganic coordination compounds called Metal-Organic Frameworks (MOFs). It is designed to inform the reader about the interesting properties displayed by these materials, but is not a comprehensive review. The chapter will cover the behaviour of a subset of MOFs that show significant structural flexibility in more detail, along with reports of crystallographic characterisation of MOFs during gas sorption. These topics are of particular relevance to work carried out in the rest of the thesis.

1.2 The Definition of Metal-Organic Frameworks

Metal-Organic Frameworks (MOFs) are currently widely studied internationally, and are broadly considered to be two or three dimensional periodic assemblies comprising metal ions or small metal clusters linked through coordination bonds via organic ligands. The wording metal-organic framework was initially coined by Yaghi and Li in 1995 to describe a particular copper-based crystalline framework with both extended channels and uncommon metal coordination.[1] The framework consisted of copper ions linked with 4,4'-bipyridyl organic ligands to give an overall formula of $[Cu(bpy)_{1.5}]NO_3(H_2O)_{1.5}$, bpy = 4,4'-bipyridine and a crystal structure as displayed in Figure 1.[1] The framework contained rectangular channels with loosely bound nitrate ions that could undergo ion exchange, and was synthesised using a hydrothermal reaction, a technique commonly used in modern MOF synthesis.

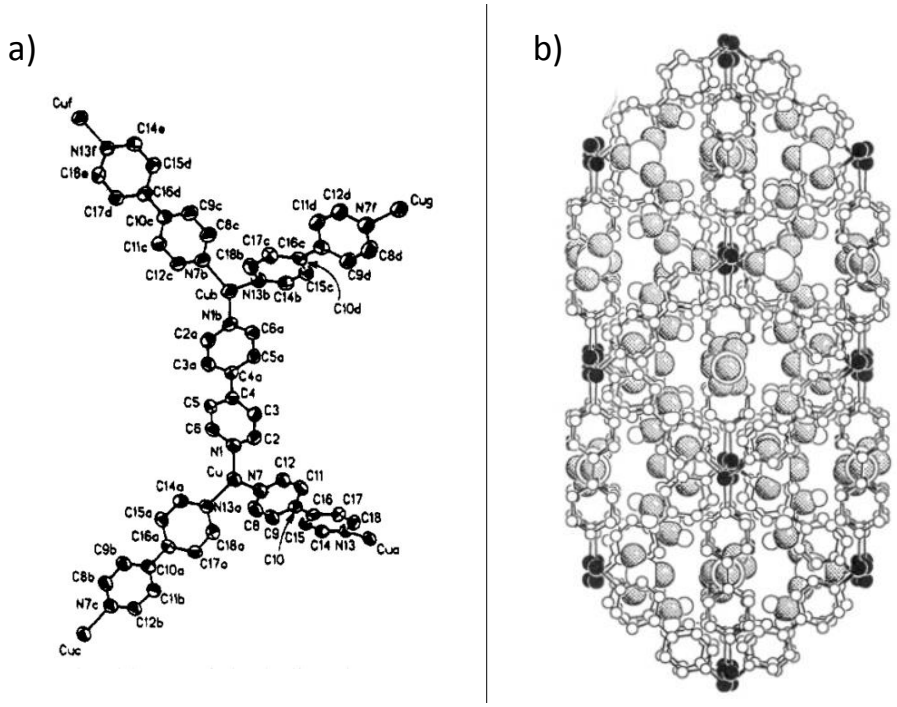

Figure 1 - a) Building block in $[Cu(4,4'\text{-bipyridine})_{1.5}]NO_3(H_2O)_{1.5}$. b) Packing of the structure showing 6 interpenetrating frameworks. Adapted with permission from O. M. Yaghi and H. Li, *J. Am. Chem. Soc.*, 1995, 117, 10401–10402. Copyright 1995 American Chemical Society[1]

Yaghi's paper unfortunately did not give an exact definition of Metal-Organic Framework, and there have been many subsequent conflicting uses of various other definitions which make defining a MOF very difficult.[2] In 2003 Janiak described both metal-organic frameworks (MOFs) and metal-organic coordination networks (MOCN) as alternative words for Coordination Polymers (CP), which he then defined as metal-ligand compounds that extend infinitely in 1, 2 or 3 dimensions.[3] However, in 2004 a review by Rowsell and Yaghi claimed that the phase coordination polymer is hazy ("most nebulous") and "simply signifies the extended connection of metal and ligand monomers through coordination bonds with no regard toward the final structure or morphology".[2] The paper then goes on to suggest MOFs should have strong bonding, linking units which are modifiable by organic synthesis and a geometrically well-defined structure (crystalline). This is further refined by Biradha *et al*. who imply that the phrase MOF is only appropriate for 3D networks.[4] They also note that the word MOF is often directly associated in the literature with compounds that exhibit both gas storage properties and porosity.[4] In 2009 an IUPAC task group was set up to address the issue and an initial discussion of the task groups work was published in 2012.[5] Provisional recommendations from IUPAC available suggest that MOFs can be defined as follows "*A Metal-Organic Framework, abbreviated to MOF, is a Coordination Polymer (or alternatively Coordination Network) with an open framework containing potential voids.*" where a coordination polymer is defined as "*A coordination*

compound continuously extending in 1, 2 or 3 dimensions through coordination bonds". Interestingly the article further states that a coordination polymer (and presumably by definition a MOF) doesn't need to be crystalline which is a property often desired for ease of characterization. Overall the author of this report considers MOFs to be a subclass of coordination polymers that tend to be, but don't have to be, 3-dimensional networks, crystalline and porous.

1.3 History

1.3.1 First Examples

While the phrase MOF was popularised by Yaghi in 1995, the concept of linking metal ions and organic ligands wasn't new. A Scifinder search by Biradha *et al*. in 2009 revealed references containing the words "coordination polymer" as early as the 1950s.[4] The results of the search, which has been updated to 2015, are shown in Table 1 and suggest a reasonable amount of research in the field up to the 1980s but a significant escalation in the 1990s. This however should not been taken as a definitive list, as more extensive Scifinder searching has revealed a paper in 1986 by Ibers *et al*. which uses the phrase metal-organic framework when describing a (phthalocyaninato)Ni(II)bromide complex.[6]

Table 1 – Updated Scifinder search results for "coordination polymers" and "metal organic frameworks" based on the original method of Biradha *et al*.[4]

Search hits for CPs and MOFs in the scientific literature using SciFinder

Years	coordination polymers	metal organic frameworks
Up to 1950	1	0
1951 – 1960	12	0
1961 – 1970	178	0
1971 – 1980	130	0
1981 – 1990	154	0
1991 – 2000	542	9
2001 – 2010	6563	2916
2011 – 2015	9145	11704

Work by Hoskins and Robson gave the first real example of a "deliberately designed and constructed infinite framework" in 1989, proposing a class of materials based on linking centres with "tetrahedral or octahedral arrays of valencies by rod-like connecting units".[7] The reported framework was based on $C(C_6H_4CN)_4$ tetrahedral ligands linking to Cu^+ ions and can be seen in Figure 2, as characterised by single crystal X-ray diffraction. The structure contained large open

spaces accommodating BF_4^- counterions and nitrobenzene molecules which were not shown in the publication or found crystallographically due to a high level of disorder.[7,8] The unresolved counterions and other molecules trapped inside the framework pores lead to a high reported R_1 value of 0.17, but this was reported before suitable programs to deal with large solvent accessible void were widely used.[7, 8]

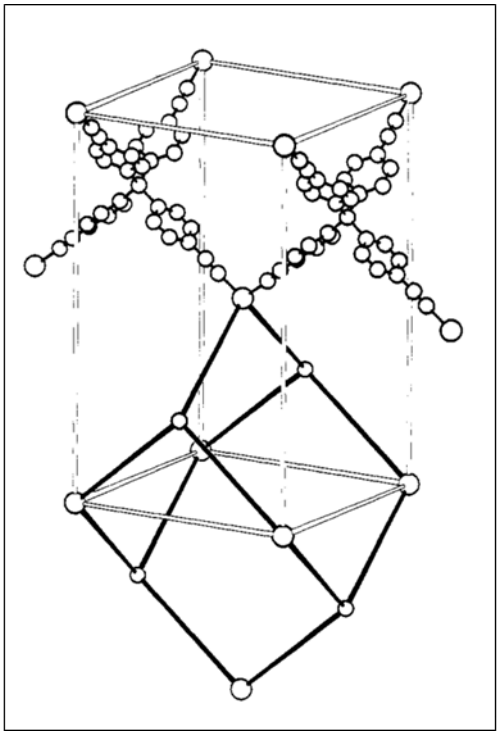

Figure 2 - Structure of the $Cu[C(C_6H_4CN)_4]$ framework reported by Hoskins and Robson, counter ions are not included. Reprinted with permission from B. F. Hoskins and R. Robson, *J. Am. Chem. Soc.*, 1989, 111, 5962–5964. Copyright 1989 American Chemical Society.[7]

1.3.2 Development

The concept of these new types of microporous solids which offered the possibilities of molecular adsorption, ion exchange and catalysis were of great interest to researchers and, research in this field rapidly took off in the 1990s.[1, 9] In 1997 Kitagawa et al reported on the first 3D porous framework capable of absorbing small gaseous molecules.[9] The framework was based on a cobalt(II) centre with 4,4'-bipyridine linkers in the formula of $[Co_2(bpy)_3(NO_3)_4].xH_2O$ and was tested for absorption of CH_4, N_2 and O_2 gases at 298 K for pressures of 1-36 atm. The crystal structure can be seen in Figure 3 and the sorption isotherms in Figure 4.

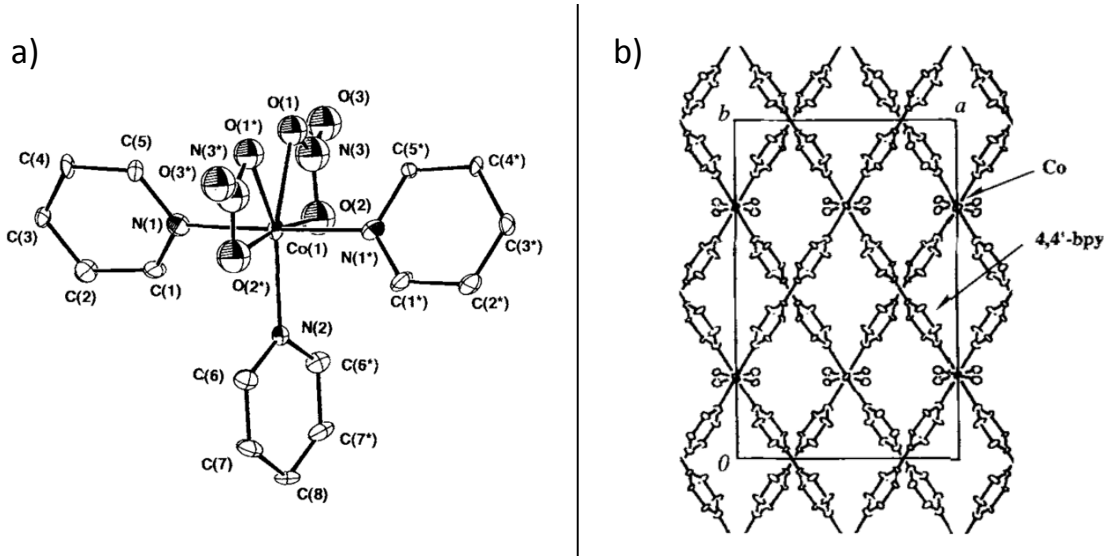

Figure 3 - Co Framework $[Co_2(4,4'Bpy)_3(NO_3)_4].xH_2O$ used for gas adsorption by Kitagawa *et al*. a) The basic building unit, b) view down the *c*-axis showing the material's pores. Adapted with permission from M. Kondo *et al*., *Angew. Chem. Int. Ed.*, 1997, 36, 1725–1727. Copyright 1997 John Wiley and Sons.[9]

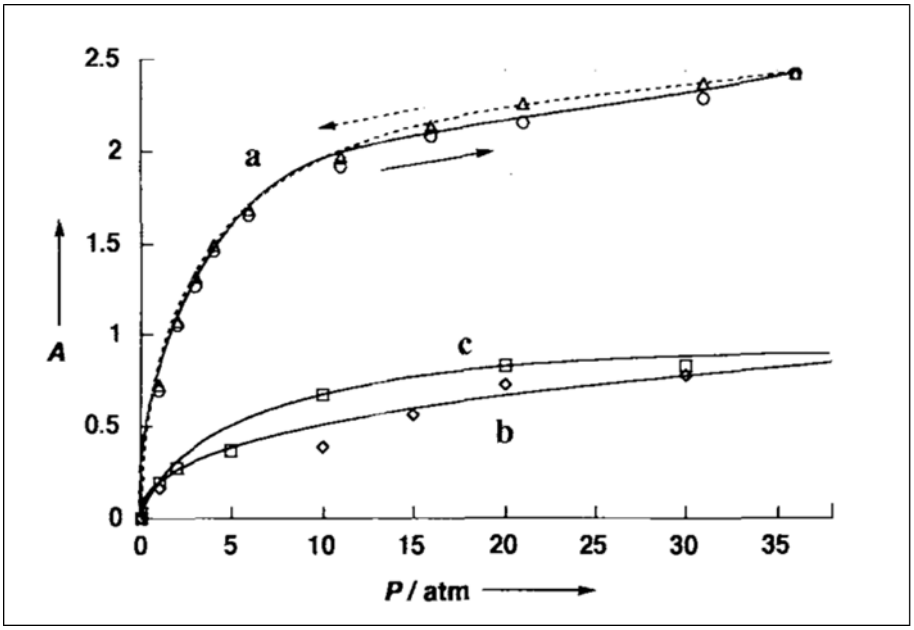

Figure 4 – Sorption isotherms of $[Co_2(b)_3(NO_3)_4]xH_2O$ with a) CH_4, b) N_2 and C) O_2 as observed by Kitagawa *et al*. Reprinted with permission from M. Kondo *et al*., *Angew. Chem. Int. Ed.*, 1997, 36, 1725–1727. Copyright 1997 John Wiley and Sons.[9]

In subsequent years there was a huge growth in new metal-organic frameworks, including the well-known and studied MOF-5 [$Zn_4O(BDC)_3$] (BDC = benzene-1,4-dicarboxylate) and HKUST-1 [$Cu_3(BTC)_2$] (BTC = 1,3,5-benzenetricarboxylate) frameworks, which were both reported in 1999.[10,11] There was also significant development of flexible MOFs, particularly MIL-53 [Cr(OH)(BDC)], which was reported by Férey et al in 2002,[12] and imidazole-based frameworks, which now have their own classification as zeolitic imidazole frameworks (ZIFs).[13, 14] The concept of mixed-linker frameworks was also widely developed, with many frameworks being synthesised that contain multiple ligands, *e.g.* dicarboxylates and diamines. A good example of a mixed-linker framework is DMOF [$Zn_2(BDC)_2(DABCO)$]; it has a zinc-based paddlewheel building unit made from 1,4-benzenedicaboxylate ligands that are pillared by DABCO (1,4-diazabicyclo[2.2.2]octane) to give a 3D structure.[15]

1.3.3 Characterisation

The majority of the frameworks above were initially characterised crystallographically using single crystal X-ray diffraction experiments; these structure solutions tend to be non-trivial due to the high level of porosity of the structures, the often disordered solvent molecules inside, and the typically low-resolution data. While single crystal analysis is the easiest method of structural characterisation, it is not always feasible to grow single crystals of sufficient size. In these cases structure solutions can be found from powder diffraction data instead. UiO-66 (a zirconium and benzenedicarboxylate-based MOF) [$Zr_6O_4(OH)_4(BDC)_6$] is a good example, it was solved in a cubic crystal system, space group: *Fm-3m* by Lillerud *et al*. in 2008,[16] and single crystals of sufficient size for X-ray diffraction were not grown until 2014.[17] The original Rietveld fit is shown in Figure 5 and shows a good match between experimental data.[16] The Behrens *et al*. used a modulated synthesis approach initially showed that a UiO-66 sister compound, a Zr-framework of the same topology but a longer ligand, formed single crystals in the same space group and topology.[18] The structure solution was then later confirmed when Lillerud and co-workers managed to grow a 100 µm single crystal on the inside of a Erlenmeyer flask that had previous been soaked in KOH to inhibit fast seeding on the glass surface.[17] Despite the lack of single crystal analysis before this the MOF received significant amounts of research attention due to its high thermal and chemical stability.

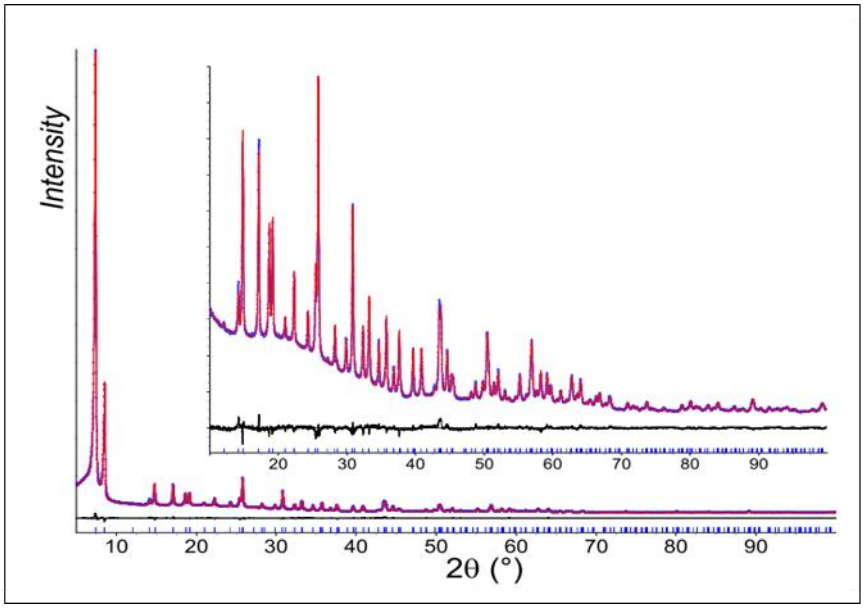

Figure 5 - Rietveld fitting for the structural solution of UiO-66 by Lillerud *et al.*, blue - experimental pattern, red - calculated pattern, black – difference. Reprinted with permission from J. H. Cavka *et al.*, *J. Am. Chem. Soc.*, 2008, 130, 13850–13851. Copyright 2008 American Chemical Society.[16]

1.4 Diversity

The field of MOFs is ever-growing and comes with a high degree of diversity. Both the metals and the organic ligands (one or several) can be varied to give many new framework structures. Alongside this, a wide range of different synthetic conditions can also give rise to different MOF topologies while containing the same ligands.

The diversity can be demonstrated using Zn-based MOFs containing benzenedicarboxylate (BDC) linkers. The well-known MOF-5 has formula $[Zn_4O(BDC)_3].x(solvent)$ with a secondary building unit (SBU) (the inorganic coordination node) consisting of Zn-oxygen clusters (formula $Zn_4(O)(O_2C)_6$) that involve 4 zinc atoms linked by 6 carboxylates surrounding a central O^{2-} ion. MOF-5 was initially synthesised by diffusion of triethylamine into a DMF/chlorobenzene solution of zinc nitrate, H_2BDC and a small amount of H_2O_2,[10] but was later, and is more commonly, synthesised using solvothermal methods.[19] The production of the MOF-5 architecture from the solvothermal synthesis however is largely dependent on the water content of the solvent. Identical conditions using fresh DEF and DEF left in the laboratory for several weeks was shown by Burrows et al to result in two different frameworks, MOF-5 and $[NH_2Et_2]_2[Zn_3(\mu\text{-bdc})_4]$ respectively.[20] $[NH_2Et_2]_2[Zn_3(\mu\text{-bdc})_4]$ contains 3 Zinc ions surrounded by a mixture of bridging and monodentate BDC ligands and two charge-balancing organic cations, and is produced due to hydrolysis of the solvent, forming the diethylammonium

counterion which templates the crystal growth. Figure 6 shows the SBU's of both MOF-5 and $[NH_2Et_2]_2[Zn_3(\mu\text{-bdc})_4]$.

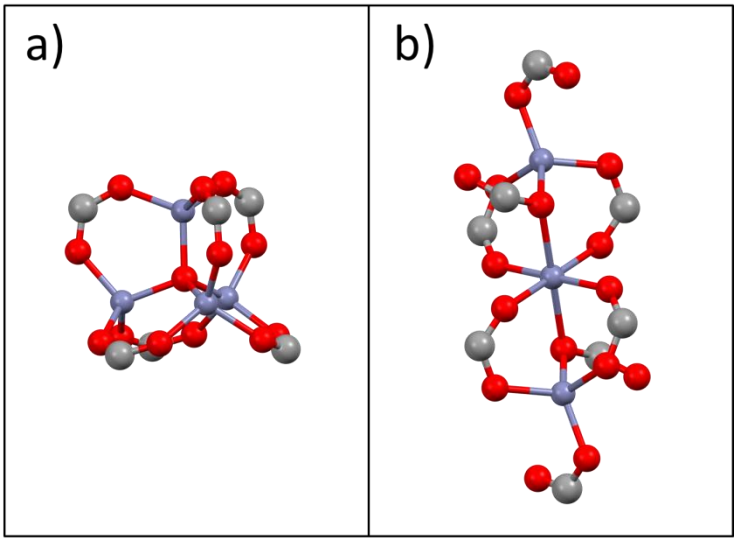

Figure 6 - Comparisons of the Secondary Building Units in a) MOF-5 and b) $[NH_2Et_2]_2[Zn_3(\mu\text{-BDC})_4]$. Carbon atoms in grey, oxygen atoms in red and zinc atoms in blue. Counterions for $[NH_2Et_2]_2[Zn_3(\mu\text{-BDC})_4]$ have been removed for clarity.

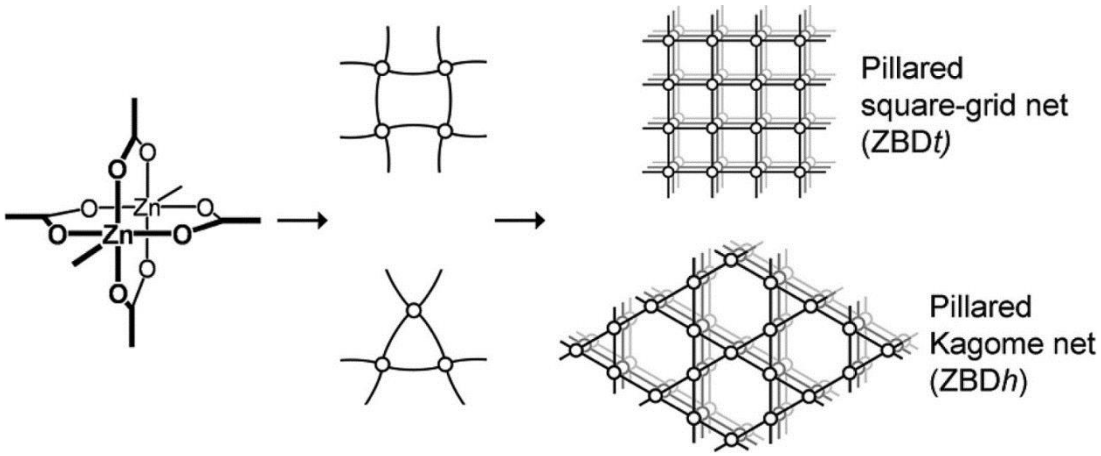

Figure 7 – The different topologies of DMOF: Pillared Square-grid net *vs* Kagome net. Reprinted with permission from H. Chun and J. Moon, *Inorg. Chem.*, 2007, 46, 4371–4373. Copyright 2007 American Chemical Society.[21]

The diversity in MOFs can be further displayed with work by Kim *et al*. who added a second ligand (DABCO).[15] This created the previously mentioned DMOF $[Zn(BDC)_2(DABCO)]$ consisting of a 2D paddlewheel formed from 4 BDC ligands and two zinc ions that are then pillared by DABCO ligands in the third dimension to give a 3D porous structure. This work was then built on by Chun *et al*. who

showed that by varying the solvent system used, the material could also be produced in different phases either a “square grid structure” giving uniform square channels or a “Kagome net” giving a mix of large hexagonal and small triangular channels, but both with the same overall connections. A comparison of the two structures can be seen in Figure 7.[21]

This is just an example using one metal and two ligands but shows that there is the potential for a wide variety of different structures. The various synthetic methods used for MOFs is reviewed by Stock *et al*.[22] and for more information on the variety of the building units adopted by various MOFs the reader is pointed towards a review article by Yaghi and O’Keeffe.[23]

Further advances in MOFs can also be made by modifying frameworks which already exist in a process commonly referred to as post-synthetic modification (PSM). This involves changes such as metal ion replacement, ligand exchange and functional group transformations based on traditional organic chemistry, and often affects the materials properties.[24–26] This will be covered later in the chapter. New and novel organic ligands can also be targeted by synthetic chemists in an aim to deliberately design characteristics of a framework such as pore size, free functional groups or specific metal linking motifs. Overall this leads to an ever-growing and expansive field.

1.5 Applications

The large internal surface areas and void volumes of MOFs combined with their chemical tunability have led them to be considered for a variety of applications including gas storage, gaseous and molecular separations, chemical sensors, biomedical uses and catalysis, all of which have been subject to their own review articles.[27–38]

1.5.1 Gas storage applications

Gas storage is probably the most prominent of these applications, with the use of MOFs as solid-based absorbents in potential industrial carbon dioxide capture and storage (CCS) receiving significant research attention. This is because global warming is becoming an increasing concern, and significant effects to the earth’s climate are being observed.[39] The global land and ocean surface temperature suggests an average warming of 0.85 ^{o}C between 1880 and 2012 and the average rate of ice loss from glaciers was “very likely” to be around 275 Gt per year between 1993 and 2009.[39] CO_2 and other anthropogenic gases are a key driver of this climate change and the concentrations of CO_2 have been shown to “exceed the highest recorded in ice cores during the past 800,000 years”.[39]

In order to try and manage the emissions of CO_2 the 2008 climate change act set a legally binding target to "ensure that the net UK carbon account for the year 2050 is at least 80% lower than the 1990 baseline".[40, 41] To achieve this target it is likely there would need to be use of both renewable energy sources and carbon capture methods, which offers a huge potential market for MOF as solid based adsorbents.

The favourable physical properties such as enormous internal surface areas (in some cases above 6,000 m^2/g), large void volumes, good thermal and chemical stabilities, and extensive tunability make MOFs highly suitable to gas capture or storage applications[28, 42] and their increasing interest can be seen by looking at the growing number of peer-reviewed publications relating to CO_2 storage in MOFs between 2000 and 2010, shown in Figure 8.[29]

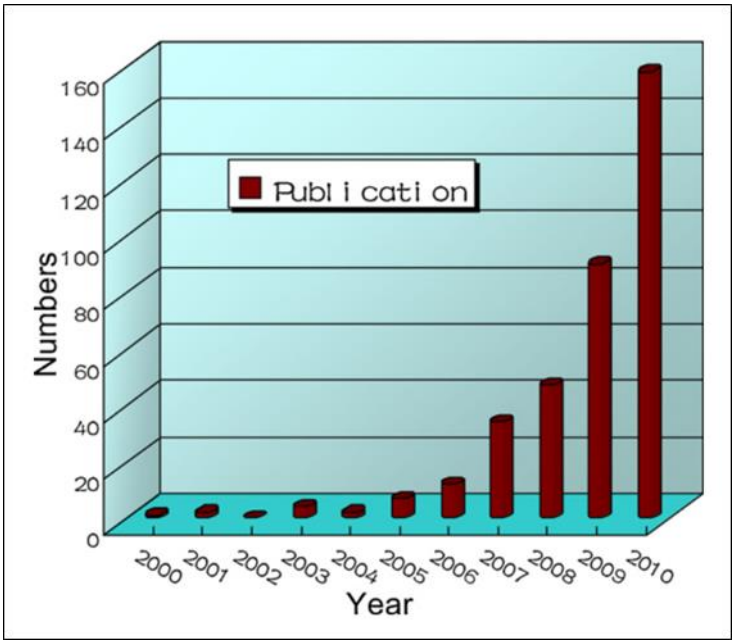

Figure 8 - Number of publications relating to CO_2 storage and/or separation. Reprinted with permission from J. R. Li *et al.*, *Coord. Chem. Rev.*, 2011, 255, 1791–1823. Copyright 2011 Elsevier.[29]

The CO_2 uptake for the frameworks is usually measured using gravimetric or volumetric measurements and relies on evacuation of the pores of the material under vacuum, followed by a steady increase of CO_2 pressure. The mass or volume change is then recorded and the results are plotted as an isotherm. A good example to illustrate these studies is work by Millward and Yaghi in 2005, who studied the CO_2 uptake of nine different MOFs over a range of pressures up to 42 bar.[43] The isotherms and structures can be seen in Figure 9. The isotherms tend to show fast initial uptakes

which then level off as the pores become saturated with gas.[43] The uptakes for the MOFs vary between 2 and 35 mmol/g depending on the MOF, with different MOFs having the best uptakes at different pressures.

In the same paper Millward and Yaghi also compare MOF-177 [$Zn_4O(BTB)_3$] (BTB = 4,4',4''-benzene-1,3,5-triyl-tribenzoate) against other materials capable of CO_2 sorption such as zeolites and carbon powder (Figure 10).[43] This shows the potential of MOFs to absorb considerably more CO_2 than their competitors due to the enormous internal spaces the can possess. It should however be noted that the comparison is against a very high capacity MOF and that at much lower pressures Zeolite 13X is far more effective.

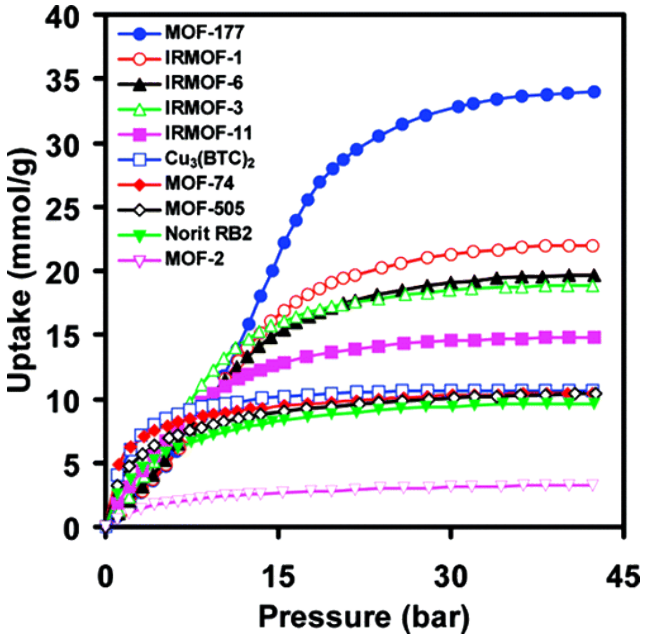

Figure 9 – CO_2 adsorption and desorption curves of various MOFs at room temperature (Filled shapes adsorption, open shapes desorption). Reprinted with permission from A. R. Millward and O. M. Yaghi, *J. Am. Chem. Soc.*, 2005, 127, 17998–17999. Copyright 2005 American Chemical Society.[43]

Similar tests have been done on a wide variety of MOFs to understand their gas sorption behaviour and a reasonably comprehensive list of the high and low pressure CO_2 uptakes of various MOFs can be found in a review by Long *et al*.[31] It is worth noting that the shape of the isotherm is important and can help elucidate the behaviour of the MOF under introduction of the gas molecules.[44] The examples above have a type I isotherm where the pores are filled up very fast initially but then level off at higher pressures as they reach saturation, but other shapes are also known and will be covered later on in the chapter.

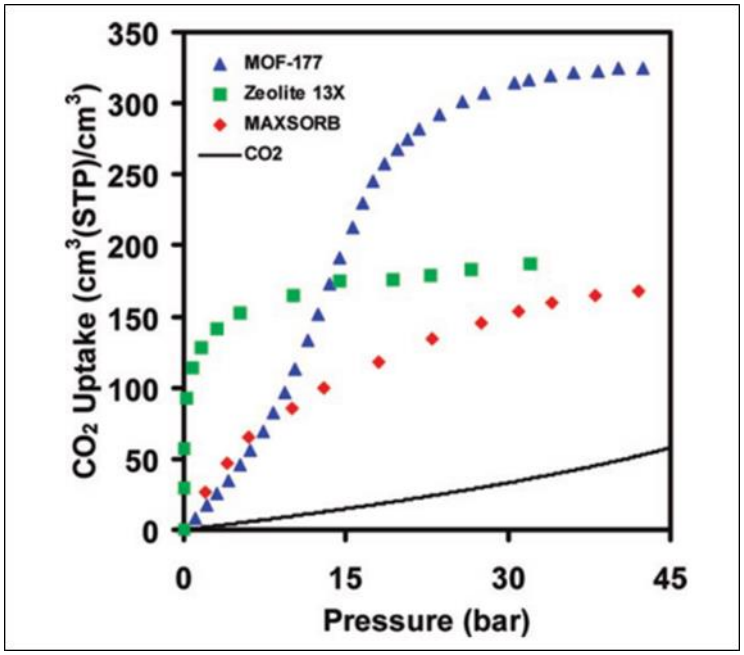

Figure 10 - Comparison of CO_2 uptake between MOF-177, Zeolite 13X and Maxsorb Carbon Powder. Reprinted with permission from A. R. Millward and O. M. Yaghi, *J. Am. Chem. Soc.*, 2005, 127, 17998–17999. Copyright 2005 American Chemical Society.[43]

1.5.2 Gas separation applications

While porous materials with a high CO_2 uptake are highly sought after, considering that only roughly 15% of waste flue gas from a typical coal-fired power plant is CO_2, with most being N_2, the ability for a MOF to selectively uptake one gas over others is also highly desired.[31] There are currently many examples of MOFs which are selective towards CO_2 over other gases and an extensive list can be found in a review by Zhou *et al*.[45] An example, shown in Figure 11, is a Cu-based MOF with a combination of both 4,4'-bipyridine and SiF_6^{2-}linkers that displays significant selectivity for CO_2 over both CH_4 and N_2.[46] Figure 11 shows wt% CO_2 at particular pressures in mmHg (between 0-1 bar), and is suggestive of very little N_2 or CH_4 uptake, while the CO_2 uptake is highly competitive with other highly adsorbing frameworks.[46] Unfortunately it is often difficult to quickly compare results from different MOFs due to inconsistencies in how isotherms are presented. The pressure can be displayed as absolute pressure (bar) or as a relative pressure P/P_0 (between 0 and 1), and the absorption can be shown in moles per gram, volume absorbed per gram, or in this case weight%. The temperature also hugely affects the uptake ability of the material, with lower temperatures giving higher values but being less likely to be industrially relevant.

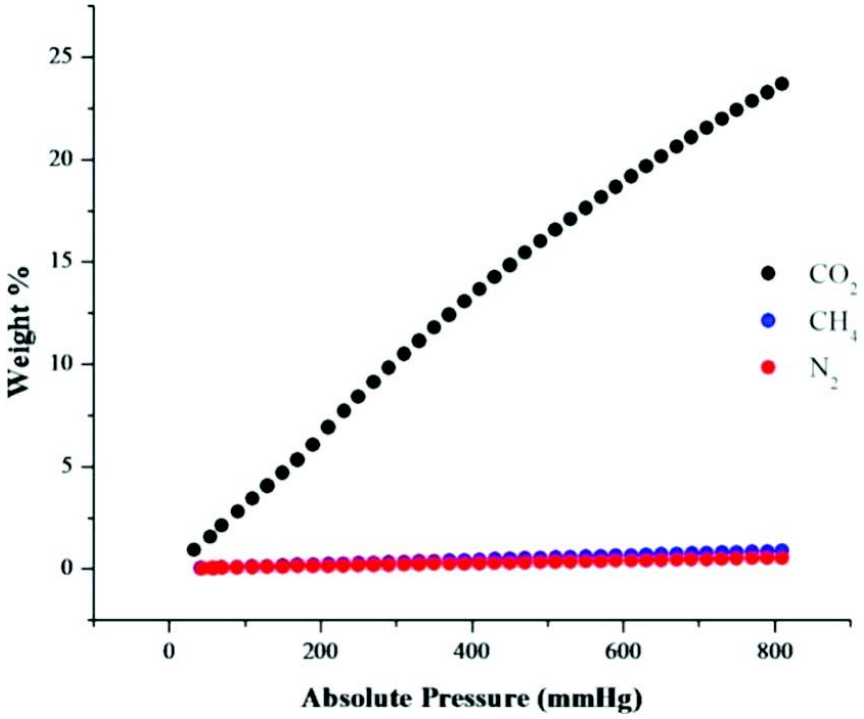

Figure 11 - Gas adsorption isotherms at 298 K for $Cu(bpy)_2(SiF_6)$. Reprinted with permission from S. D. Burd *et al.*, *J. Am. Chem. Soc.*, 2012, 134, 3663–3666. Copyright 2012 American Chemical Society.[46]

The dramatic ability of a framework to uptake a specific gas over another opens the field for MOFs to be used as gas stream separation materials. Yaghi and co-workers reported a good example of this in 2009 using Mg-MOF-74 [$Mg_2(dhtp)(OH_2)_2$] (dhtp = dihydroxyterephthalte) to purify a mixed stream of CH_4 and CO_2.[47] Figure 12 shows the percentage composition of the two gases over time while a 80:20 CH_4:CO_2 mixed gas stream is fed through a column packed with the MOF. The output for the first 4 minutes was observed to consist of 100% CH_4, with none of the CO_2 being able to pass through the framework, due to material's high affinity for CO_2 adsorption. After 4 minutes however the framework became saturated and the output composition returned to the initial 80:20.[47] The paper suggests that there is little evidence to indicate any CH_4 is adsorbed, proving both that the MOF is saturated only with CO_2 and that in a separation application all of the CH_4 could be collected. The selectivity is claimed to be due to an open magnesium site within the MOF providing a place for the CO_2 to bind. It has been observed that isostructural MOFs with different metal centres show different uptake volumes indicating that the metal is key in the adsorption process.[48] More information on using MOFs for separations can be found in various review articles. [29, 45]

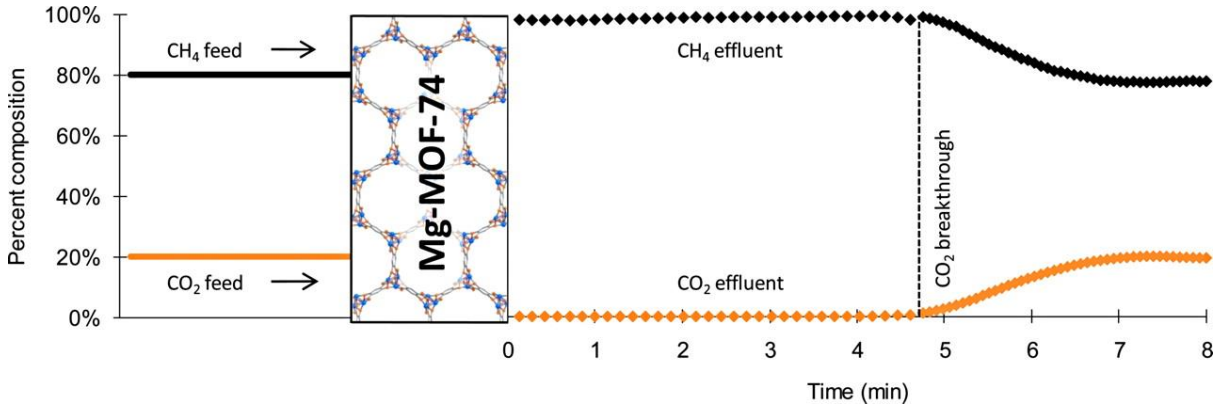

Figure 12 - CO_2 breakthrough experiment on Mg-MOF-74 showing separation of CO_2 and CH_4. Reprinted with permission from D. Britt *et al.*, *Proc. Natl. Acad. Sci. U. S. A.*, 2009, 106, 20637–20640. Copyright 2009 United States National Academy of Sciences.[47]

1.6 *In situ* Diffraction Studies

The gas uptake properties of MOFs can be probed by crystallographic techniques as well as through gravimetric adsorption measurements. These crystallographic diffraction measurements can offer very useful structural information on both the locations of the gas molecules inside the porous cavities of the MOF and any structural changes that occur to the framework itself. These results are of particular interest in determining the mechanism behind gas adsorption, understanding the molecular interactions involved, and ultimately designing new improved framework materials.

While information related to the binding of gases inside MOFs has also been determined by other methods such as: inelastic neutron scattering (H_2 adsorption in MOF-5)[49], Raman spectroscopy (CO_2 adsorption in ZIF-8 [$Zn(MeIm)_2$] (MeIm = 2-methylimidazolate) and [$Zn(SiF_6)(pyz)_2$] pyz = pyrazine)[50, 51], IR spectroscopy (CO and CO_2 adsorption in UiO-66, and NO adsorption in MIL-88(Fe) [$Fe^{III}_3O(CH_3OH)_3\{fum\}\{O_2C\text{-}CH_3\}$] (fum = fumarate))[52, 53] and solid-state NMR (CO and CO_2 adsorption in HKUST-1)[54], crystallographic characterisation is well known for providing very definitive and reliable structural information, and was successfully employed to study the adsorption of acetylene and carbon monoxide in metal-exchanged zeolites decades before MOFs were even developed.[55–58]

The study of gas sorption in MOFs by *in situ* crystallographic methods was first reported by Kitagawa, Takata and co-workers in 2002, shortly after the initial reports of gas uptake in these materials, while examining physisorbed O_2 in CPL-1 [Cu([pzdc)(pyz)] (pzdc =2,3-pyrazinedicarboxylate).[59] The maximum entropy method (MEM)/Rietveld method, developed by Takata[60–62] was used to construct a precise electron-density map from refinements against high-resolution synchrotron X-ray powder

diffraction patterns collected under an oxygen atmosphere (0.8 bar at 90K).[63] The oxygen sites were clearly identifiable as peanut-shaped electron densities located in the middle of the channels and accounting for 15.8(1) electrons. One oxygen was observed per Cu atom which corresponded well to the adsorption isotherms and interestingly the ordering of the molecules resembled O_2 in the solid state, despite being above its boiling point, pointing to a significant confinement effect.[59] Figure 13 shows the MEM electron densities of both the anhydrous and gas-loaded framework, clearly showing the presence of the confined gas molecules.

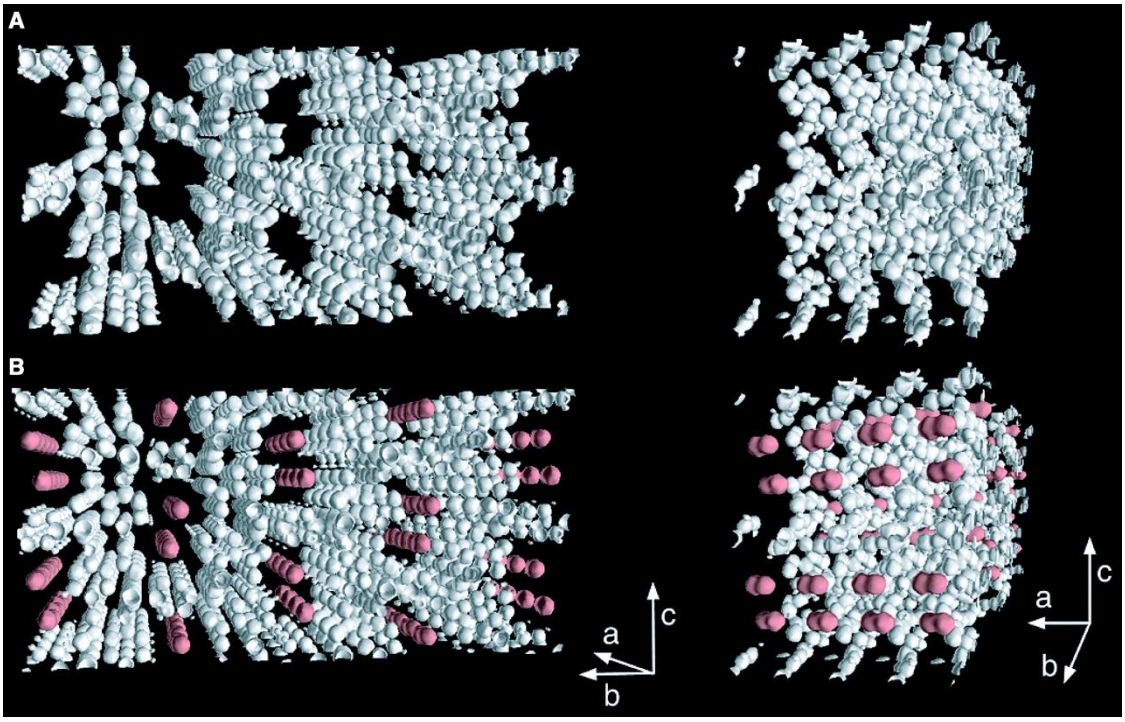

Figure 13 - MEM electron densities of a) anhydrous CPL-1 without O_2 molecules at 120 K and b) CPL-1 with adsorbed O_2 at 90 K. Reprinted with permission from R. Kitaura *et al*., *Science*, 2002, 298, 2358–2361. Copyright 2002 American Association for the Advancement of Science.[59]

In addition to oxygen, the adsorption of a wide number of different gases in CPL-1 has been studied crystallographically including N_2, Ar, CH_4, H_2 and C_2H_2.[64–68] The confinement of C_2H_2 (acetylene) was shown to be the most interesting, with the framework exhibiting both intermediate and saturated phases that displayed different acetylene-to-framework interactions.[68] At low loadings the acetylene forms a meta-stable phase with an interaction between the two metal-coordinated carboxylate oxygen atoms, but at high loadings a slight rotation of the acetylene accompanied by a rotation of the pyrazine rings occurs, aligning the acetylene molecules with the two uncoordinated carboxylate oxygen atoms and forming stronger hydrogen bonds. The behaviour explains the gradient changes

observed in the adsorption isotherm which can be seen in relation to the determined crystal structures in Figure 14.[68] Isotherms showing these non-standard isotherm shapes usually arise due to similar phase changes occurring upon gas adsorption resulting from the inherent flexibility in the frameworks. These effects will be studied in more detail later on in this chapter. The impressive adsorption behaviour of CPL-1 showed acetylene at storage densities 200 times the compression limit of free acetylene, clearly showing the advantage of these types of materials for gas storage material.

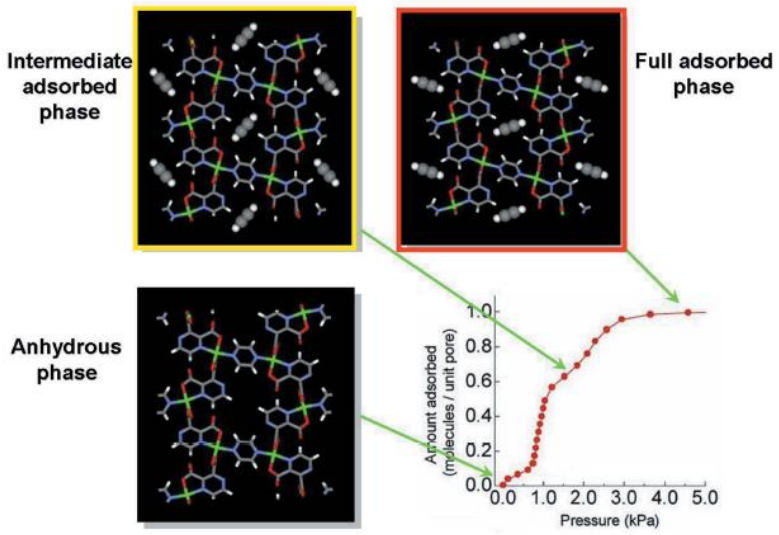

Figure 14 - Crystal structure of CPL-1 viewed along the a-axis, in its evacuated form, partially filled intermediate phase and fully filled saturated phase. Reprinted with permission from M. Takata, *Acta Crystallogr. A.*, 2008, 64, 232–245. Copyright 2008 International Union of Crystallography.[63]

The channels with CPL-1 are relatively small and only offer very specific locations of the contained guest molecules. Many MOFs however have significantly larger void spaces with the potential for many crystallographically independent adsorption sites, leading to more difficult characterisation. MOF-5 was the first such 3D large void MOF to be studied and 8 different adsorption sites were determined from single crystal analysis of the Ar and N_2 loaded material.[69] Five sites were located close to the framework taking advantage of possible interactions, and three sites formed a second layer within the main part of the channels, as shown in Figure 15.[69] The sites exhibited different partial occupancies allowing the authors to rank the preferential locations, and the same positions were determined for both Ar and N_2, albeit with different relative populations, implying they were intrinsic to the framework. Unsurprisingly the most populated site (α) was observed to be close to the metal cluster, where it could interact with three carboxylate groups and three Zn atoms but

some of the other binding sites interestingly showed previously unobserved interactions with aromatic moieties such as with the edge of the aromatic ring (site ε).[69]

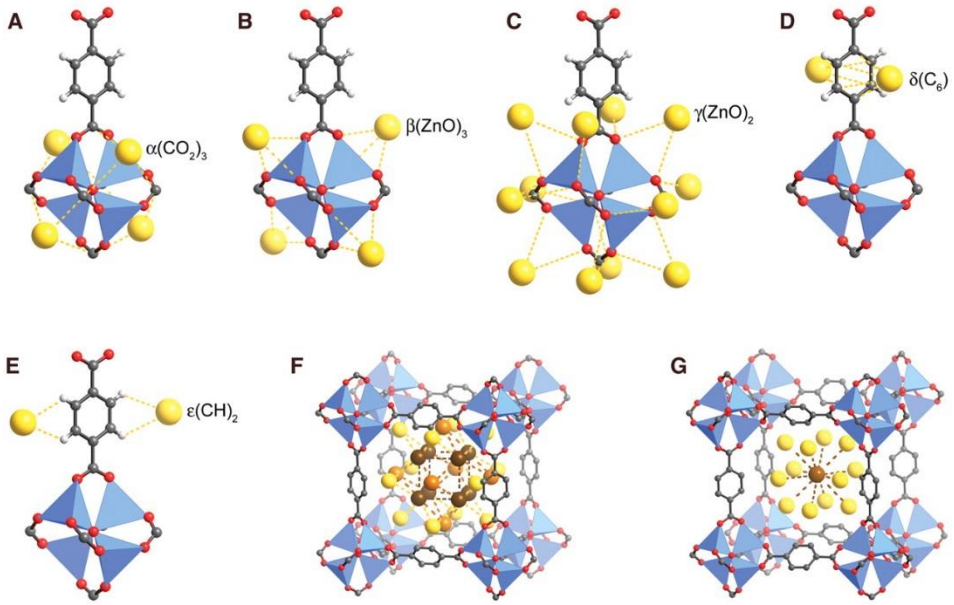

Figure 15 - The various adsorption sites determined for MOF-5 by *in situ* single crystal analysis under an argon atmosphere at 30 K. Reprinted with permission from . L. C. Rowsell *et al*., *Science*, 2005, 309, 1350–1354. Copyright 2005 American Association for the Advancement of Science.[69]

Determining the adsorption locations of hydrogen molecules in MOF-5 was also of particular relevance; however, due to the fact that the scattering intensity in X-ray diffraction is directly related to the atoms electron density, the accurate location of hydrogen atoms, not to mention partially occupied gas molecules, is often elusive. To overcome the problem two independent studies, published close to each other, employed neutron diffraction techniques where the scattering length of hydrogen is similar to other elements. Yaghi, Howard and co-workers extended their previous work using single crystal analysis[70] and Yildirim and Hartman used neutron powder diffraction but with D_2 instead of H_2 and a deuterated MOF.[71] The replacement of hydrogen with deuterium is fairly common place in neutron diffraction studies, removing the difficulties associated with hydrogen having a large incoherent scattering cross-section. Both studies used low temperatures (<5 K), providing localisation of the hydrogen gas molecules, which often interact only weakly with the framework. Both studies found hydrogen locations corresponding to the α and β sites displayed in Figure 15 for Ar adsorption, and Yildrium and Hartman also observed the γ and δ sites as well.[70, 71] This is in reasonable agreement with inelastic neutron scattering experiments suggesting locations of

hydrogen in the α and γ sites.[49, 72] It is an encouraging result, especially considering two independent research groups drew similar conclusions from different challenging experiments.

A variety of different frameworks have been studied using a combination of powder and single crystal diffraction of both X-rays and neutrons. It is worth noting that X-ray analysis can been carried out both at synchrotron facilities, a good example being CO_2, H_2, CH_4 and C_2H_6 adsorption in Sc(BDC) on the Swiss Norwegian beamline at ESRF,[73] or custom modifications to laboratory diffractometers, *e.g.* N_2, CO_2 and C_2H_2 adsorption in MAF-2 [Cu(etz)] (Hetz = 3,5-diethyl-1,2,4-triazole).[74] Neutron diffraction experiments are obviously limited to large facilities and often requires deuteration of the samples, but can be used to study other gases such as CD_4 as well as D_2.[75, 76] A full review of all of the materials studied by these techniques is beyond the scope of this chapter, but the reader is directed to the appendix which contains a published review article covering many of the reported studies in more detail and giving a more complete list of the currently known experiments.[77] This review was written to increase awareness of the benefits of *in situ* diffraction techniques and report the current progress and findings. It is hoped that a solid understanding of how different MOFs adsorb gases should help tailor them to certain applications in the future.

1.7 Functionalization of MOFs

1.7.1 Pendant functional groups

One of the tunable properties of MOFs is the ability for chemical functional groups to be easily incorporated into the framework structure, often pointing directly into the materials channels, changing and hopefully improving the adsorption properties. The method involves synthesis of frameworks with linkers that contain groups designed not to coordinate to the metal in the initial synthesis but to provide stronger host-guest interactions to molecules inside the pore. Formation of functionalities such as OH can also occur within the construction of the frameworks secondary building unit.

A nice example of the changes in gas sorption due to interior functionalization was reported by Blom *et al*. in 2008, studying 3 different amino-modified MOFs constructed from either terephthalic acid or 2-aminoterephthalic acid.[78] The reported CO_2 uptake capacities at 298 K across the entire P/P_0 range are shown in Figure 16, and it can be seen that all three modified MOFs performed better in terms of uptake than their non-amino counterpart despite the reduction in pore volume associated with the NH_2 group. The functionality was also shown to increase the adsorption energy of CO_2.[78]

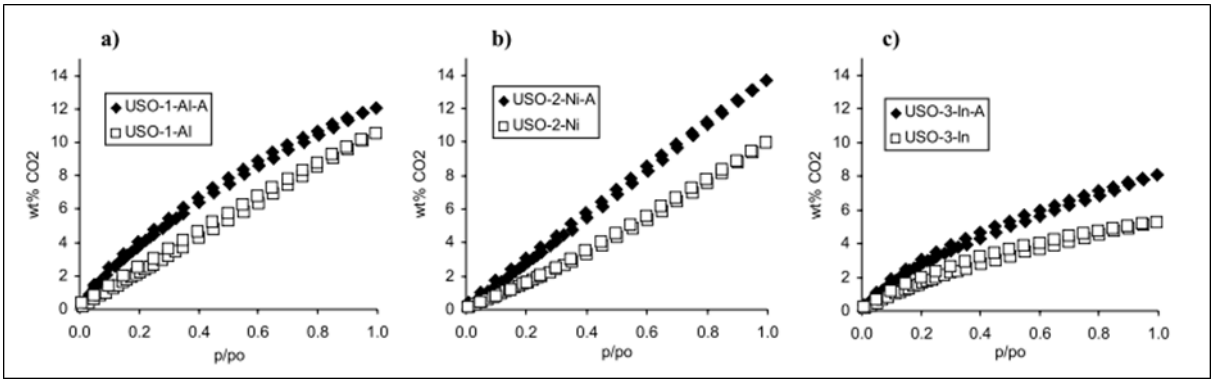

Figure 16 - CO_2 adsorption and desorption isotherms for 3 different amine-functionalised MOFs at 298 K, USO-1 [Al(OH)(BDC)] (Mil-53(Al)), USO-2 [Ni_2(BDC)(DABCO)], USO-3 [In(OH)(BDC)] (MIL-68(In)). Reprinted with permission from B. Arstad *et al*., *Adsorption*, 2008, 14, 755–762. Copyright 2008 Springer.[78]

1.7.2 *In situ* crystallographic studies

In situ crystallographic data can provide strong evidence for the importance of these functional groups in binding to gases. Work by Vaidhyanathan *et al*. using single crystal diffraction to directly observe the CO_2 within $Zn_2(Atz)_2(Ox)$ (Atz = 3-amino-1,2,4-triazole, Ox = oxalate) is a good demonstration.[79, 80] In the study, two crystallographically independent CO_2 molecules were found within the pore at occupancies of 0.8 and 0.5, which indicated a loading of 1.3CO_2 per formula unit consistent with the gravimetric adsorption data. A $N^{\delta-}\cdots C^{\delta+}$ interaction is clearly visible between the lone pair on the free amine group and the adsorbed CO_2 molecule. The position of the hydrogen atoms were determined crystallographically confirming they are bent out of the plane and the nitrogen lone pair is not delocalised into the triazole ring. The hydrogen atoms on the amine group also exhibit hydrogen bonds to the oxygen atoms of the CO_2 molecules. The CO_2 positions were in good agreement with both GCMC and dispersion-corrected periodic DFT calculations and the crystal structure refinement led to an R-factor of 2.7%. It therefore seems likely that the lone pair of the amine group is responsible for holding the CO_2 in place. The two CO_2 molecules also show a favourable T-shaped $C^{\delta+}\cdots O^{\delta-}$ interaction with each other, as shown in Figure 17.[80]

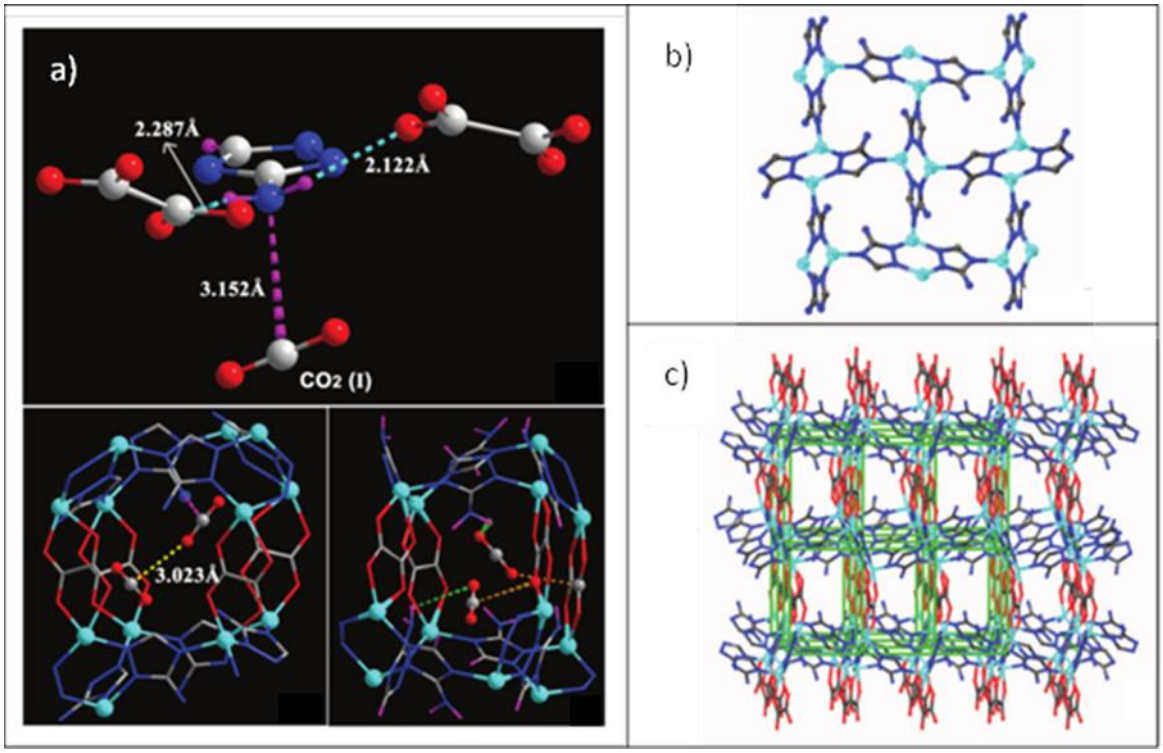

Figure 17 - a) CO_2 binding positions found by single crystal diffraction in $Zn_2(Atz)_2(Ox)$, b) a Zn-Atz layer, c) 3D structure of the MOF (Atz = 3-amino-1,2,4-triazole, ox = oxalate). Adapted with permission from R. Vaidhyanathan *et al*., *Science*, 2010, 330, 650–653. Copyright 2010 American Association for the Advancement of Science.[79, 80]

Similar favourable nitrogen interactions from triazole-containing MOFs to CO_2 molecules have been observed for MAF-X7 $(Me_2NH_2)(H\text{-}DMF)[Co_2Cl_4(ppt)_2]$ (H_2ppt = 3-(2-phenol)-5-(4-pyridyl)-1,2,4-triazole) and MAF-23 $[Zn_2(BTM)_2]$ (H_2BTM = Bis(5-methyl-1H-1,3,4-triazol-3-yl)methane).[81, 82] MAF-X7 shows one CO_2 site with a contact between the central carbon and the triazolate 4-nitrogen[81] and MAF-23 displays two sites held in claw-like interactions from nitrogen atoms on different triazolate rings at N···C distances which were generally smaller than the van der Waals radii.[82]

Amino or imino nitrogen atoms are not the only functionalities observed to affect the adsorption of gases. Yang and Schroder using a combination of powder diffraction with both inelastic neutron scattering and DFT calculations showed that the main binding site for CO_2 and SO_2 in NOTT-300 $[Al_2(OH)_2(L)]$ (H_4L = biphenyl-3,3',5,5'-tetracarboxylic acid) is due to interaction with a hydroxyl group on the framework.[83] The gas molecules sit in a hydrogen-bonding pocket containing a μ_2-OH group that points towards the main channel (see Figure 18). There is also a secondary site which mainly interacts with the first CO_2, implying it fills up after the first site is occupied, however, the authors did not publish any refinements at lower gas pressures to indicate only 1 site is initially occupied.[83]

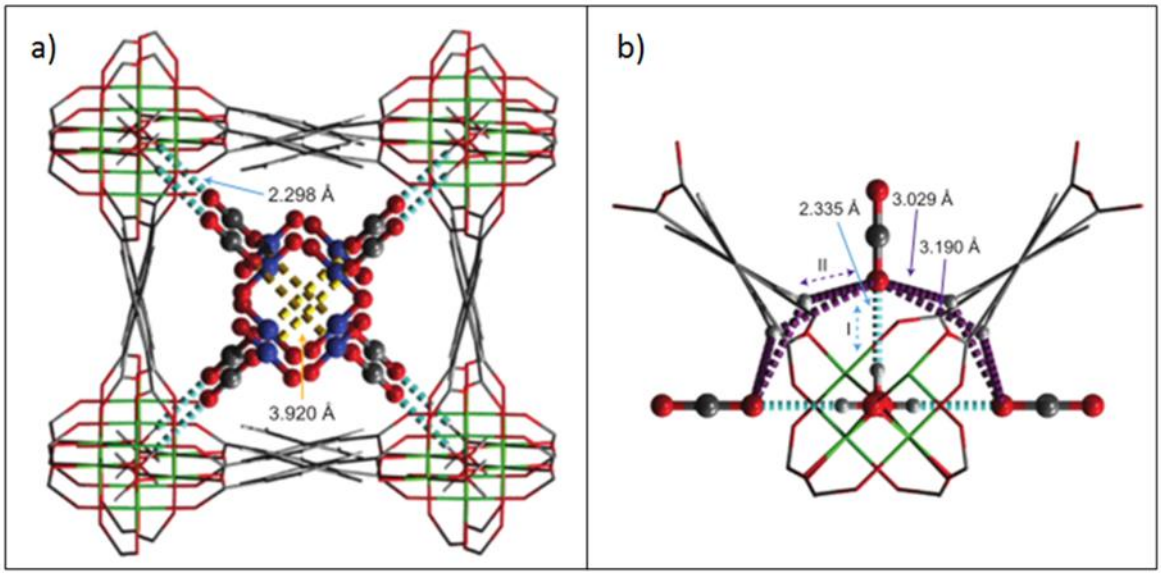

Figure 18 - CO_2 locations in CO_2-loaded NOTT-300 a) showing both binding sites (grey and blue), b) Close up showing interaction with hydroxyl group and benzyl hydrogens. Adapted with permission from S. Yang *et al.*, *Nat. Chem.*, 2012, 4, 887–894. Copyright 2012 Nature Publishing Group.[83]

1.7.3 Open metal sites

The strongest direct interactions with trapped gas molecules often arise due to open metal sites within the framework. These interactions were alluded to earlier in the chapter when discussing the separation of CO_2 and CH_4 using Mg-MOF-74 (also known as CPO-27). *In situ* diffraction studies on both the Ni and Mg analogue of MOF-74 under a CO_2 atmosphere have shown that a CO_2 molecule becomes bound end-on (through one of its oxygen atoms) to an unsaturated metal site with bond lengths shorter than the sum of van der Waals radii.[84, 85] The bound CO_2 molecules were observed to have a bent geometry, with a O=C=O angle of 162° for the Ni version[84] and 160.5° for the Mg version.[85] The authors reporting the finding of the Mg version attributed the larger than expected bending effect to (unmodelled) crystallographic disorder, due to the significant energy penalty such deviation from linearity might incur. This theory was further supported by a subsequent neutron powder diffraction study suggesting a more reasonable angle of 170°. This study also found evidence of a secondary adsorption site within the main pores.[86] Figure 19 shows the determined coordination environment of the CO_2 in Ni-MOF-74.[84] In addition to CO_2, both NO and H_2S have also been shown to become bound to the metal centre in MOF-74, with particular interest in the in vitro release of the gases for medical purposes.[87, 88] Unfortunately Ni is fairly toxic and a more suitable metal would be needed for the application. It was suggested that the Zn analogue would be the most appropriate, but it proved problematic in the initial solvent removal process (often termed the activation step).

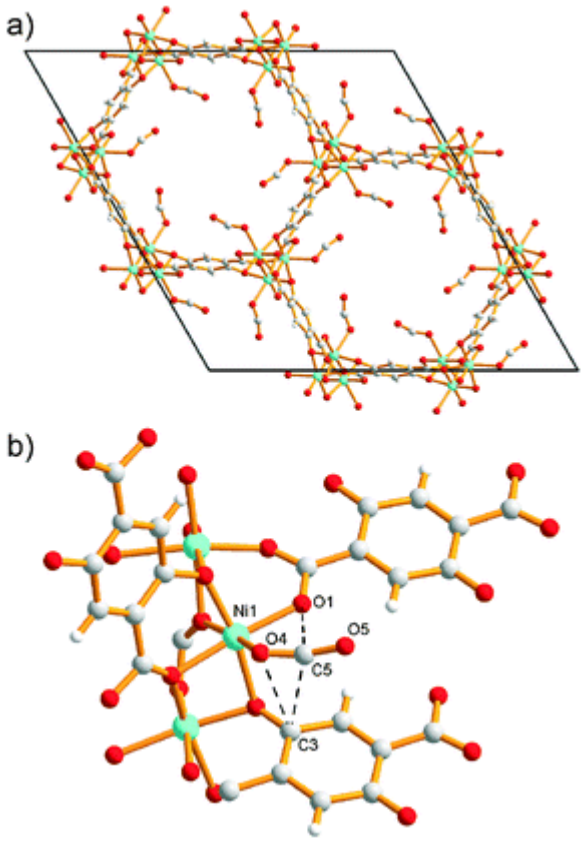

Figure 19 - Crystal structure of MOF-74 Ni (CPO-27-Ni) with adsorbed CO_2, a) hexagonal channel viewed along (001) direction. b) Coordination environment of the CO_2 molecules. Adapted with permission from P. D. C. Dietzel *et al*., *Chem. Commun.*, 2008, 2, 5125–5127. Copyright 2008 Royal Society of Chemistry.[84]

Similar binding of gases due to open metal sites has been shown for several other MOFs including the Mn and Cu analogues of $[Mn(DMF)_6]_3[(Mn_4Cl)_3(BTT)_8(H_2O)_{12}]_2$ (BTT = 1,3,5-benzenetristetrazolate)[89, 90] and the well-known HKUST-1 ($[Cu_3(BTC)_2]$).[85, 91–95] The adsorption of CO_2, D_2, CD_4 in HKUST-1 all showed multiple binding sites for each gas, but the primary location for all gases occupied the uncoordinated axial sites of the Cu paddlewheels (see Figure 20 which shows the various binding sites of D_2).[91] In contrast, work studying the adsorption of noble gases in HKUST-1 displayed no evidence of interaction with the Cu atoms.[95] $[Mn(DMF)_6]_3[(Mn_4Cl)_3(BTT)_8(H_2O)_{12}]_2$ similarly displayed a strong interaction from the exposed Mn^{2+} site to D_2 molecules, but like some MOF-74 analogues, activation turned out to be problematic, with residual methanol molecules occupying 83% of the frameworks exposed metal sites, even after extensive heating.[89] The Cu version proved far easier to activate and, although it showed a longer range M···D_2 contact, a significantly higher site occupancy of 93% was reported.[90]

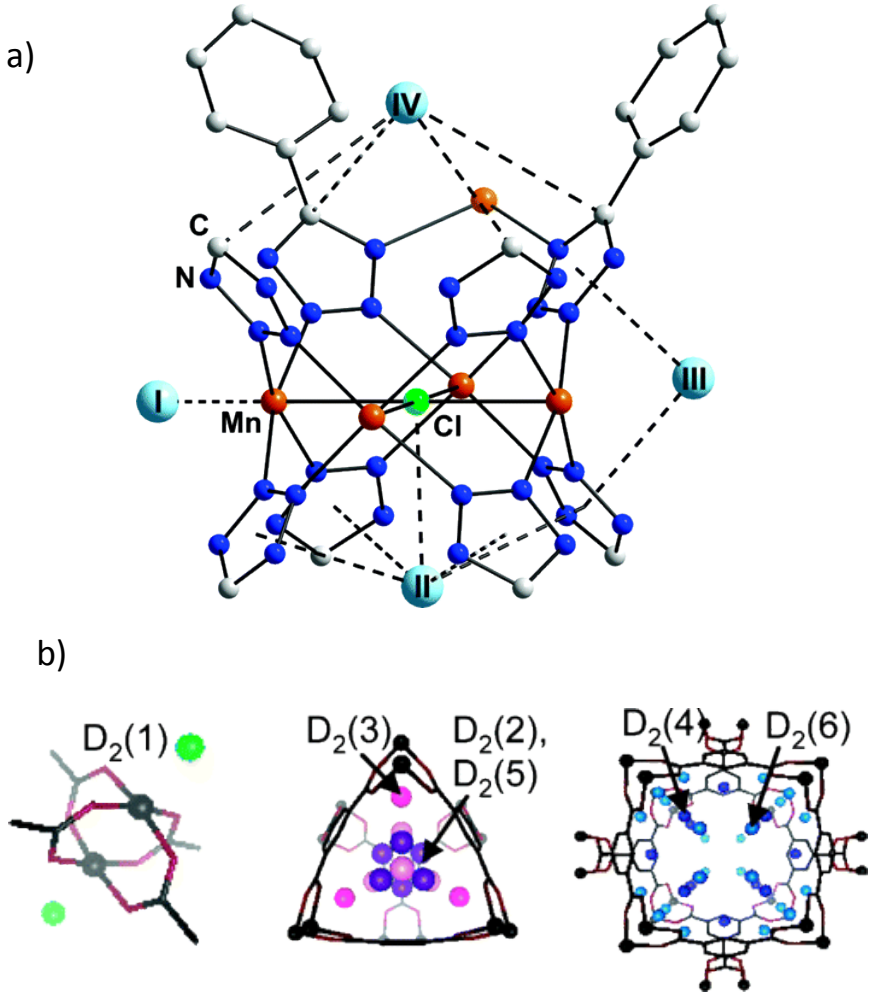

Figure 20 - Adsorption sites of D_2 as determined by neutron powder diffraction, for a) $[Mn(DMF)_6]_3[(Mn_4Cl)_3(BTT)_8(H_2O)_{12}]_2$ and b) HKUST-1. Adapted with permission from M. Dincă *et al.*, *J. Am. Chem. Soc.*, 2006, 128, 16876–83 and V. K. Peterson *et al.*, *J. Am. Chem. Soc.*, 2006, 128, 15578–15579. Copyright 2006 American Chemical Society.[89, 91]

Open metal sites are a promising way of improving the frameworks absorption properties, however they are likely to be hard to deliberately design in a self-assembly reaction. Likewise it is hard to introduce novel functional groups into MOFs, particularly ones capable of coordinating to metal centres during MOF synthesis and thereby changing the desired framework topology.

1.7.4 Post-synthetic modification

A more practical alternative to introduce new functionalities to MOFs is to add them once the framework has been synthesised by a process called post-synthetic modification (PSM). The process involves transport of a reagent through the pores of the MOF, followed by chemical reaction to give a new functionality.

The concept was presented by Wang and Cohen in 2007 showing the modification of the amine group in the amino-BDC version of MOF-5 [$Zn_4O(ABDC)$] (ABDC = 2-aminobenzene-1,4-dicarboxylate) (also known as IRMOF-3) to a methyl amide.[96] The reaction was carried out at room temperature in DCM using acetic anhydride. A schematic is presented in Figure 21. After modification the framework was digested, breaking apart the structure so that mass spectrometry and solution-phase NMR spectroscopy could be used to observe the changes to the ligand. The conversion was recorded to be about 80% based on integration of the ^1H NMR spectrum.[96]

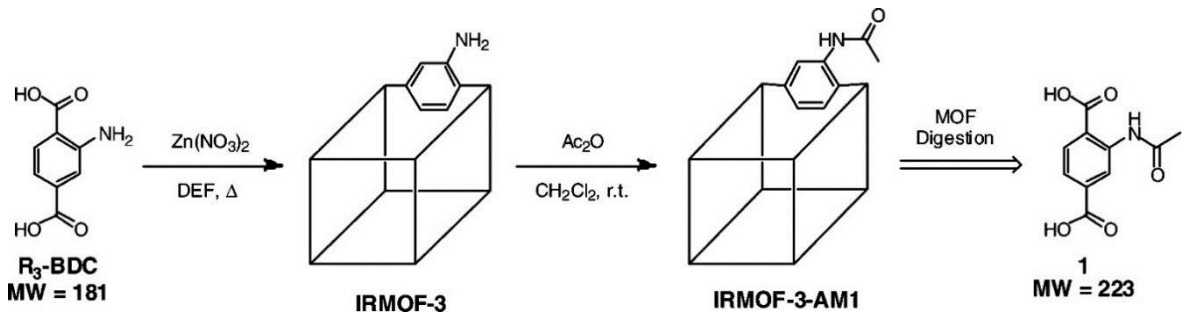

Figure 21 – Schematic for the post-synthetic modification of IRMOF-3 from an amine to a methyl amide. Reprinted with permission from Z. Wang and S. M. Cohen, *J. Am. Chem. Soc.*, 2007, 129, 12368–12369. Copyright 2007 American Chemical Society.[96]

Since Wang and Cohen's pioneering work there has been a wide variety of differing reactions carried out on the organic linkers inside metal-organic frameworks. Some of the frameworks studied include; IRMOF-3,[97–100] [Zn_2(TCPB)(DPG)] (TCPB = 1,2,4,5-tetrakis(4-carboxyphenyl)benzene, DPG = meso-1,2-bis(4-pyridyl)-1,2-ethanediol),[101] DMOF,[102] UMCM-1 [$Zn_4O(BDC)(BTB)_2$],[102] UiO-66,[103–105] MIL-53,[106] MIL-101 [$M_3F(H_2O)_2(\mu_3\text{-}O)(BDC)_3$],[107] MIL-68 [V(OH)(BDC)],[108] CAU-1 [$Al_4(OH)_2(OCH_3)_4(BDC)$],[109] IRMOF-16 [$Zn_4O(L)_3$] (L = 1,4-di(4-carboxy-2-hydroxyphenyl)benzene),[110] various PIZOFs [$Zr_6O_4(OH)_4(O_2C\text{-}PE\text{-}P(R_1,R_2)\text{-}EP\text{-}CO_2)_6$] (P = phenylene, E = ethynylene),[111] and [$Zn_2(TDC)_2L$] (H_2TDC = 9,10-triptycenedicaroxylic acid, L = 3-(but-3-enyl)-3'-4,4'-bipyridine).[112] Many of these studies show introduction of new functionalities previously unseen in MOFs, and Figure 22 shows some of the complicated multistep reactions carried out on IRMOF-3, that take advantage of partial conversions in each step.[98] Post-synthetic modification of MOFs is a large research area but was fairly extensively reviewed by Cohen et al in 2011 and 2012.[24, 25]

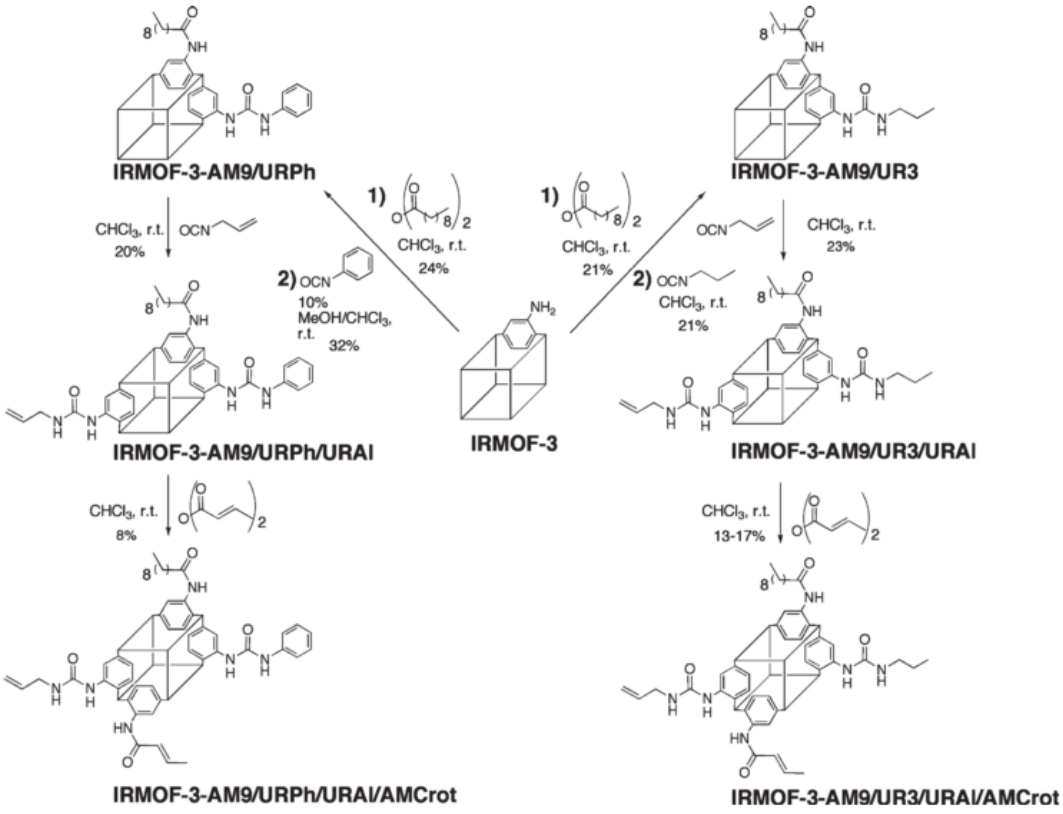

Figure 22 – Multistep post-synthetic modification reactions carried on IRMOF-3. Reprinted with permission from S. J. Garibay *et al*., *Inorg. Chem.*, 2009, 48, 7341–7349. Copyright 2009 American Chemical Society.[98]

Many of the examples of PSM use organic reactions to attach new groups to the frameworks, but similar results can also be achieved by grafting alkylamines onto coordinatively unsaturated metal centres. *i.e.* coordination to open metal sites. This was first demonstrated using MIL-101 and analysed for its effect on the catalytic properties.[113] This idea was extended by Long and co-workers to look at the effect of grafting a double ended alkylamine on the gas uptake properties of $H_3[(Cu_4Cl)_3(BTTri)_8]$ (H_3BTTri = 1,3,5-tris(1H-1,2,3-triazol-5-yl)benzene).[114] The process is shown in Figure 23 and resulted in an improved uptake of CO_2 at low pressures, but a significant reduction at higher pressures, this was rationalised due to an increased attraction to CO_2 but a reduced pore volume.[114] While this strategy is an interesting one it removes the free open metal sites which have previously been shown to be one of the main binding locations and it would be more ideal to have both a free alkyl chain and an open metal site in the framework.

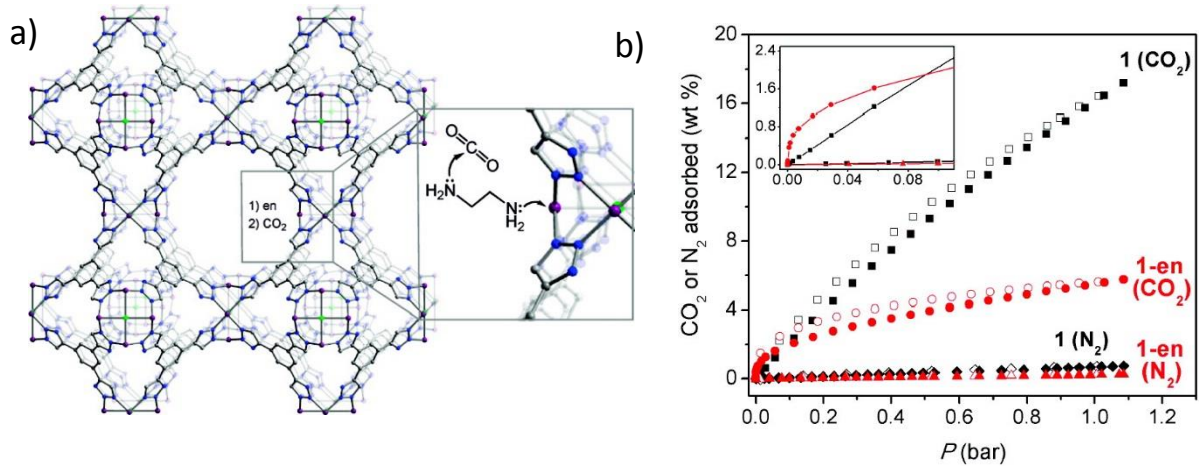

Figure 23 - a) Schematic for the two-step adsorption of CO_2 inside $H_3[(Cu_4Cl)_3(BTTri)_8]$ involving a alkylamine coordinated the MOFs open metal site, b) gravimetric adsorption values for the parent material (1) and the alkylamine-modified version (1-en). Adapted with permission from A. Demessence *et al.*, *J. Am. Chem. Soc.*, 2009, 131, 8784–8786. Copyright 2009 American Chemical Society.[114]

Post-synthetic reactions are not limited to changes of the organic linkers or introduction of new functional groups, several examples also show conversion of the metal centres. Nice examples include work on exchanging Al and Fe centres in MIL-53 resulting in a mixed metal species (see Figure 24)[115] and capture of metal ions in anionic MOF $[Mn_3(L)_2]^{2-}.2[NH_2(CH_3)_2]^+$ (H_4L = tetrakis[4-(carboxyphenyl)oxamethyl]methane acid) , resulting in a neutral framework.[116]

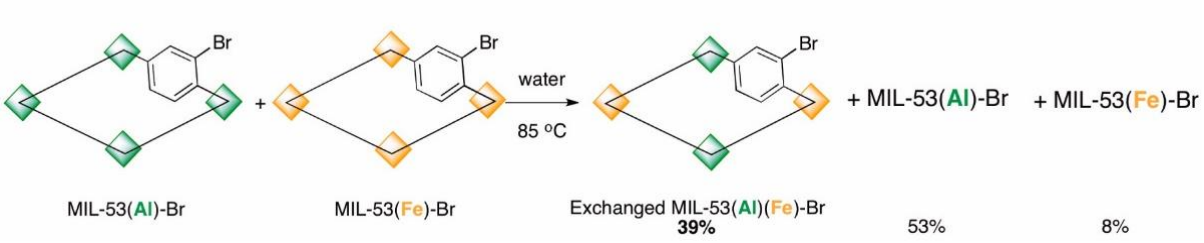

Figure 24 – Post-synthetic metal exchange of Al and Fe MIL-53. Adapted with permission from M. Kim *et al.*, *J. Am. Chem. Soc.*, 2012, 134, 18082–18088. Copyright 2012 American Chemical Society.[115]

1.8 *Flexible MOFs*

One of the most interesting aspects of metal-organic frameworks is their potential for dynamic behaviour in response to external stimuli. This refers to the ability of certain frameworks to drastically change their shape, structure or unit cell volume either when heated, undergoing guest exchange, being placed under pressure or exposed to light. The relative number of these highly flexible frameworks is fairly low and a recent review by Schneemann *et al*. suggest that "among the about 20,000 coordination networks structures…. less than 100 compounds reveal substantial breathing transitions or related stimuli responsive properties".[117] The majority of MOFs are considered to be rigid and only experience small changes to their structures, *i.e.* thermal expansion as would be expected of most solid state compounds, but a few exhibit much larger structural changes that can be of great benefit in terms of the materials properties.

1.8.1 The breathing behaviour of MIL-53

Desolvation and water uptake

The most well-known, and by far the most studied, flexible MOF is MIL-53. The framework is constructed from linear chains of M^{3+} ions connected through bridging OH^- groups and coordinated carboxylates. The carboxylates are part of a benzenedicarboxylate (BDC) linker which connect the other chains resulting in a 3D structure with a diamond shape 1D channel and an overall formula $M^{III}(OH)(BDC)$. The structure was first reported with a Cr^{3+} ion and after synthesis the pores contained a free terephthalic acid molecule.[12] The free acid could be removed by heating, giving a new high-temperature phase material similar to the as-synthesised version but with a slightly expanded pore containing no guest molecules. Upon cooling the material to room temperature the material immediately absorbed atmospheric water undergoing a drastic phase change that resulted in a major collapse of the pore shape. The phase change altered the symmetry of the framework going from orthorhombic *Imcm* to monoclinic *C*2/*c*. Views of the three structures can be seen in Figure 25, as solved by powder X-ray diffraction. Figure 25 d) also shows a view perpendicular to the pores showing the linked chromium ions. The structural change is analogous to a collapsible wine rack, when open it can hold wine bottles but when collapsed contains very little space.

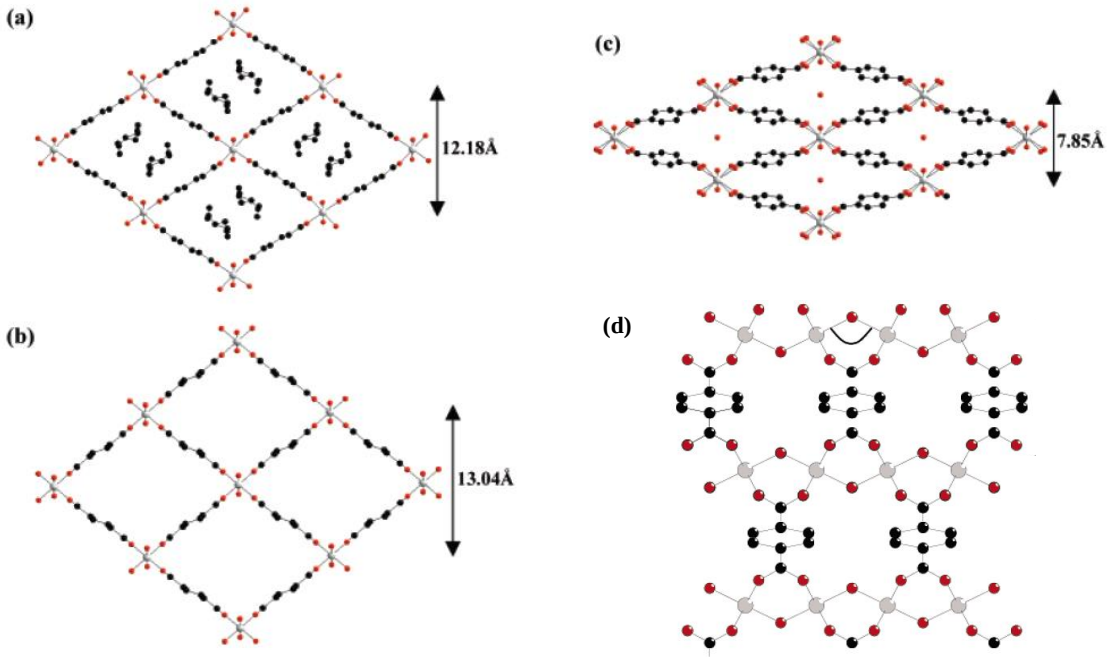

Figure 25 - View down the pore for a) as-synthesised MIL-53 containing partial occupancy guest acid molecules, b) high temperature MIL-53 with empty channel and c) low temperature Mil-53 with adsorbed water molecule in the centre of the pore space. d) Shows a view perpendicular to the pore of high temperature MIL-53 demonstrating the linked chain of Cr^{3+} ions. Adapted with permission from C. Serre *et al.*, *J. Am. Chem. Soc.*, 2002, 124, 13519–13526. Copyright 2012 American Chemical Society.[12]

The hydration effect is reversible and the transition can be easily followed using variable temperature powder X-ray diffraction (PXRD). Figure 26 demonstrates the transition occurring as the sample is heated.

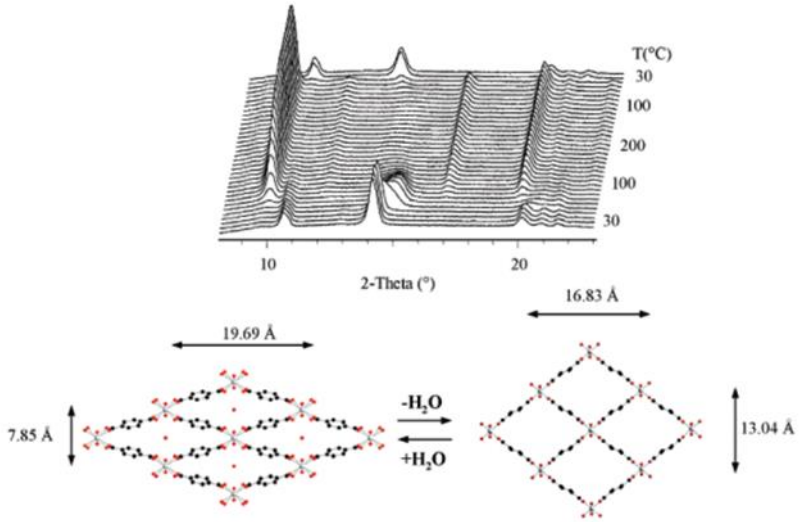

Figure 26 - Reversible structural transitions upon hydration / dehydration of MIL-53(Cr) followed through variable temperature PXRD. Adapted with permission from C. Serre *et al.*, *J. Am. Chem. Soc.*, 2002, 124, 13519–13526. Copyright 2012 American Chemical Society.[12]

The reason behind the huge structural contraction was investigated by Loiseau *et al*. on the aluminium analogue of MIL-53 by using solid state NMR (^{1}H, ^{13}C, ^{27}Al) techniques.[118] The contained water molecules were found to interact with the carboxylate oxygens through hydrogen bonds and these favourable interactions are thought to be responsible for the large structural change. Figure 27 shows some suggested hydrogen bond interactions holding the framework structure in this closed state.

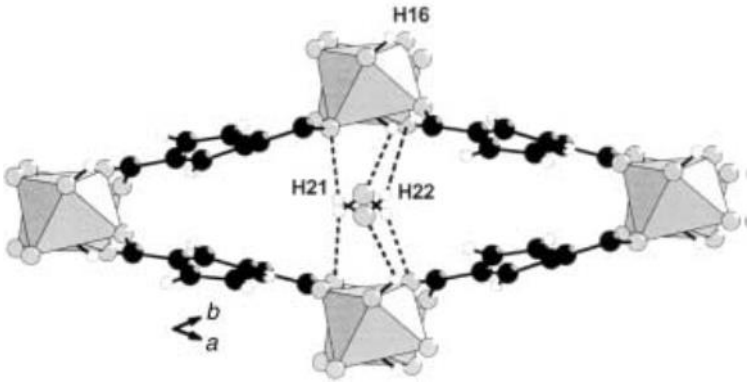

Figure 27 - Hydrogen bonding interactions in the low temperature structure of MIL-53(Al), as established using the partial charges and hardness analysis method (PACHA).[119, 120] Adapted with permission from T. Loiseau *et al*., *Chem. Eur. J.*, 2004, 10, 1373–1382. Copyright 2004 John Wiley and Sons.[118]

Effect on gas uptake properties

The gas uptake properties of both the open high temperature (dehydrated) phase, often termed large-pore, and the closed water containing (hydrated) phase, often termed narrow-pore, were investigated by gravimetric absorption methods.[121, 122] An initial analysis of the pores shapes would suggest that the dehydrated version should rapidly adsorb large amounts of CO_2 into its channel, whereas the hydrated version should essentially be non-porous, but in reality the two samples were seen to absorb almost the same amount of CO_2. The isotherms are significantly different, but both display distinct steps in their profiles. The isotherm of the dehydrated version (displayed in Figure 28 a) shows two steps: an initial filling of gas at low pressures, a levelling off, and then a second adsorption above 5 bar. The hydrated version (Figure 28 b) in contrast shows only one step, with no adsorption until pressures are above 10 bar. These interesting adsorption behaviours are a direct result of the framework's flexibility and were followed nicely by *in situ* crystallographic analysis.[122, 123] The dehydrated version is shown to rapidly close on the initial adsorption step, which Rietveld refinements of the powder diffraction data, in conjunction with *in situ* IR spectroscopy and periodic DFT calculations, showed was due to formation of an electron donor-acceptor interactions between

the adsorbed CO_2 molecules and the hydroxyl oxygen atom in the framework. Higher CO_2 pressures then break these CO_2-hydroxyl interactions and force the MOF back to the open-pore structure to accommodate more CO_2.[123] The hydrated version shows similar behaviour to the second step of the dehydrated version because it is already locked shut by the confined water molecules, but the gating pressure is higher due to a greater interaction strength between the water molecules and the framework.[122] During desorption a large hysteresis is observed in both cases implying that once loaded, the MOF holds onto its contained gas molecules even while the pressure is decreased. This is obviously favourable in certain applications and is fairly common among flexible MOFs. The *in situ* diffraction studies show that the hysteresis arises because the framework converts back to the narrow pore phase at lower pressures on desorption than it converts to the large pore phase on adsorption. The *in situ* powder diffraction study showing both adsorption and desorption from the dehydrated version can be seen in Figure 29.[123] The CH_4 isotherms are also displayed in Figure 28 and show no steps. This is presumably because CH_4 is unable to interact with the framework as strongly and induce the initial closing; similarly CH_4 is unable to break the interactions holding the framework closed in the hydrated MIL-53. Further *in situ* analysis on the dehydrated version shows that this narrow pore to large pore behaviour on CO_2 adsorption is cyclable over several runs.[123]

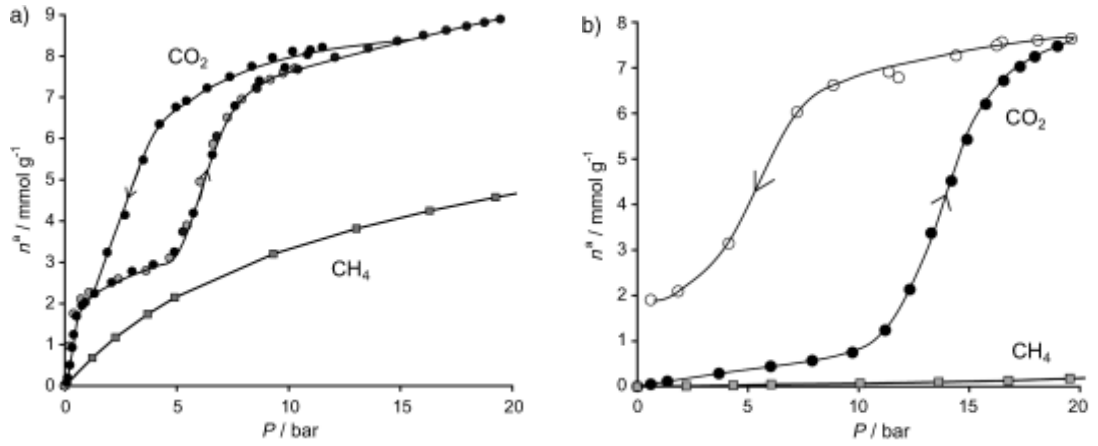

Figure 28 - Gravimetric CO_2 and CH_4 adsorption isotherms for a) dehydrated version and b) hydrated version of MIL-53(Cr). Adapted with permission from P. L. Llewellyn *et al*., *Angew. Chem. Int. Ed.*, 2006, 45, 7751–7754. Copyright 2006 John Wiley and Sons.[122]

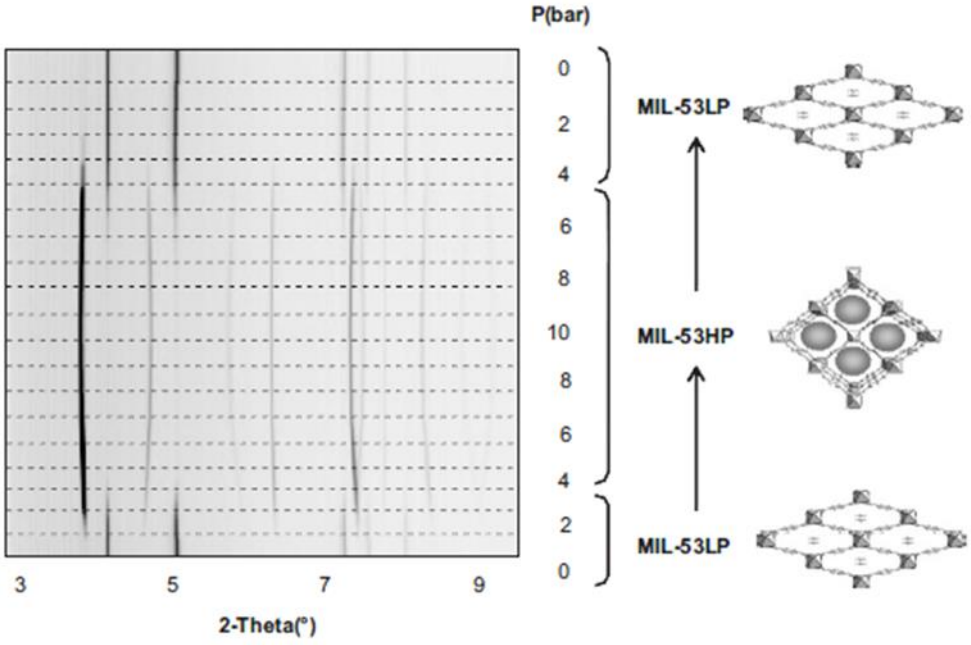

Figure 29 - *In situ* PXRD study of CO_2 adsorption on dehydrated MIL-53(Cr). Adapted with permission from C. Serre *et al*., *Adv. Mater.*, 2007, 19, 2246–2251. Copyright 2007 John Wiley and Sons.[123]

Differences due to the metal

A large number of MIL-53 analogues with different metal ions have been synthesised; including iron[124], gallium[125], indium[126], manganese[127], scandium[128] and cobalt[129] and several publications have explored the effect of cation mixing[130] and mixed-valent ions[131]. In these studies changing the metal ion has been shown to result in significant differences to the breathing behaviour. The Fe version is a great example, showing a more complicated behaviour than just an open dehydrated and closed hydrated form. In the presence of many organic solvents it exists, much like the Cr and Al analogues, in the large pore form, however, upon desolvation, while the Cr and Al versions exist in an open empty pore structure, the anhydrous Fe versions collapses to a very narrow pore form which is tightly closed and displays no porosity.[124, 132] Upon adsorption of water MIL-53(Fe) converts to a similar hydrated closed form to that of the hydrated Cr and Al analogues but the transitions occurs through an additional intermediate phase.[124, 132] This results in a 4-phase breathing behaviour that is displayed in Figure 30.

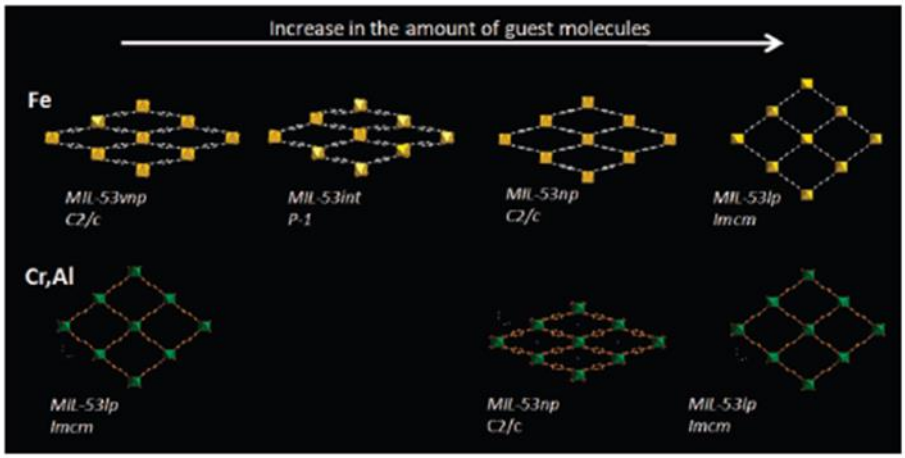

Figure 30 - Structural evolution of MIL-53 (Fe - Top and Cr, Al - Bottom) with increasing amounts of guest molecules. Reprinted with permission from P. L. Llewellyn *et al*., *J. Am. Chem. Soc.*, 2009, 131, 13002–12008. Copyright 2009 American Chemical Society.[132]

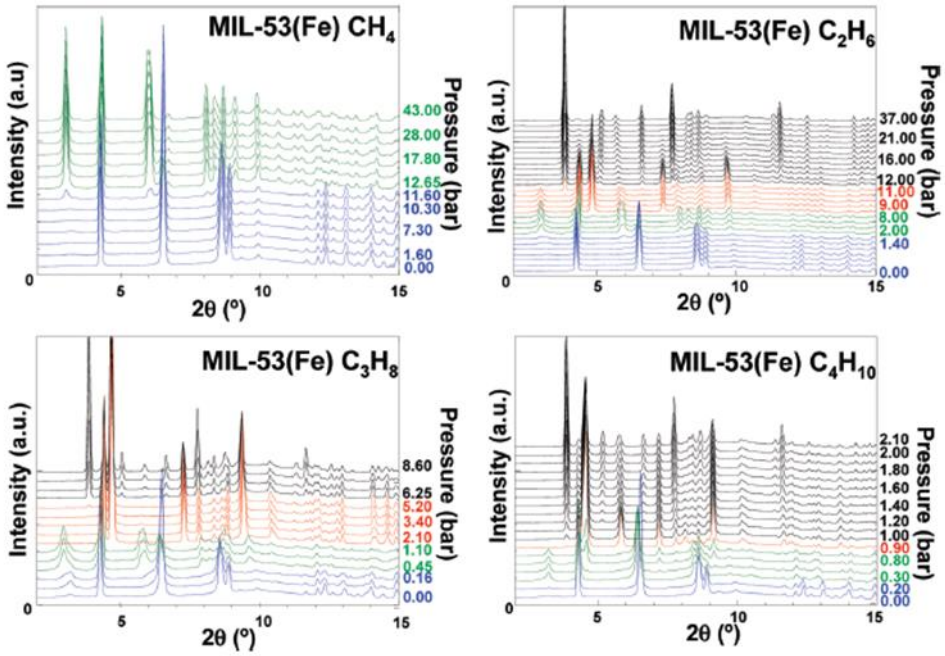

Figure 31 - *In situ* PXRD studies of adsorption of various linear alkanes at 303 K. Colour relates to the major phase present (blue, anhydrous; green, intermediate; red, narrow pore; black, large pore form. Reprinted with permission from P. L. Llewellyn *et al*., *J. Am. Chem. Soc.*, 2009, 131, 13002–12008. Copyright 2009 American Chemical Society.[132]

In situ studies on the adsorption of short chain hydrocarbons in MIL-53 Fe (Figure 31) have shown that the framework undergoes successive transitions between the 4 phases displayed in Figure 30, with increasing gas pressures. Even more interestingly the gating pressures between these transitions have been shown to vary significantly based on the length of the alkyl chain. Adsorption of C_4H_{10} resulted in the framework undergoing transitions between all four phases at very low

pressures, being fully converted to the open from by 2 bar.[132] Uptake of C_3H_8 and C_2H_6 showed transitions between all four phases but requiring higher pressures for the transitions to occur, and CH_4 exhibits a transition between the very narrow pore and the intermediate form at around 12 bar and then display no further changes even when applying pressure up to 43 bar.[132]

The adsorption of CO_2 and short chain alkanes by the MIL-53 series has been fairly extensively investigated, including multiple *in situ* crystallographic studies.[122, 123, 132–138] The breathing effects relating to adsorption of mixed CH_4 and CO_2 streams have also been recorded for the Cr version due to the industrial relevance of separating these gases.[139] The work showed that for equimolar or higher levels of CO_2 the breathing behaviours followed the normal pattern where the introduction of gas initially closes the pores before reopening at higher gas pressures, however, for CH_4 rich streams the MOF constantly remained in the open form not displaying any breathing effect, similar to adsorption of pure CH_4.[139] A variety of other guests have also been studied, including gases such as nitrogen, carbon monoxide, oxygen, argon and hydrogen disulphide, as well as a range of organic solvent like molecules.[134, 140–145]

Applications in Separations

Some interesting research has also reported on the ability of MIL-53 to separate different organic molecules including mixtures of pyridine and 2,3-lutidine[146], aniline and phenol[147], and various xylene isomers.[148, 149] The separation of the xylene isomers is particularly impressive with the ability under chromatographic conditions at 323 K to resolve all the components contained in a BTEX mixture (benzene, toluene, ethylbenzene, para-xylene, meta-xylene and ortho-xylene).[149] Figure 32 shows the chromatograms at both 293 K and 323 K.

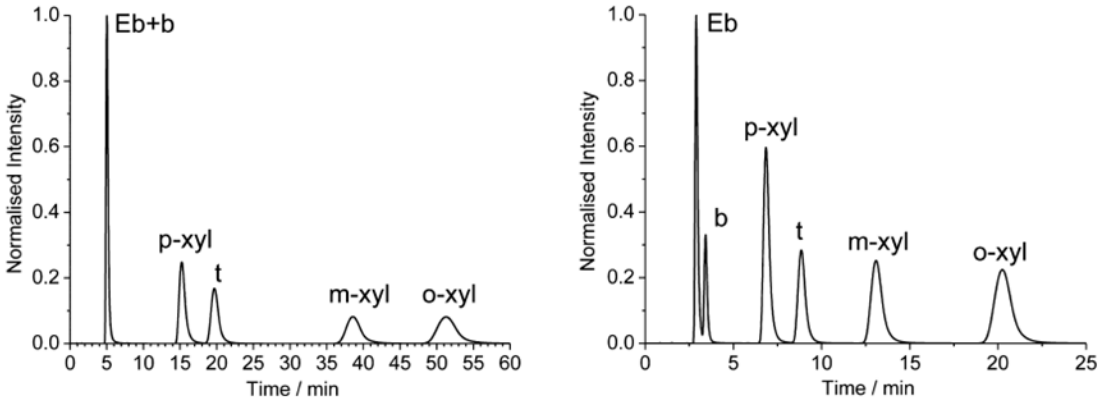

Figure 32 - Chromatograms for the separation of BTEX mixtures at left - 293K and right - 323K. Eb, ethylbenzene; b, benzene; p-xyl, para-xylene; t, toluene; m-xyl, meta-xylene; o-xyl, ortho-xylene. Adapted with permission from R. El Osta *et al*., *Chem. Mater.*, 2012, 24, 2781–2791. Copyright 2012 American Chemical Society.[149]

Effect of functionalization

Similar to more rigid frameworks, the chemical modifiability of the ligand can also be used to further refine adsorption properties of MIL-53. This has been done by modifying the BDC ligand with pendant groups including; Cl, Br, CF_3, CH_3, NH_2, NO_2, OH, CO_2H and F,[150–154, 126, 155] and using mixed ligand systems of normal BDC and NH_2-BDC, observing how changing the relative ratios of the two ligands affect the adsorption based breathing behaviour.[156] Figure 33 shows a nice visual demonstration of how certain functionalised MIL-53 Fe systems affect the transitions between different phases upon CO_2 adsorption.[154]

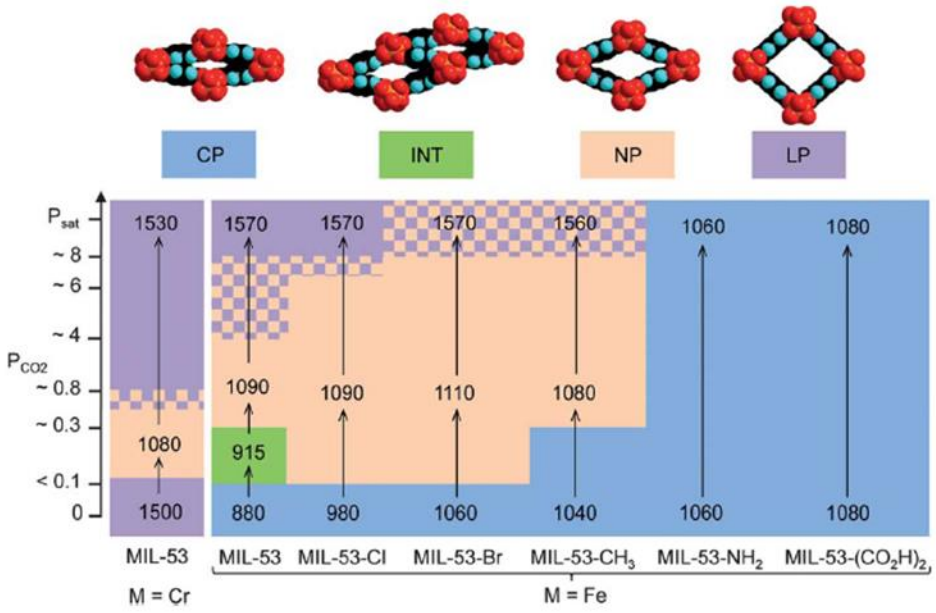

Figure 33 - Transitions between various pore opening stages in modified MIL-53 with increasing CO_2 pressure as determined by PXRD, numbers refer to unit cell volumes. Reprinted with permission from T. Devic *et al.*, *J. Mater. Chem.*, 2012, 22, 10266-10273. Copyright 2012 Royal Society of Chemistry.[154]

Techniques Used

Research into MIL-53 has been incredibly active over the past decade and to understand the dynamics of the framework a wide range of techniques aside from gravimetric or normal crystallographic measurements have been employed. These include solid state ^{1}H and ^{27}Al NMR[157], ^{129}Xe NMR[158], inelastic neutron scattering[159, 160], quasi-elastic neutron scattering[161, 162], pulse chromatography[163], various calorimetric measurements[164–166], thermodynamic isotherm models[167], high pressure crystallography[168] and electron spin resonance spectroscopy.[169] In addition to the experimental techniques, computational methods have been frequently used to try and both predict and understand the breathing behaviours.[136, 170–190] Overall the literature on MIL-53 is very extensive

and an entire literature review could be written just looking at all the various studies that have been reported.

1.8.2 Other Breathing MOFs

Although MIL-53 has dominated the field of flexible MOFs, there are other frameworks exhibiting these large dynamic motions. Many of these examples show transitions between open and closed forms upon removal of guests with various numbers of intermediate phases and stepped isotherm profiles. Examples of these flexible MOFs are included in Table 2.

Table 2 - MOFs displaying transitions between open and closed Phases

MOF / Formula	Relevant Abbreviations	Ref
MIL-105 / $Cr(OH)[O_2C\text{-}C_6(CH_3)_4\text{-}CO_2]$		191
Cu(BDTri).DMF	H_2BDTri = 1,4-benzenedi(1*H*-1,2,3-triazole)	192
$[Zn_6\text{-}(IDC)_4(OH)_2(Hprz)_2]$	IDC = imidazole-4,5-dicarboxylate	193
$NaLa[(PO_3H)_2\text{-}CH\text{-}C_6H_4\text{-}CH(PO_3H)_2]$		194
$[Na_2Cu\text{-}(2,4\text{-pyrdc})(H_2O)(\mu\text{-}OH_2)_2]$	2,4-pyrdc = pyridine-2,4-dicarboxylate	195
$[Cu(2,5\text{-pyrdc})(NH_3)](2H_2O)$	2,5-pyrdc = pyridine-2,5-dicarboxylate	195
$[Cd(IBA)_2]$	HIBA = 4-(1H-imidazole-1-yl)benzoic acid	196
CaH_6DTMP	H_8DTMP = hexamethylenediamine tetrakis(methylenephosphonic acid)	197
$Ln(btc)(H_2O)$	btc = benzenetricarboxylate	198
DUT-13 / $[Zn_4O(BenzTB)_{3/2}]$	H_4BenzTB = N,N,N',N'-benzidinetetrabenzoic acid	199
SUMOF-6 / $[Ln_2(bpydc)_3(H_2O)_3]$	bpydc = 2,2'-bipyridine-5,5'dicarboxylate	200
$[La(BTB)(H_2O)]$	BTB = 1,3,5-tris(4-carboxyphenyl)benzene	201
Co(BDP)	BDP = 1,4-benzenedipyrozolate	202
$Zn_3(btz)_2(bdc)_2$	btz = 1H-benzotriazole	203
$Zn_3(tz)_2(bdc)_2$	tz = 1,2,3-1H-triazole	203
$[Pr_4(H2O)_{18}Cu_4(H_2O)_8bta_5]$	bta = 1,3,4,5 - benzenetetracarboxylate	204
$La(H_5$DTMP)	H_8DTMP = hexamethylenediamine tetrakis(methylenephosphonic acid)	205
$Co(HL^{dc})$	HL^{dc} = 5-{4-[3-carboxy-2,6-bis(pyridin4-yl)pyridine-4-yl]-phenyl}benzene-1,3-dicarboxylic acid	206
$[Zn_3(OH)_2(BTCA)_2]$	H_2btca = benzotriazole-5-carboxylic acid	207
COMOC-2 / VO(BPDC)	biphenyl-4,4'-dicarboxylate	208
PCN-72 / Mg(TTTP)	TTTP = 2', 3', 5', 6'-tetramethyl-[1,1':4',1''-terphenyl]-4,4''-dicarboxylate	209
[Cd(HBTC)-BPE]	H3BTC = 1,3,5-benzenetricarboxylic acid, BPE = 1,2-bis(4-pyridyl)ethane	210

$[Ca(BDC)(DMF)(H_2O)]$		[211]
$[Zn_2(BTC)(OH)(H_2O)]$	BTC = 1,3,5-benzenetricarboxylate	[212]
$Cu_3(H_2L^2)(bpa)_2$	H_8L^2 = N,N,N',N'tetrakis(phosphonomethyl)-hexamethylenediamine, bpa = 1,2-bis(4-pyridyl)ethane	[213]
MIL-47(V^{III}) / V^{IV}(O)BDC		[214]
$\{Cu_4[CuI(bcpdmpm)_2]_2(EtOH)_2(H_2O)_2\}(NO_3)_2$	H_2bcpdmpm = bis(4-carboxyphenyl)-3,5-dimethyl-1*H*-pyrazolyl)methane	[215]
$[Co_3(bpydc)_2(HCOO)_2H_2O]$	bpydc = 2,2'-bipyridine-5,5'dicarboxylate	[216]
$[Zn_3(bpydc)_2(HCOO)_2]$	bpydc = 2,2'-bipyridine-5,5'dicarboxylate	[216]
CAU-10-H / [Al(OH)(1,3-BDC)]	1,3-BDC = benzene-1,3-dicarboxylate	[217]
$[Cu_4(\mu_4\text{-}O)(\mu_2\text{-}OH)_2(Me_2trz\text{-}pba)_4]$	Me_2trz-pba = 4-(dimethyl-4H-1,2,4-triazol-4-yl)benzoate	[218]
[Zn(bpaipa)]	H_2bpaipa = 5-(bis(pyridine-2-ylmethyl)amino)isophthalic acid	[219]
DynaMOF-100 / $[Zn_4O(L)_3(DMF)_2]$	H_2L = 4-[4-tert-butyl-2-(4-carboxyphenoxy)phenoxy]benzoic acid	[220]
$[Zn_5(4\text{-}pca)_4(ade)_2(H_2O)_2]$	4-H_2Pca = 4-pyrazolecarboxylic acid, Hade = adenine	[221]
$[NH_2(CH_3)_2][Zn_3(4\text{-}pca)_3(ade)]$		[222]

The flexible MOFs in Table 2 display a wide variety of differing motifs and functionalities, for example Co(BDP)[202], which displays four steps during N_2 adsorption between its open and closed versions, via three intermediates, is a bispyrazolate-containing framework where the ligands are coordinated to the metal centres through the pyrazolate rings in contrast to the carboxylate bonds in MIL-53. Unfortunately detailed analysis of all these flexible frameworks is beyond the scope of this chapter. Many of these examples do, however, contain interesting phenomena, for example [Cu(BDTri)]·DMF exhibits structural flexibility, but replacing the coordinated solvent (DMF) with DEF stops the transitions,[192] MIL-47(V^{III}) ([V(OH)(BDC)]) shows multi-step phase transitions similar to MIL-53(Fe), but if the metal centre is V^{IV} (*i.e.* [V(O)(BDC)]) the MOFs flexibility is drastically reduced,[214] and DynaMOF-100 displays structural transitions back to its solvated phase upon adsorption of styrene but not the very similar sized ethylbenzene, offering the potential as a good separation material.[220] Figure 34 shows a schematic for this effect.[220]

Research on $[Ca(BDC)(DMF)(H_2O)]$ has also revealed that the dynamics can vary within one single crystal due to non-uniform transformations, DMF being lost from the outsides of the crystal first, becoming non-porous and stopping the DMF contained in the core easily leaving.[211]

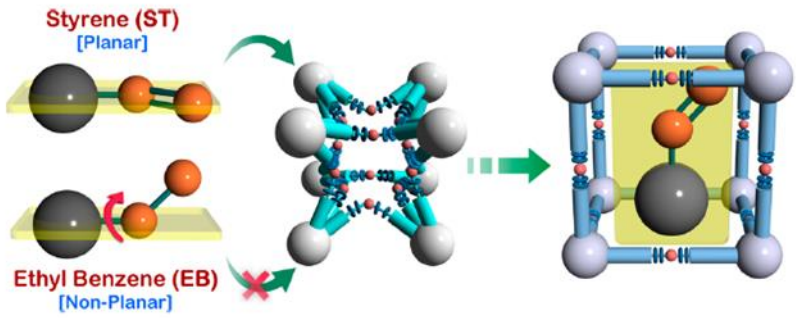

Figure 34 - Schematic showing the guest responsive behaviour of DynaMOF-100 which preferentially adsorbs styrene over ethylbenzene. Reprinted with permission from S. Mukherjee *et al*., *Inorg. Chem.*, 2015, 54, 4403–4408. Copyright 2015 American Chemical Society.[220]

Paddlewheel MOFs

Several examples of paddlewheel MOFs also display these breathing transitions upon removal of guests including; DMOF ($[Zn_2(BDC)_2(DABCO)]$),[223–228] TetZB $[Zn_2(L)(bpy)]$ (H_4L = tetrakis[4-carboxyphenyl)oxamethyl]methane),[229] $[Zn_2(cpa)_2(bpy)]$ (cpa = 4-(methoxycarbonyl)benzoate),[230] $[Zn_2(btdc)_2(bpy)]$ (btdc = 2,2'-bithiophene-5,5'-dicarboxylate),[231] DUT-8(M) $[M_2(ndc)_2(dabco)]$ (ndc = naphthalene-2,6-dicarboxylate)[232–235] and $[Cu_2(bdc)_2(bpy)]$.[236] The breathing of these frameworks can be quite sensitive to changes to the material; DMOF and amino-DMOF are shown to exist mainly in an open large-pore form (with the exception of adsorption of isopropanol in the parent compound which causes the large-pore to narrow-pore to large-pore transitions)[224] but by post-synthetically modifying the amine group to an amide group with different length alkyl substituents, a breathing effect can be introduced.[225] Similarly by using differing pendant alkoxy groups on the BDC linker, a breathing range upon loss of solvent can be introduced and finely tuned along with the gas uptake properties.[226–228] Figure 35 shows the various changes to the powder patterns and unit cell volumes going from the solvated to desolvated phases of various modified DMOF frameworks and Figure 36 shows the different volumetric gas uptake profiles.[228]

The paddlewheel MOFs are often interpenetrated which can also be an important factor in controlling the breathing, for example the 2-fold interpenetrated version of $[Zn_2(btdc)_2(bpy)]$ showing distinct closed-to-open-pore transitions upon loss and gain of guest molecules while the 3-fold interpenetrated version remains rigid.[231] In addition, the crystallite size also turns out to be relevant and Sakata *et al*. show for $[Cu_2(bdc)_2(bpy)]$ that by downsizing the crystals a shape memory can be introduced.[236] Under normal behaviour, loss of guest molecules results in a reversible closing of the structure, removing the inherent void space, but for significantly smaller crystallite sizes the framework remain temporarily in an open structure until further thermal treatment.[236]

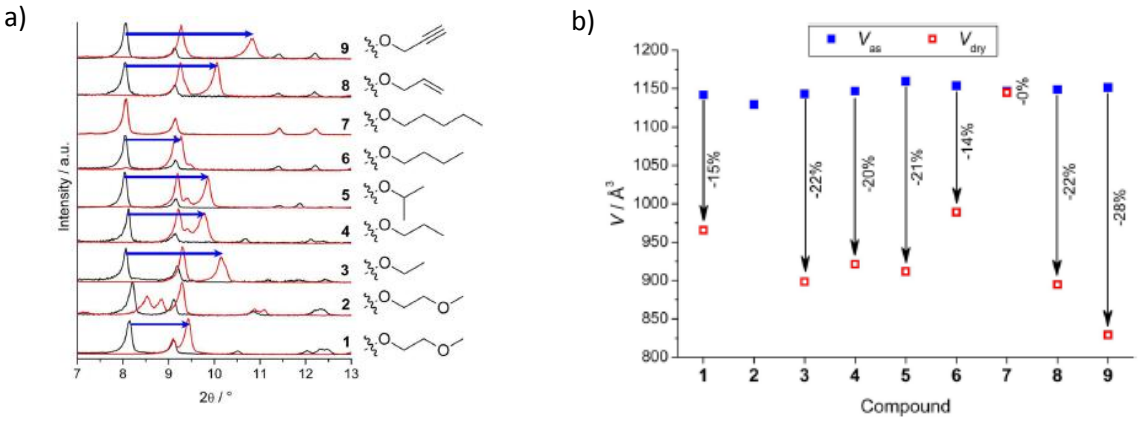

Figure 35 - a) Changes to powder diffraction patterns upon solvent removal for a range of modified DMOF species, b) corresponding changes to unit cell volumes upon desolvation. Adapted with permission from S. Henke *et al*., *J. Am. Chem. Soc.*, 2012, 134, 9464–9474. Copyright 2012 American Chemical Society.[228]

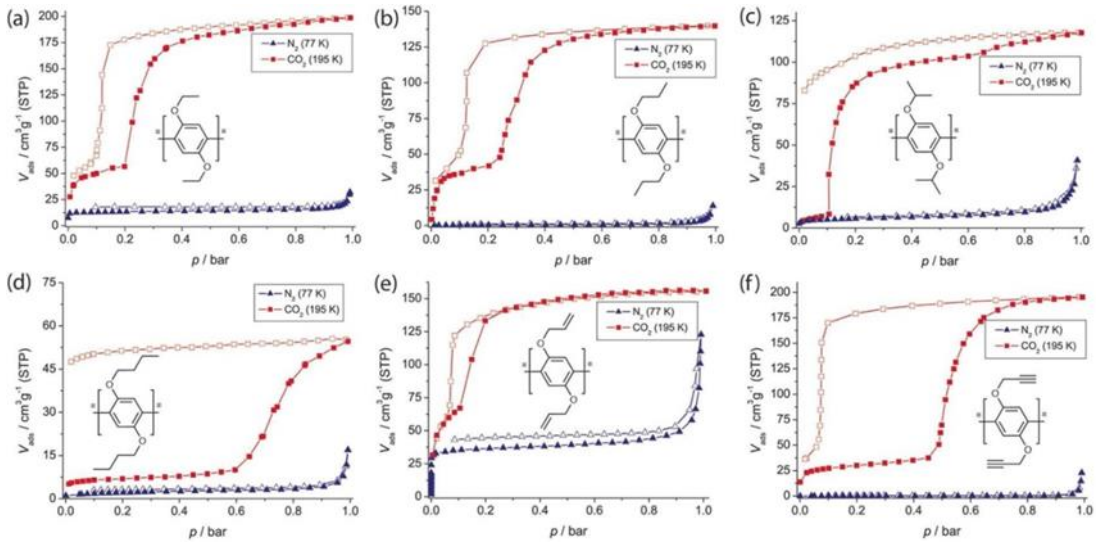

Figure 36 - CO_2 and N_2 adsorption / desorption isotherms for various functionalised DMOF species. a) 3, b) 4, c) 5, d) 6 and e) 8 and f) 9. Adapted with permission from S. Henke *et al*., *J. Am. Chem. Soc.*, 2012, 134, 9464–9474. Copyright 2012 American Chemical Society.[228]

1.8.3 Different flexible motions

MIL-53 and many of the other similar compounds mentioned above are generally classed as breathing MOFs, showing the narrow-pore to large-pore transitions. This is, however, not the only dynamic motion available to MOFs, with flexibility also arising from the rotation of the organic linkers, the movement of interpenetrated chains, or a change to the dimensionality of the connectivity in the material (e.g. a 2D MOF to a 3D MOF).

Linker Rotation

The rotation of linkers is a particularly interesting property that can lead to what has been called gate-opening effects. The effect is summarised in the schematic displayed in Figure 37 and involves a movement of the organic linkers out of the way of the channel windows essentially opening a door to the pores of the material.

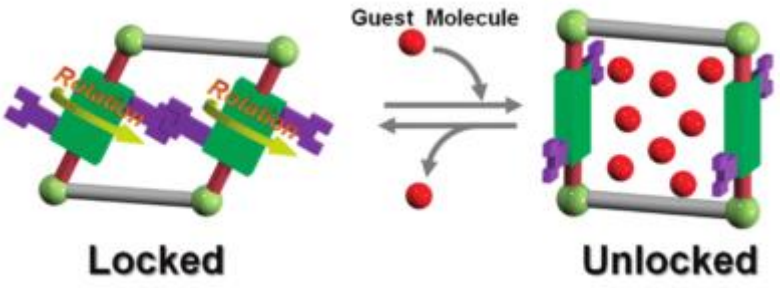

Figure 37 - Schematic for gate-opening effects due to ligand rotation in $[Cd_2(pzdc)_2L(H_2O)_2]$. Reprinted with permission from J. Seo *et al*., *J. Am. Chem. Soc.*, 2009, 131, 12792–12800. Copyright 2009 American Chemical Society.[237]

A good example of this gate opening phenomena is ZIF-8 $[Zn(MeIm)_2]$, where the initial investigations into the structures flexibility were carried out using high pressure crystallography.[238] A single crystal was enclosed in a diamond-anvil cell with a hydrostatic medium of 4:1 methanol / ethanol, and the pressure slowly increased. The starting material contained guest solvent, equivalent to 12 MeOH molecules per unit cell (based on SQUEEZE[239] analysis of electron density) which was shown to increase as the pressure was raised due to the methanol / ethanol being forced into the pore. At a particular gating pressure there was a substantial increase of the absorbed MeOH molecules to 41 per unit cell due to the framework undergoing a single-crystal-to-single-crystal phase transitions based on a twisting / swing of the imidazolate ligands. This twisting was like the opening of a door shown in Figure 37 that subsequently increased the size of windows in the material and the accessible pore volume. Figure 38 shows the two phases observed and how the channel space has increased.[238] Further work on ZIF-8 using Rietveld refinements of *in situ* PXRD data obtained during nitrogen uptake show that the structure can also be modified in the same way by gas adsorption, which explains how ZIF-8 has been shown to adsorb gas molecules whose kinetic diameters are larger than the normal window size and should have been excluded based on size.[240]

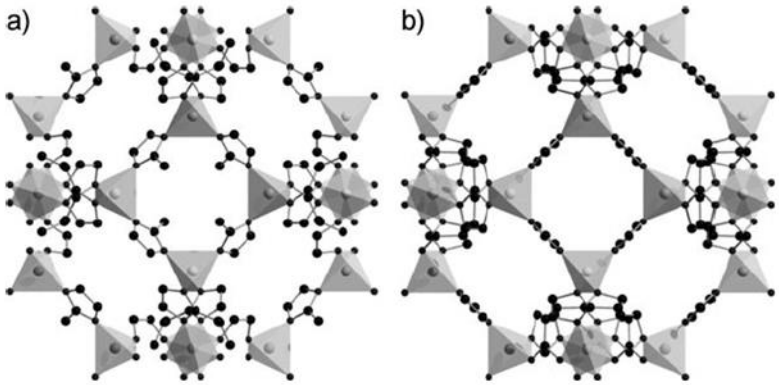

Figure 38 - ZIF-8 at a) ambient pressure and b) at 1.47 GPa in its new gate-opened phase. Adapted with permission from S. A. Moggach *et al*., *Angew. Chem. Int. Ed.*, 2009, 48, 7087–7089. Copyright 2009 John Wiley and Sons.[238]

Similar ligand rotations and gate-opening effects have been reported for other imidazolate frameworks, namely ZIF-7 [$Zn(BzIm)_2$] (BzIm = benzimidazolate) [241, 242] and ZIF-4 [$Zn(Im)_2$] (Im = imidazolate)[243] as well as other framework such as [$Cd_2(pzdc)_2L(H_2O)_2$] (L = 2,5-bis(2-hydroxyethoxy)-1,4-bis(4-pyridyl)benzene).[237] Flexibility due to ligand changes is not limited to gate-opening effects. Frameworks [$Co_2(epda)_2(bpa)(H_2O)_2$] ($H_2epda$ = 5-ethyl-pyridine-2,3-dicarboxylic acid, bpa = 1,2-bi(4-pyridyl)ethane))[244] and [$Cu_2(L)_2(SO_4)(Br)_2$] (L = 4,4'-(1,4-(trans-2-butene)diyl)bis(1,2,4-triazole)) [245] are nice examples of open- and closed-pore structures being driven by the flexibility of the ligands. [$Co_2(epda)_2(bpa)(H_2O)_2$] demonstrates an expanded and shrunken form due to rotation of its pillar ligand and [$Cu_2(L)_2(SO_4)(Br)_2$] (Figure 39) shows a rotation of part of its partially flexible ligand between two positions upon removal of solvent.[244, 245]

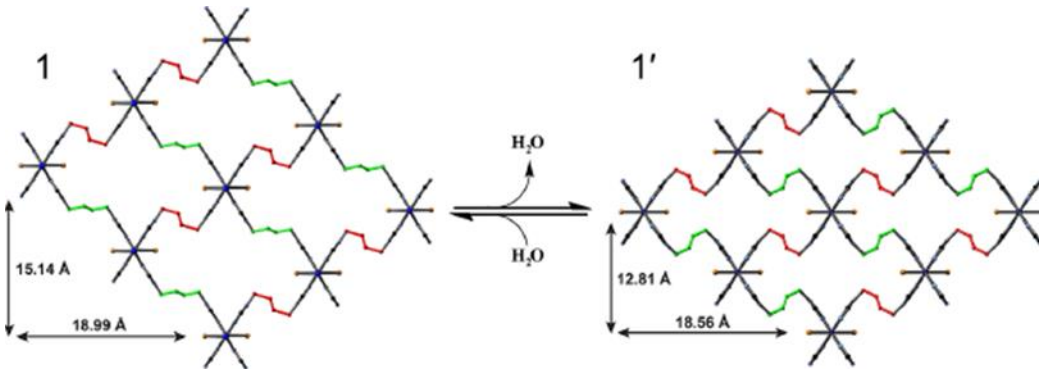

Figure 39 - Effect on solvent removal on [$Cu_2(L)_2(SO_4)(Br)_2$]. Reprinted with permission from C. R. Murdock *et al*., *Inorg. Chem.*, 2013, 52, 2182–2187. Copyright 2013 American Chemical Society.[245]

The conformational changes of ligands can also be of advantage for various reasons, for example $[Zn_2(bpeb)(obc)_2]$ (bpeb = 1,4-bis[2-(4-pyridyl)ethenyl]benzene, H_2obc = 4,4'-oxybisbenzoic acid) displays a shift in the UV adsorption when undergoing solvent-dependent SC-SC transitions between *trans-cis-trans* and *trans-trans-trans* forms of the bpeb ligand,[246] and $[Zn_2(L)(H_2O)_2]NO_3$ (L = 1,3-bis-(3,5-dicarboxyphenyl)imidaolate) exhibits SC-SC conformational changes of its imidazolium group which allows transmetallation reactions to occur.[247]

Movement of interpenetrated chains

Another interesting type of flexibility is the movement of interpenetrated chains. This kind of behaviour is most dramatic for 2D coordination polymers such as $[Cu(dhbc)_2(bpy)]$, in which large shifts of interdigitated chains can occur reducing or increasing the gap between different layers,[248] but similar subnetwork displacement effects can also be seen in 3D frameworks such $[(CuCN)_3L(guest)_x]_n$ (L = 2,6-bis((3,5-dimethyl-1H-pyrazol-4-yl)methyl)pyridine), in which a phase transition based on the sliding of the two interpenetrated chains is observed on guest uptake,[249] and NOTT-202 ($(Me_2NH_2)_{1.75}[In(L)]_{1.75}$, H_4L = biphenyl-3,3',5,5'-tetra-(phenyl-4-carboxylic acid)) which undergoes rearrangement of the interweaving of the two independent networks upon guest removal.[250] NOTT-202 is a very interesting structure due to its partial interpenetration, an unusual feature in which the two crystallographically independent networks have different chemical occupancies. The network with only a partial occupancy of 0.75 consists of two disordered components, neither of which could be fully occupied as they would not fit inside the other network. Similarly there cannot be a half-occupancy of both the disordered parts because it would lead to steric clashes. This results in a 0.375 occupancy of both the disordered components of the partially interpenetrated network and leads to the overall 1.75 interpenetration (Figure 40).[250]

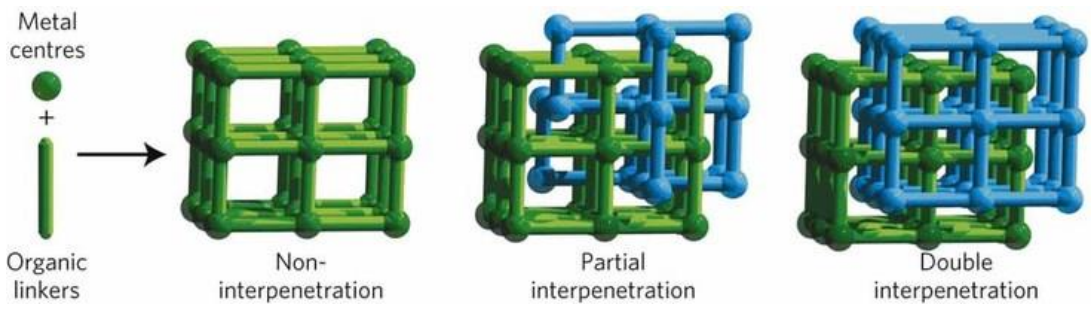

Figure 40 - Schematic demonstrating the idea of a partially interpenetrated MOF. Reprinted with permission from S. Yang *et al.*, *Nat. Mater.*, 2012, 11, 710–716. Copyright 2012 Nature Publishing Group.[250]

3D to 2D structural changes

Some flexible motions can be quite dramatic resulting in a complete change in the structure, and potentially its dimensionality, rather than just changes to the pore shape. A recent paper by Manna *et al*. reporting on the behaviour of $[Cd(L)_3(ClO)_4]$ (L =1,4-bis(4-pyridyl)-2,3-diaza-1,3-butadiene) upon guest removal, is a good demonstration, showing transitions from a 3D porous framework to a 2D sheet structure where the only remaining pore space is filled by the anions.[251] The transition occurs in a SC-SC manner and the structure change can be seen in Figure 41.[251] Similar 3D-to-2D transitions have also been reported for ELM-11 ($[Cu(bpy)(H2O)_2(BF)_2]\cdot bpy$)[252–254] and $[Ag(dpzm)]ClO_4$ (dpzm = di-2-pyrazinylmethane).[255]

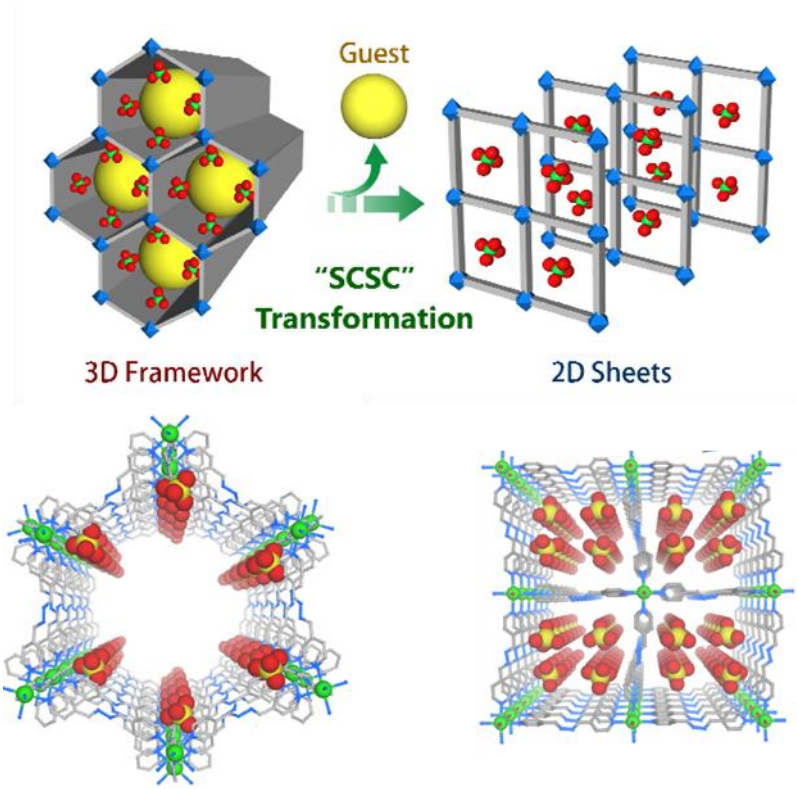

Figure 41 - Single transformation from 3D framework to 2D sheets exhibited by $[Cd(L)_3(ClO)_4]$. Adapted with permission from B. Manna *et al*., *CrystEngComm*, 2015, 17, 1166–1169. Copyright 2015 Royal Society of Chemistry.[251]

Effect of the SBU

The dynamic behaviour exhibited by MOFs can have significant effects on the metal coordination and the secondary building unit; this is best demonstrated by looking at work by Seo *et al*. on solvent removal in the zinc paddlewheel structure $[Zn_2(bdc)_2(L^2)]$ (L^2 = 2,3-difluoro-1,4-bis(4-pyridyl)benzene).[256] The deformation of the framework showed significant effects on the zinc coordination bonds, including the breaking of some Zn–O bonds involving carboxylates bridging

between the two zinc atoms. The framework undergoes a transition from its solvated form to its dried form via two intermediates and then converts to a fifth phase upon rehydration. The effects on the paddlewheel geometry for each of these phases can be seen in Figure 42.[256] Other MOF SBUs have also been similarly studied including CPO-27 (MOF-74)[257] and $[Co(Hoba)_2]\cdot 2H_2O$ (H_2oba = 4,4'-oxybis(benzoic acid)).[258]

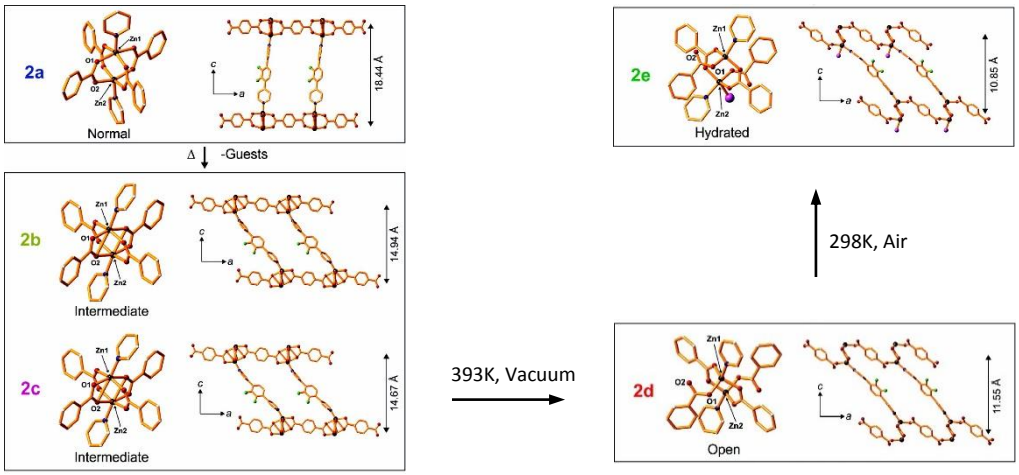

Figure 42 - Structural transformation occurring upon guest removal in $[Zn_2(tp)_2(L^2)]$. Adapted with permission from J. Seo *et al*., *J. Am. Chem. Soc.*, 2011, 133, 9005–9013. Copyright 2011 American Chemical Society[256]

Thermal Expansion

The flexibility of MOFs can also result in very interesting thermal expansion behaviour and work by Omary and co-workers studying the two-step nitrogen isotherm of FMOF-1 $Ag_2[Ag_4\text{-}Tz_6]$ (Tz = 3,5-bis(trifluoromethyl)-1,2,4-triazolate) (shown in Figure 43 a) demonstrates the significant differences observed upon cooling a sample in a nitrogen stream *vs* in a vacuum sealed capillary (Figure 43 b).[259, 260] The sample cooled while under vacuum follows standard positive thermal expansion behaviour but the sample under nitrogen exhibits much more significant changes and a reversal to negative thermal expansion behaviour below 119 K. This is shown to be correlated to the location of the N_2 gas molecules in the framework, and changes in the materials structure during its two-step breathing process.[260]

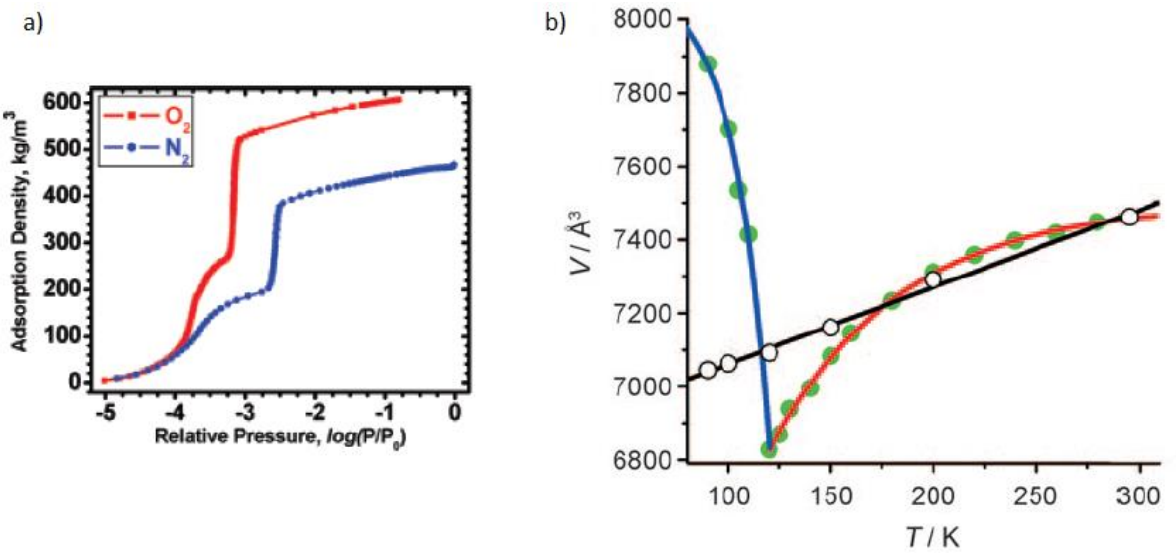

Figure 43 - a) Adsorption data for O_2 and N_2 uptake in FMOF-1, b) thermal expansion behaviour of FMOF-1 under vacuum (white circles) and under N_2 (green circles). Adapted with permission from C. Yang *et al.*, *J. Am. Chem. Soc.*, 2007, 129, 15454–15455 and C. Yang *et al.*, *Angew. Chem. Int. Ed.*, 2009, 48, 2500–2505. Copyright 2007 American Chemical Society and 2009 John Wiley and Sons.[259, 260]

1.8.4 Response to Guests

So far the dynamic responses shown for various metal-organic frameworks have mainly been due to transitions between different crystalline forms upon solvent removal or guest uptake, such as the narrow- to large-pore transitions seen in gas loading of MIL-53, the gating seen in ZIF-8 or the interpenetration shifts in [Cu(dhbc)$_2$(4,4'-bpy)], but many flexible MOFs also show a high responsiveness when being soaked in different guest solutions. These changes arise due to an induced accommodation of differing guest molecules and can be large or quite subtle changes. [Fe(pydc)(4,4'-bipy)][261], [Co$_2$(ma)(ina)] (ma = Malate, ina = isonicotinate)[262] , [Co(5-NH$_2$-bdc)(bpy)$_{0.5}$(H$_2$O)][263], [Zn(PNMI)] (PNMI = N-(4-pyridyl)-1,4,5,8-naphathlenetetracarboxymonoimide)[264] are all examples showing relatively small changes upon incorporation of various alcohols, [Zn$_2$(ndc)$_2$DPNI$_2$] (DPNI = N,N'-di(4-pyridyl)-1,4,5,8-naphthalenetetracarboxydiimide)[265] changes upon adsorption of DMF, *n*-heptanol, nitrobenzene and chloroform and [Cu$_3$(TP)$_4$(N$_3$)$_2$(DMF)$_2$] (TP = 4-tetrazole pyridine) responds to different cyclic organics.[266] The response to different guests offers the possibility of development of a sensor material and [Zn$_2$(bdc)$_2$(dpNDI)] (dpNDI = N,N'-di(4-pyridyl)-1,4,5,8-naphthalenediimide) has been shown to produce reasonable differences in the visible adsorption region for many broadly similar aromatic guests.[267]

Subtle changes upon different guest adsorption are also observed for MIL-53 despite it being well known for its narrow-to-large pore transitions; loading MIL-53 Fe with guests, even dropwise, was observed to result in a distinct transition to a guest-loaded MOF at a particular pore opening. This

pore opening does not seem to have to be fully open or even correspond to one of the phases upon normal desolvation or CO_2 uptake. Figure 44 shows the response of MIL-53(Fe) to various guests compared to the theoretical evolution of volume *vs* the ratios of the pore dimensions.[145, 268] The data match well and suggest that different solvents / guests, presumably due to the interaction strengths, result in a different degree of pore opening along what is a potentially a continuum of different structures. It could be envisaged that by picking a suitable guest any point along the theoretical evolution trend line could be achieved. Immersion of MIL-53(Fe) in any of the solvents was observed to result in immediate full exchange and structural transition, but by introducing the solvent dropwise into hydrated MIL-53 in water, and monitoring using synchrotron radiation, a kinetic study was achieved.[145, 268] In almost all cases only Bragg reflections of the hydrated and final solvated phase were observed, with only the relative intensities of the two phases and not the peak positions seen to change over time. This implied definitive transitions due to a stepwise motion. Light alcohols such as ethanol and methanol were however shown not to completely follow this pattern with intermediate transient phases being observed that both match the theoretical volume evolution curve and show a slow movement over time.[145, 268] The intermediates are suggested to arise due to hydrogen bonding with water-alcohol mixtures, but might be a suggestion of continual structural evolution under certain conditions rather than a stepwise motion.

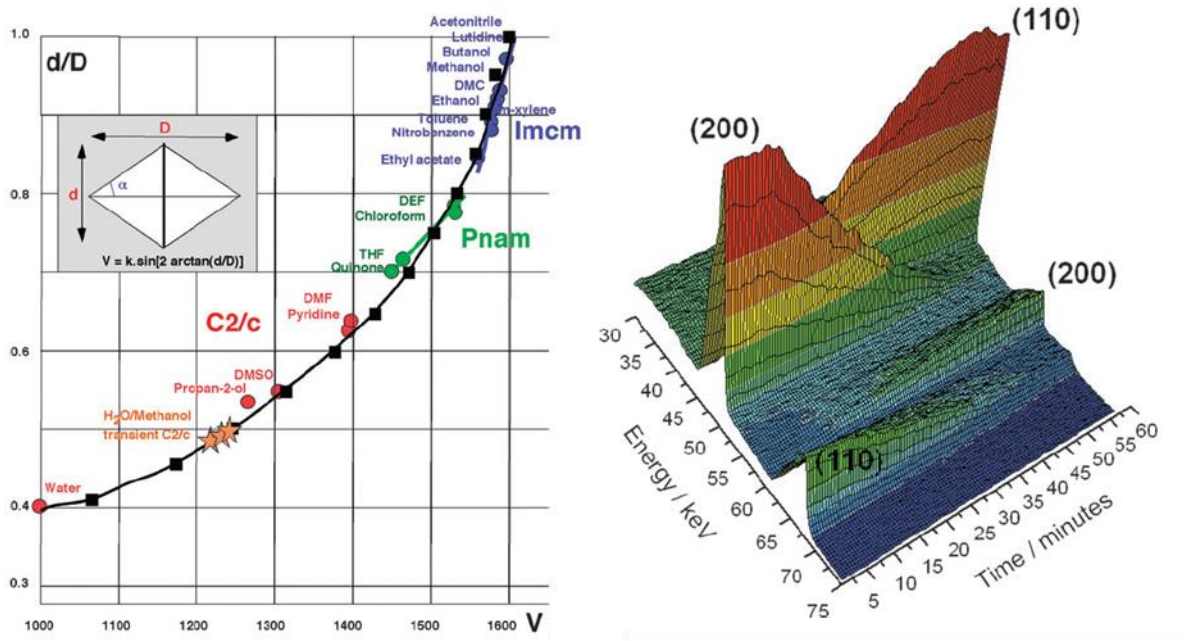

Figure 44 – Left, comparisons between the differing fully solvent exchanged frameworks (coloured circles) and the theoretical evolution of volume *vs* the ratio of pore dimensions in Fe-MIL-53 (black line). Orange stars refer to transient phases for methanol uptake at 0, 25 and 40 minutes. Right, the evolution of powder diffraction patterns during the dropwise additions on lutidine. Adapted with permission from G. Férey and C. Serre, *Chem. Soc. Rev.*, 2009, 38, 1380–1399. Copyright 2009 Royal Society of Chemistry[268]

Other flexible MOFs show similar behaviour where a continuum of structures might potentially be accessible for different solvents. MCF-18 ($[M_3(\mu\text{-}OH)(L)_3]$ (L = 2,6-di-p-carboxyphenyl-4-4'-bipyridine)[269] and $[In_2(OH)_2(obb)_2]$ (obb = 4,4'-oxybis(benzoate)) [270] are good examples, and Figure 45 shows the seemingly continual changes observed in the powder diffraction pattern upon loading of different guests in MCF-18.[269] This kind of analysis is particularly relevant for frameworks such as MCF-18 where the flexibility does not result in any change to the symmetry of the material.

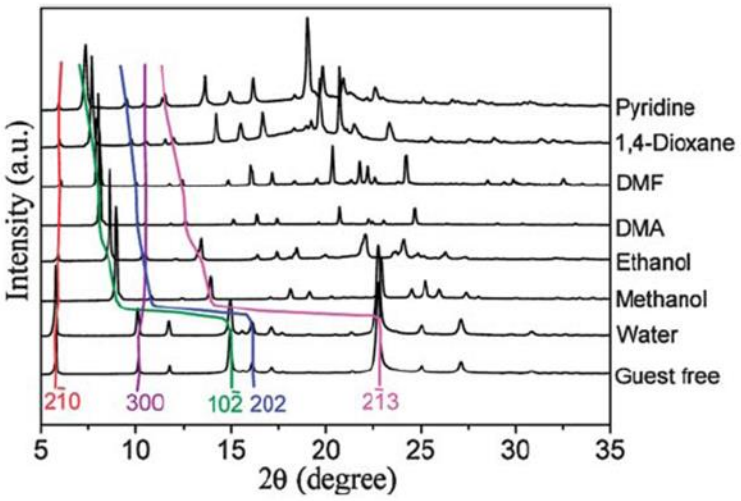

Figure 45 - Structural evolution of MCF-18 upon adsorption of different guests. Adapted with permission from Y. S. Wei *et al.*, *Chem. Sci.*, 2013, 4, 1539-1546. Copyright 2013 Royal Society of Chemistry.[269]

Although these MOFs provide the potential for accessing a range of structures by adsorption of different solvents, with the exception of alcohol adsorption in MIL-53, the changes occur through defined phase transitions to the fully loaded structure. It is very rare for MOFs to show continuous changes upon loss or adsorption of one particular guest. MIL-88 is the prototypical example of this kind of continuous behaviour, showing a continual evolution of its powder pattern upon loss and re-adsorption of water (see Figure 46).[271] The flexibility in MIL-88 is very impressive, showing huge guest-dependent structural changes with increases of up to 170% in its unit cell volume, for certain versions of the MOF.[272] These are some of, if not the largest, transitions seen in flexible frameworks to date, but unfortunately the crystallinity of the material upon desolvation was not sufficient for structural determinations directly from crystallography, and computational methods were required to help model the structure, limiting the ease/efficiency of many *in situ* diffraction studies. Similarly, the variable-temperature powder patterns (Figure 46) only hint at the continuousness of the process and do not provide definitive evidence that the "swelling" mode can give access to all of the breathing range. While MIL-88 has been subject to several further studies including changes to the

metal centre[128, 273] and modification to the organic linker[274], little is still understood about its rare breathing effect, and not much is reported on the effect of adsorption of gases.[52, 128] Similarly, while other frameworks, such as NOTT-202, have also shown some evidence of a continuous structural flexing, in this case only on adsorption of CO_2 below the triple point of the gas, the relative volume changes are quite low (≈2%) and the motion is not well characterised.[250]

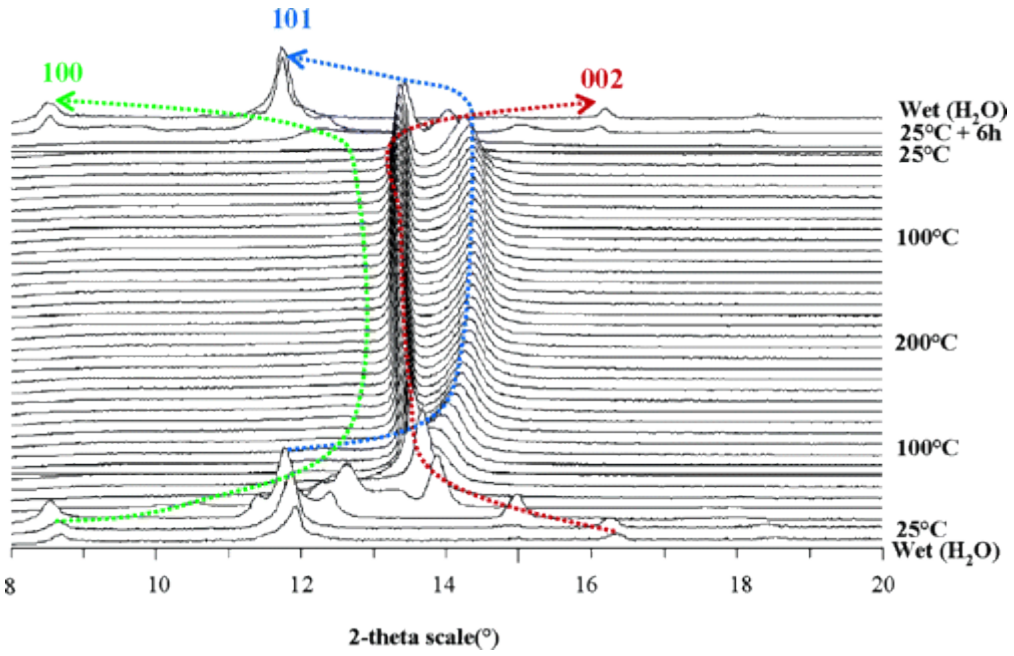

Figure 46 - Variable temperature X-ray diffraction patterns of MIL-88A showing the structural effect of loss and gain of water molecules. Reprinted with permission from C. Mellot-Draznieks *et al.*, *J. Am. Chem. Soc.*, 2005, 127, 16273–16278. Copyright 2005 American Chemical Society.[271]

To advance this field a framework showing a large clear continuous breathing effect upon loading of guests needs to be developed, ideally one which can be easily characterised through crystallographic methods, so the structural evolution can be easily monitored, and one which can be modified to change the various interactions responsible for the effects. By comparing this framework to others such as MIL-69 and DUT-4 (the same framework [Al(OH)(ndc)] in narrow- and large-pore forms that cannot be interconverted)[275] along with previous analysis by Férey and Serre on the rules and consequences of breathing,[268] an understanding of the thermodynamic barriers of the flexibility of MOFs can be developed, which will hopefully lead to the design of new frameworks with tunable properties.

1.9 Conclusions

This chapter has shown that a wide range of different metal-organic frameworks (MOFs) have so far been published in the scientific literature, demonstrating the large structural diversity present in the field. The differences between various MOF designs / topologies have led to significant changes to the porosity, gas uptake and other desirable properties of these materials, which can be refined using additional synthetic modifications. The structures of MOFs can be highly dynamic, responding to guest removal and external stimuli in differing ways, and understanding these flexible motions is an important task for the tailoring of MOFs for specific applications. *In situ* crystallographic characterisation can be of particular use in understanding these behaviours, especially when used to monitor changes under operation conditions. The current literature on dynamic frameworks is dominated by MOFs which exhibit step changes through defined phase transformations and very little is currently known regarding MOFs which display continuous motions. This is therefore an area which should be expanded to increase the understanding in the field and maximise the benefit of stimuli responsive MOFs.

1.10 References

1 O. M. Yaghi and H. Li, *J. Am. Chem. Soc.*, 1995, 117, 10401–10402.

2 J. L. C. Rowsell and O. M. Yaghi, *Microporous Mesoporous Mater.*, 2004, 73, 3–14.

3 C. Janiak, *Dalton. Trans.*, 2003, 2781-2804.

4 K. Biradha, A. Ramanan, and J. J. Vittal, *Cryst. Growth Des.*, 2009, 9, 2969–2970.

5 S. R. Batten, N. R. Champness, X.-M. Chen, J. Garcia-Martinez, S. Kitagawa, L. Öhrström, M. O'Keeffe, M. P. Suh, and J. Reedijk, *CrystEngComm*, 2012, 14, 3001-3004.

6 S. M. Palmer, J. M. Stanton, B. M. Hoffman, and J. A. Ibers, *Inorg. Chem.*, 1986, 25, 2296–2300.

7 B. F. Hoskins and R. Robson, *J. Am. Chem. Soc.*, 1989, 111, 5962–5964.

8 B. F. Hoskins and R. Robson, *J. Am. Chem. Soc.*, 1990, 112, 1546–1554.

9 M. Kondo, T. Yoshitomi, H. Matsuzaka, S. Kitagawa, and K. Seki, *Angew. Chem. Int. Ed.*, 1997, 36, 1725–1727.

10 H. Li, M. Eddaoudi, M. O'Keeffe, and O. Yaghi, *Nature.*, 1999, 402, 276–279.

11 S. S. Chui, *Science.*, 1999, 283, 1148–1150.

12 C. Serre, F. Millange, C. Thouvenot, M. Noguès, G. Marsolier, D. Louër, and G. Férey, *J. Am. Chem. Soc.*, 2002, 124, 13519–13526.

13 Y. Tian, C. Cai, Y. Ji, X. You, S. Peng, and G. Lee, *Angew. Chem. Int. Ed.*, 2002, 41, 1384–1386.

14 K. S. Park, Z. Ni, A. P. Côté, J. Y. Choi, R. Huang, F. J. Uribe-Romo, H. K. Chae, M. O'Keeffe, and O. M. Yaghi, *Proc. Natl. Acad. Sci. U. S. A.*, 2006, 103, 10186–10191.

15 D. N. Dybtsev, H. Chun, and K. Kim, *Angew. Chem. Int. Ed.*, 2004, 43, 5033–5036.

16 J. H. Cavka, S. Jakobsen, U. Olsbye, N. Guillou, C. Lamberti, S. Bordiga, and K. P. Lillerud, *J. Am. Chem. Soc.*, 2008, 130, 13850–13851.

17 S. Øien, D. Wragg, H. Reinsch, S. Svelle, S. Bordiga, C. Lamberti, and K. P. Lillerud, *Cryst. Growth Des.*, 2014, 14, 5370–5372.

18 A. Schaate, P. Roy, A. Godt, J. Lippke, F. Waltz, M. Wiebcke, and P. Behrens, *Chem. Euro. J.*, 2011, 17, 6643–6651.

19 M. Eddaoudi, J. Kim, N. Rosi, D. Vodak, J. Wachter, M. O'Keeffe, and O. M. Yaghi, *Science*, 2002, 295, 469–472.

20 A. D. Burrows, K. Cassar, R. M. W. Friend, M. F. Mahon, S. P. Rigby, and J. E. Warren, *CrystEngComm*, 2005, 7, 548-550.

21 H. Chun and J. Moon, *Inorg. Chem.*, 2007, 46, 4371–4373.

22 N. Stock and S. Biswas, *Chem. Rev.*, 2012, 112, 933–969.

23 M. O'Keeffe and O. M. Yaghi, *Chem. Rev.*, 2012, 112, 675–702.

24 K. K. Tanabe and S. M. Cohen, *Chem. Soc. Rev.*, 2011, 40, 498–519.

25 S. M. Cohen, *Chem. Rev.*, 2012, 112, 970–1000.

26 Y.-X. Tan, Y.-P. He, and J. Zhang, *Inorg. Chem.*, 2012, 51, 9649–9654.

27 U. Mueller, M. Schubert, F. Teich, H. Puetter, K. Schierle-Arndt, and J. Pastré, *J. Mater. Chem.*, 2006, 16, 626-636.

28 D. M. D'Alessandro, B. Smit, and J. R. Long, *Angew. Chem. Int. Ed.*, 2010, 49, 6058–6082.

29 J. R. Li, Y. Ma, M. C. McCarthy, J. Sculley, J. Yu, H.-K. Jeong, P. B. Balbuena, and H.-C. Zhou, *Coord. Chem. Rev.*, 2011, 255, 1791–1823.

30 Q. Wang, J. Luo, Z. Zhong, and A. Borgna, *Energy Environ. Sci.*, 2011, 4, 42-55.

31 K. Sumida, D. L. Rogow, J. A Mason, T. M. McDonald, E. D. Bloch, Z. R. Herm, T.-H. Bae, and J. R. Long, *Chem. Rev.*, 2012, 112, 724–781.

32 M. P. Suh, H. J. Park, T. K. Prasad, and D.-W. Lim, *Chem. Rev.*, 2012, 112, 782–835.

33 J. Liu, P. K. Thallapally, B. P. McGrail, D. R. Brown, and J. Liu, *Chem. Soc. Rev.*, 2012, 41, 2308–2322.

34 Y. Liu, Z. U. Wang, and H. Zhou, *Greenh. Gases Sci. Technol.*, 2012, 2, 239–259.

35 L. E. Kreno, K. Leong, O. K. Farha, M. Allendorf, R. P. Van Duyne, and J. T. Hupp, *Chem. Rev.*, 2012, 112, 1105–1125.

36 P. Horcajada, R. Gref, T. Baati, P. K. Allan, G. Maurin, P. Couvreur, G. Férey, R. E. Morris, and C. Serre, *Chem. Rev.*, 2012, 112, 1232–1268.

37 M. Yoon, R. Srirambalaji, and K. Kim, *Chem. Rev.*, 2012, 112, 1196–1231.

38 A. Bétard and R. A. Fischer, *Chem. Rev.*, 2012, 112, 1055–1083.

39 IPCC, 2013: Summary for Policymakers. In: *Climate Change 2013: the Physical Science Basis*. C*ontribution of Working Group I to the fifth Asessment Report of the Intergovernmental Panel on Climate Change*, T. F. Stocker, D. Qin, G.-K. Plattner, M. Tignor, S.K. Allen, J. Boschung, A. Nauels, Y. Xia, V. Bex, and P. M. Midgley

40 *Climate Change Act 2008*, Legislation.gov.uk, website accessed 2012.

41 Department of Energy and Climate UK, *Annual Statement of Emissions for 2012*.

42 H.-C. Zhou, J. R. Long, and O. M. Yaghi, *Chem. Rev.*, 2012, 112, 673–674.

43 A. R. Millward and O. M. Yaghi, *J. Am. Chem. Soc.*, 2005, 127, 17998–17999.

44 A. J. Fletcher, K. M. Thomas, and M. J. Rosseinsky, *J. Solid State Chem.*, 2005, 178, 2491–2510.

45 J. R. Li, J. Sculley, and H. C. Zhou, *Chem. Rev.*, 2012, 112, 869–932.

46 S. D. Burd, S. Ma, J. A. Perman, B. J. Sikora, R. Q. Snurr, P. K. Thallapally, J. Tian, L. Wojtas, and M. J. Zaworotko, *J. Am. Chem. Soc.*, 2012, 134, 3663–3666.

47 D. Britt, H. Furukawa, B. Wang, T. G. Glover, and O. M. Yaghi, *Proc. Natl. Acad. Sci. U. S. A.*, 2009, 106, 20637–20640.

48 S. R. Caskey, A. G. Wong-Foy, and A. J. Matzger, *J. Am. Chem. Soc.*, 2008, 130, 10870–10871.

49 N. L. Rosi, J. Eckert, M. Eddaoudi, D. T. Vodak, J. Kim, M. O'Keeffe, and O. M. Yaghi, *Science*, 2003, 300, 1127–1129.

50 P. Kanoo, S. K. Reddy, G. Kumari, R. Haldar, C. Narayana, S. Balasubramanian, and T. K. Maji, *Chem. Commun.*, 2012, 48, 8487–8589.

51 G. Kumari, K. Jayaramulu, T. K. Maji, and C. Narayana, *J. Phys. Chem. A*, 2013, 117, 11006–11102.

52 a. C. McKinlay, J. F. Eubank, S. Wuttke, B. Xiao, P. S. Wheatley, P. Bazin, J.-C. Lavalley, M. Daturi, A. Vimont, G. De Weireld, P. Horcajada, C. Serre, and R. E. Morris, *Chem. Mater.*, 2013, 25, 1592–1599.

53 A. D. Wiersum, E. Soubeyrand-Lenoir, Q. Yang, B. Moulin, V. Guillerm, M. Ben Yahia, S. Bourrelly, A. Vimont, S. Miller, C. Vagner, M. Daturi, G. Clet, C. Serre, G. Maurin, and P. L. Llewellyn, *Chem. Asian J.*, 2011, 6, 3270–3280.

54 F. Gul-E-Noor, M. Mendt, D. Michel, A. Pöppl, H. Krautscheid, J. Haase, and M. Bertmer, *J. Phys. Chem. C*, 2013, 117, 7703–7712.

55 A. A. Amaro and K. Seff, *J. Phys. Chem.*, 1973, 77, 906–910.

56 P. E. Riley and K. Seff, *J. Am. Chem. Soc.*, 1973, 95, 8180–8182.

57 P. E. Riley and K. Seff, *Inorg. Chem.*, 1974, 13, 1355–1360.

58 P. E. Riley, K. B. Kunz, and K. Seff, *J. Am. Chem. Soc.*, 1975, 97, 537–542.

59 R. Kitaura, S. Kitagawa, Y. Kubota, T. C. Kobayashi, K. Kindo, Y. Mita, A. Matsuo, M. Kobayashi, H.-C. Chang, T. C. Ozawa, M. Suzuki, M. Sakata, and M. Takata, *Science*, 2002, 298, 2358–2361.

60 M. Takata, B. Umeda, E. Nishibori, M. Sakata, Y. Saitot, M. Ohno, and H. Shinohara, *Nature*, 1995, 377, 46–49.

61 M. Takata, E. Nishibori, and M. Sakata, *Z. Kristallogr.*, 2001, 216, 71–86.

62 H. Tanaka, M. Takata, E. Nishibori, K. Kato, T. Iishi, and M. Sakata, *J. Appl. Crystallogr.*, 2002, 35, 282–286.

63 M. Takata, *Acta Crystallogr. A.*, 2008, 64, 232–245.

64 R. Kitaura, R. Matsuda, Y. Kubota, S. Kitagawa, M. Takata, T. C. Kobayashi, and M. Suzuki, *J. Phys. Chem. B*, 2005, 109, 23378–23385.

65 Y. Kubota, M. Takata, R. Matsuda, R. Kitaura, S. Kitagawa, K. Kato, M. Sakata, and T. C. Kobayashi, *Angew. Chem. Int. Ed.*, 2005, 44, 920–923.

66 Y. Kubota, M. Takata, R. Matsuda, R. Kitaura, S. Kitagawa, and T. C. Kobayashi, *Angew. Chem. Int. Ed. Engl.*, 2006, 45, 4932–4936.

67 Y. Kubota, M. Takata, T. Kobayashi, and S. Kitagawa, *Coord. Chem. Rev.*, 2007, 251, 2510–2521.

68 R. Matsuda, R. Kitaura, S. Kitagawa, Y. Kubota, R. V Belosludov, T. C. Kobayashi, H. Sakamoto, T. Chiba, M. Takata, Y. Kawazoe, and Y. Mita, *Nature*, 2005, 436, 238–241.

69 J. L. C. Rowsell, E. C. Spencer, J. Eckert, J. a K. Howard, and O. M. Yaghi, *Science*, 2005, 309, 1350–1354.

70 E. C. Spencer, J. a K. Howard, G. J. McIntyre, J. L. C. Rowsell, and O. M. Yaghi, *Chem. Commun.*, 2006, 278–280.

71 T. Yildirim and M. Hartman, *Phys. Rev. Lett.*, 2005, 95, 215504.

72 J. L. C. Rowsell, J. Eckert, and O. M. Yaghi, *J. Am. Chem. Soc.*, 2005, 127, 14904–14910.

73 S. R. Miller, P. a Wright, T. Devic, C. Serre, G. Férey, P. L. Llewellyn, R. Denoyel, L. Gaberova, and Y. Filinchuk, *Langmuir*, 2009, 25, 3618–3626.

74 J.-P. Zhang and X.-M. Chen, *J. Am. Chem. Soc.*, 2009, 131, 5516–5521.

75 H. Wu, W. Zhou, and T. Yildirim, *J. Am. Chem. Soc.*, 2007, 129, 5314–535.

76 H. Wu, W. Zhou, and T. Yildirim, *J. Phys. Chem. C*, 2009, 113, 3029–3035.

77 E. J. Carrington, I. J. Vitórica-Yrezábal, and L. Brammer, *Acta Crystallogr. Sect. B Struct. Sci. Cryst. Eng. Mater.*, 2014, 70, 1–19.

78 B. Arstad, H. Fjellvåg, K. O. Kongshaug, O. Swang, and R. Blom, *Adsorption*, 2008, 14, 755–762.

79 R. Vaidhyanathan, S. S. Iremonger, K. W. Dawson, and G. K. H. Shimizu, *Chem. Commun.*, 2009, 5230–5232.

80 R. Vaidhyanathan, S. S. Iremonger, G. K. H. Shimizu, P. G. Boyd, S. Alavi, and T. K. Woo, *Science*, 2010, 330, 650–653.

81 J.-B. Lin, W. Xue, J.-P. Zhang, and X.-M. Chen, *Chem. Commun. (Camb).*, 2011, 47, 926–928.

82 P.-Q. Liao, D.-D. Zhou, A.-X. Zhu, L. Jiang, R.-B. Lin, J.-P. Zhang, and X.-M. Chen, *J. Am. Chem. Soc.*, 2012, 134, 17380–17383.

83 S. Yang, J. Sun, A. J. Ramirez-Cuesta, S. K. Callear, W. I. F. David, D. P. Anderson, R. Newby, A. J. Blake, J. E. Parker, C. C. Tang, and M. Schröder, *Nat. Chem.*, 2012, 4, 887–894.

84 P. D. C. Dietzel, R. E. Johnsen, H. Fjellvåg, S. Bordiga, E. Groppo, S. Chavan, and R. Blom, *Chem. Commun.*, 2008, 2, 5125–5127.

85 H. Wu, J. M. Simmons, G. Srinivas, W. Zhou, and T. Yildirim, *J. Phys. Chem. Lett.*, 2010, 1, 1946–1951.

86 W. L. Queen, C. M. Brown, D. K. Britt, P. Zajdel, M. R. Hudson, and O. M. Yaghi, *J. Phys. Chem. C*, 2011, 115, 24915–24919.

87 A. C. McKinlay, B. Xiao, D. S. Wragg, P. S. Wheatley, I. L. Megson, and R. E. Morris, *J. Am. Chem. Soc.*, 2008, 130, 10440–10444.

88 P. K. Allan, P. S. Wheatley, D. Aldous, M. I. Mohideen, C. Tang, J. a Hriljac, I. L. Megson, K. W. Chapman, G. De Weireld, S. Vaesen, and R. E. Morris, *Dalton Trans.*, 2012, 41, 4060–4066.

89 M. Dincă, A. Dailly, Y. Liu, C. M. Brown, D. a Neumann, and J. R. Long, *J. Am. Chem. Soc.*, 2006, 128, 16876–83.

90 M. Dincă, W. S. Han, Y. Liu, A. Dailly, C. M. Brown, and J. R. Long, *Angew. Chem. Int. Ed.,* 2007, 46, 1419–1422.

91 V. K. Peterson, Y. Liu, C. M. Brown, and C. J. Kepert, *J. Am. Chem. Soc.*, 2006, 128, 15578–15579.

92 V. K. Peterson, C. M. Brown, Y. Liu, and C. J. Kepert, *J. Phys. Chem. C*, 2011, 115, 8851–8857.

93 H. Wu, J. M. Simmons, Y. Liu, C. M. Brown, X.-S. Wang, S. Ma, V. K. Peterson, P. D. Southon, C.

J. Kepert, H.-C. Zhou, T. Yildirim, and W. Zhou, *Chem. Eur. J*, 2010, 16, 5205–5214.

94 J. Getzschmann, I. Senkovska, D. Wallacher, M. Tovar, D. Fairen-Jimenez, T. Düren, J. M. van Baten, R. Krishna, and S. Kaskel, *Microporous Mesoporous Mater.*, 2010, 136, 50–58.

95 Z. Hulvey, K. V. Lawler, Z. Qiao, J. Zhou, D. Fairen-Jimenez, R. Q. Snurr, S. V. Ushakov, A. Navrotsky, C. M. Brown, and P. M. Forster, *J. Phys. Chem. C*, 2013, 117, 20116–20126.

96 Z. Wang and S. M. Cohen, *J. Am. Chem. Soc.*, 2007, 129, 12368–12369.

97 Z. Wang and S. M. Cohen, *Angew. Chem. Int. Ed.*, 2008, 47, 4699–4702.

98 S. J. Garibay, Z. Wang, K. K. Tanabe, and S. M. Cohen, *Inorg. Chem.*, 2009, 48, 7341–7349.

99 D. Britt, C. Lee, F. J. Uribe-Romo, H. Furukawa, and O. M. Yaghi, *Inorg. Chem.*, 2010, 49, 6387–6389.

100 A. D. Burrows and L. L. Keenan, *CrystEngComm*, 2012, 14, 4112-4114.

101 T. Gadzikwa, O. K. Farha, K. L. Mulfort, J. T. Hupp, and S. T. Nguyen, *Chem. Commun.*, 2009, 3720–3722.

102 Z. Wang, K. K. Tanabe, and S. M. Cohen, *Inorg. Chem.*, 2009, 48, 296–306.

103 S. J. Garibay and S. M. Cohen, *Chem. Commun..*, 2010, 46, 7700–7702.

104 M. Kandiah, S. Usseglio, S. Svelle, U. Olsbye, K. P. Lillerud, and M. Tilset, *J. Mater. Chem.*, 2010, 20, 9848-9851.

105 M. Kim, S. J. Garibay, and S. M. Cohen, *Inorg. Chem.*, 2011, 50, 729–731.

106 S. J. Garibay, Z. Wang, and S. M. Cohen, *Inorg. Chem.*, 2010, 49, 8086–91.

107 S. Bernt, V. Guillerm, C. Serre, and N. Stock, *Chem. Commun.*, 2011, 47, 2838–2840.

108 J. Canivet, S. Aguado, G. Bergeret, and D. Farrusseng, *Chem. Commun.*, 2011, 47, 11650–11652.

109 T. Ahnfeldt, D. Gunzelmann, J. Wack, J. Senker, and N. Stock, *CrystEngComm*, 2012, 14, 4126-4136.

110 J. Kim, D. O. Kim, D. W. Kim, J. Park, and M. S. Jung, *Inorg. Chim. Acta*, 2012, 390, 22–25.

111 P. Roy, A. Schaate, P. Behrens, and A. Godt, *Chem. Eur. J.*, 2012, 18, 6979–6985.

112 K. Hindelang, S. I. Vagin, C. Anger, and B. Rieger, *Chem. Commun.*, 2012, 48, 2888–2890.

113 Y. K. Hwang, D.-Y. Hong, J.-S. Chang, S. H. Jhung, Y.-K. Seo, J. Kim, A. Vimont, M. Daturi, C. Serre, and G. Férey, *Angew. Chem. Int. Ed.*, 2008, 47, 4144–4148.

114 A. Demessence, D. M. D'Alessandro, M. L. Foo, and J. R. Long, *J. Am. Chem. Soc.*, 2009, 131, 8784–8786.

115 M. Kim, J. F. Cahill, H. Fei, K. a Prather, and S. M. Cohen, *J. Am. Chem. Soc.*, 2012, 134, 18082–18088.

116 J. Tian, L. V. Saraf, B. Schwenzer, S. M. Taylor, E. K. Brechin, J. Liu, S. J. Dalgarno, and P. K. Thallapally, *J. Am. Chem. Soc.*, 2012, 134, 9581–9584.

117 A. Schneemann, V. Bon, I. Schwedler, I. Senkovska, S. Kaskel, and R. A. Fischer, *Chem. Soc. Rev.*, 2014, 43, 6062–6096.

118 T. Loiseau, C. Serre, C. Huguenard, G. Fink, F. Taulelle, M. Henry, T. Bataille, and G. Férey, *Chem. Eur. J.*, 2004, 10, 1373–1382.

119 M. Henry, *ChemPhysChem*, 2002, 561.

120 M. Henry, *ChemPhysChem*, 2002, 607.

121 S. Bourrelly, P. L. Llewellyn, C. Serre, F. Millange, T. Loiseau, and G. Férey, *J. Am. Chem. Soc.*, 2005, 127, 13519–13521.

122 P. L. Llewellyn, S. Bourrelly, C. Serre, Y. Filinchuk, and G. Férey, *Angew. Chem. Int. Ed.*, 2006, 45, 7751–7754.

123 C. Serre, S. Bourrelly, A. Vimont, N. A. Ramsahye, G. Maurin, P. L. Llewellyn, M. Daturi, Y. Filinchuk, O. Leynaud, P. Barnes, and G. Férey, *Adv. Mater.*, 2007, 19, 2246–2251.

124 F. Millange, N. Guillou, R. I. Walton, J.-M. Grenèche, I. Margiolaki, and G. Férey, *Chem. Commun.*, 2008, 4732-4734.

125 C. Volkringer, T. Loiseau, N. Guillou, G. Férey, E. Elkaïm, and A. Vimont, *Dalton. Trans.*, 2009, 53, 2241-2249.

126 P. Serra-Crespo, E. Gobechiya, E. V Ramos-Fernandez, J. Juan-Alcañiz, A. Martinez-Joaristi, E. Stavitski, C. E. A Kirschhock, J. A Martens, F. Kapteijn, and J. Gascon, *Langmuir*, 2012, 28, 12916–12922.

127 G. Xu, X. Zhang, P. Guo, C. Pan, H. Zhang, and C. Wang, *J. Am. Chem. Soc.*, 2010, 132, 3656–3657.

128 J. P. S. Mowat, S. R. Miller, A. M. Z. Slawin, V. R. Seymour, S. E. Ashbrook, and P. a. Wright, *Microporous Mesoporous Mater.*, 2011, 142, 322–333.

129 A. S. Munn, G. J. Clarkson, and R. I. Walton, *Acta Crystallogr. Sect. B Struct. Sci. Cryst. Eng. Mater.*, 2014, 70, 11–18.

130 F. Nouar, T. Devic, H. Chevreau, N. Guillou, E. Gibson, G. Clet, M. Daturi, A. Vimont, J. M. Grenèche, M. I. Breeze, R. I. Walton, P. L. Llewellyn, and C. Serre, *Chem. Commun.*, 2012, 48, 10237-10239.

131 M. I. Breeze, G. Clet, B. C. Campo, A. Vimont, M. Daturi, J. M. Grenèche, A. J. Dent, F. Millange, and R. I. Walton, *Inorg. Chem.*, 2013, 52, 8171–8182.

132 P. L. Llewellyn, P. Horcajada, G. Maurin, T. Devic, N. Rosenbach, S. Bourrelly, C. Serre, D. Vincent, S. Loera-Serna, Y. Filinchuk, and G. Férey, *J. Am. Chem. Soc.*, 2009, 131, 13002–12008.

133 S. Bourrelly, P. L. Llewellyn, C. Serre, F. Millange, T. Loiseau, and G. Férey, *J. Am. Chem. Soc.*, 2005, 127, 13519–13521.

134 T. K. Trung, P. Trens, N. Tanchoux, S. Bourrelly, P. L. Llewellyn, S. Loera-Serna, C. Serre, T. Loiseau, F. Fajula, and G. Férey, *J. Am. Chem. Soc.*, 2008, 130, 16926–16932.

135 T. K. Trung, I. Déroche, A. Rivera, Q. Yang, P. Yot, N. Ramsahye, S. D. Vinot, T. Devic, P. Horcajada, C. Serre, G. Maurin, and P. Trens, *Microporous Mesoporous Mater.*, 2011, 140, 114–119.

136 P. L. Llewellyn, G. Maurin, T. Devic, S. Loera-Serna, N. Rosenbach, C. Serre, S. Bourrelly, P. Horcajada, Y. Filinchuk, and G. Férey, *J. Am. Chem. Soc.*, 2008, 130, 12808–12814.

137 N. Guillou, S. Bourrelly, P. L. Llewellyn, R. I. Walton, and F. Millange, *CrystEngComm*, 2015, 17, 422–429.

138 L. Chen, J. P. S. Mowat, D. Fairen-Jimenez, C. A. Morrison, S. P. Thompson, P. A. Wright, and T. Düren, *J. Am. Chem. Soc.*, 2013, 135, 15763–15773.

139 L. Hamon, P. L. Llewellyn, T. Devic, A. Ghoufi, G. Clet, V. Guillerm, G. D. Pirngruber, G. Maurin, C. Serre, G. Driver, W. van Beek, E. Jolimaître, A. Vimont, M. Daturi, and G. Férey, *J. Am. Chem. Soc.*, 2009, 131, 17490–17499.

140 P. Rallapalli, K. P. Prasanth, D. Patil, R. S. Somani, R. V. Jasra, and H. C. Bajaj, *J. Porous Mater.*, 2011, 18, 205–210.

141 L. Hamon, C. Serre, T. Devic, T. Loiseau, F. Millange, G. Férey, and G. De Weireld, *J. Am. Chem. Soc.*, 2009, 131, 8775–8777.

142 L. Hamon, H. Leclerc, A. Ghoufi, L. Oliviero, A. Travert, J. Lavalley, T. Devic, C. Serre, G. Férey, G. De Weireld, A. Vimont, and G. Maurin, *J. Phys. Chem. C*, 2011, 115, 2047–2056.

143 S. Bourrelly, B. Moulin, A. Rivera, G. Maurin, S. Devautour-Vinot, C. Serre, T. Devic, P. Horcajada, A. Vimont, G. Clet, M. Daturi, J. C. Lavalley, S. Loera-Serna, R. Denoyel, P. L. Llewellyn, and G. Férey, *J. Am. Chem. Soc.*, 2010, 132, 9488–9498.

144 R. I. Walton, A. S. Munn, N. Guillou, and F. Millange, *Chem. Eur. J.*, 2011, 17, 7069–7079.

145 F. Millange, C. Serre, N. Guillou, G. Férey, and R. I. Walton, *Angew. Chem. Int. Ed.*, 2008, 47, 4100–4105.

146 F. Millange, N. Guillou, M. E. Medina, G. Férey, A. Carlin-Sinclair, K. M. Golden, and R. I. Walton, *Chem. Mater.*, 2010, 22, 4237–4245.

147 Y. Xiao, T. Han, G. Xiao, Y. Ying, H. Huang, Q. Yang, D. Liu, and C. Zhong, *Langmuir*, 2014, 30, 12229–12235.

148 V. Finsy, C. E. a Kirschhock, G. Vedts, M. Maes, L. Alaerts, D. E. De Vos, G. V. Baron, and J. F. M. Denayer, *Chem. Eur. J.*, 2009, 15, 7724–7731.

149 R. El Osta, A. Carlin-Sinclair, N. Guillou, R. I. Walton, F. Vermoortele, M. Maes, D. de Vos, and F. Millange, *Chem. Mater.*, 2012, 24, 2781–2791.

150 T. Devic, P. Horcajada, C. Serre, F. Salles, G. Maurin, B. Moulin, D. Heurtaux, G. Clet, A. Vimont, J.-M. Grenèche, B. Le Ouay, F. Moreau, E. Magnier, Y. Filinchuk, J. Marrot, J.-C. Lavalley, M. Daturi, and G. Férey, *J. Am. Chem. Soc.*, 2010, 132, 1127–1136.

151 N. A. Ramsahye, T. K. Trung, S. Bourrelly, Q. Yang, T. Devic, G. Maurin, P. Horcajada, P. L.

Llewellyn, P. Yot, C. Serre, Y. Filinchuk, F. Fajula, G. Férey, and P. Trens, *J. Phys. Chem. C*, 2011, 115, 18683–18695.

152 S. Biswas, T. Ahnfeldt, and N. Stock, *Inorg. Chem.*, 2011, 50, 9518–9526.

153 E. Stavitski, E. A Pidko, S. Couck, T. Remy, E. J. M. Hensen, B. M. Weckhuysen, J. Denayer, J. Gascon, and F. Kapteijn, *Langmuir*, 2011, 27, 3970–3976.

154 T. Devic, F. Salles, S. Bourrelly, B. Moulin, G. Maurin, P. Horcajada, C. Serre, A. Vimont, J.-C. Lavalley, H. Leclerc, G. Clet, M. Daturi, P. L. Llewellyn, Y. Filinchuk, and G. Férey, *J. Mater. Chem.*, 2012, 22, 10266-10273.

155 S. Biswas, T. Rémy, S. Couck, D. Denysenko, G. Rampelberg, J. F. M. Denayer, D. Volkmer, C. Detavernier, and P. Van Der Voort, *Phys. Chem. Chem. Phys.*, 2013, 15, 3552-3561.

156 M. Pera-Titus, T. Lescouet, S. Aguado, and D. Farrusseng, *J. Phys. Chem. C*, 2012, 116, 9507–9516.

157 C. Lieder, S. Opelt, M. Dyballa, H. Henning, E. Klemm, and M. Hunger, *J. Phys. Chem. C*, 2010, 114, 16596–16602.

158 M.-A. Springuel-Huet, A. Nossov, Z. Adem, F. Guenneau, C. Volkringer, T. Loiseau, G. Férey, and A. Gédéon, *J. Am. Chem. Soc.*, 2010, 132, 11599–11607.

159 Y. Liu, J.-H. Her, A. Dailly, A. J. Ramirez-Cuesta, D. a. Neumann, and C. M. Brown, *J. Am. Chem. Soc.*, 2008, 130, 11813–11818.

160 A. S. Munn, A. J. Ramirez-Cuesta, F. Millange, and R. I. Walton, *Chem. Phys.*, 2013, 427, 30–37.

161 F. Salles, H. Jobic, A. Ghoufl, P. L. Llewellyn, C. Serre, S. Bourrelly, G. Férey, and G. Maurin, *Angew. Chem. Int. Ed.*, 2009, 48, 8335–8339.

162 F. Salles, S. Bourrelly, H. Jobic, T. Devic, V. Guillerm, P. Llewellyn, C. Serre, G. Ferey, and G. Maurin, *J. Phys. Chem. C*, 2011, 115, 10764–10776.

163 S. Couck, T. Rémy, G. V Baron, J. Gascon, F. Kapteijn, and J. F. M. Denayer, *Phys. Chem. Chem. Phys.*, 2010, 12, 9413-9418.

164 S. Devautour-Vinot, G. Maurin, F. Henn, C. Serre, T. Devic, and G. Férey, *Chem. Commun.*, 2009, 47, 2733–2735.

165 N. Rosenbach, A. Ghoufi, I. Déroche, P. L. Llewellyn, T. Devic, S. Bourrelly, C. Serre, G. Férey, and G. Maurin, *Phys. Chem. Chem. Phys.*, 2010, 12, 6428–6437.

166 J. Rodriguez, I. Beurroies, T. Loiseau, R. Denoyel, and P. L. Llewellyn, *Angew. Chem. Int. Ed*, 2015, 4709–4713.

167 M. Pera-Titus, M. Savonnet, and D. Farrusseng, *J. Phys. Chem. C*, 2010, 114, 17665–17674.

168 I. Beurroies, M. Boulhout, P. L. Llewellyn, B. Kuchta, G. Férey, C. Serre, and R. Denoyel, *Angew. Chem. Int. Ed.*, 2010, 49, 7526–7529.

169 M. Mendt, B. Jee, N. Stock, T. Ahnfeldt, M. Hartmann, D. Himsl, and A. Pöppl, *J. Phys. Chem. C*, 2010, 114, 19443–19451.

170 N. a. Ramsahye, G. Maurin, S. Bourrelly, P. L. Llewellyn, T. Devic, C. Serre, T. Loiseau, and G. Ferey, *Adsorption*, 2007, 13, 461–467.

171 A. Ghoufi, G. Maurin, and G. Férey, *J. Phys. Chem. Lett.*, 2010, 1, 2810–2815.

172 A. Ghoufi, A. Subercaze, Q. Ma, P. G. Yot, Y. Ke, I. Puente-Orench, T. Devic, V. Guillerm, C. Zhong, C. Serre, G. Férey, and G. Maurin, *J. Phys. Chem. C*, 2012, 116, 13289–13295.

173 F.-X. Coudert, A. U. Ortiz, V. Haigis, D. Bousquet, A. H. Fuchs, A. Ballandras, G. Weber, I. Bezverkhyy, N. Geoffroy, J. Bellat, G. Ortiz, G. Chaplais, J. Patarin, and A. Boutin, *J. Phys. Chem. C*, 2014, 118, 5397–5405.

174 N. a Ramsahye, G. Maurin, S. Bourrelly, P. L. Llewellyn, T. Loiseau, C. Serre, and G. Férey, *Chem. Commun.*, 2007, 3261–3263.

175 N. A Ramsahye, G. Maurin, S. Bourrelly, P. Llewellyn, T. Loiseau, and G. Ferey, *Phys. Chem. Chem. Phys.*, 2007, 9, 1059–1063.

176 F. Salles, A. Ghoufi, G. Maurin, R. G. Bell, C. Mellot-Draznieks, and G. Férey, *Angew. Chem. Int. Ed.*, 2008, 47, 8487–8491.

177 N. A. Ramsahye, G. Maurin, S. Bourrelly, P. L. Llewellyn, C. Serre, T. Loiseau, T. Devic, and G. Ferey, *J. Phys. Chem. C*, 2008, 112, 514–520.

178 F. X. Coudert, C. Mellot-Draznieks, A. H. Fuchs, and A. Boutin, *J. Am. Chem. Soc.*, 2009, 131, 3442–3443.

179 F. X. Coudert, C. Mellot-Draznieks, A. H. Fuchs, and A. Boutin, *J. Am. Chem. Soc.*, 2009, 131, 11329–11331.

180 D. Dubbeldam, R. Krishna, and R. Q. Snurr, *J. Phys. Chem. C*, 2009, 113, 19317–19327.

181 A. Ghoufi and G. Maurin, *J. Phys. Chem. C*, 2010, 114, 6496–6502.

182 A. V. Neimark, F. X. Coudert, A. Boutin, and A. H. Fuchs, *J. Phys. Chem. Lett.*, 2010, 1, 445–449.

183 C. Triguero, F.-X. Coudert, A. Boutin, A. H. Fuchs, and A. V Neimark, *J. Phys. Chem. Lett.*, 2011, 2, 2033–2037.

184 A. V. Neimark, F.-X. Coudert, C. Triguero, A. Boutin, A. H. Fuchs, I. Beurroies, and R. Denoyel, *Langmuir*, 2011, 27, 4734–4741.

185 D. Bousquet, F.-X. Coudert, and A. Boutin, *J. Chem. Phys.*, 2012, 137, 044118

186 D. Bousquet, F. X. Coudert, A. G. J. Fossati, A. V. Neimark, A. H. Fuchs, and A. Boutin, *J. Chem. Phys.*, 2013, 138, 174706.

187 A. Ghysels, L. Vanduyfhuys, M. Vandichel, M. Waroquier, V. Van Speybroeck, and B. Smit, *J. Phys. Chem. C*, 2013, 117, 11540–11554.

188 E. García-Pérez, P. Serra-Crespo, S. Hamad, F. Kapteijn, and J. Gascon, *Phys. Chem. Chem. Phys.*, 2014, 16, 16060-16066.

189 F.-X. Coudert, M. Jeffroy, A. H. Fuchs, A. Boutin, and C. Mellot-Draznieks, *J. Am. Chem. Soc.*, 2008, 130, 14294–14302.

190 F.-X. Coudert, *Phys. Chem. Chem. Phys.*, 2010, 12, 10904.

191 C. Serre, F. Millange, T. Devic, N. Audebrand, and W. Van Beek, *Mater. Res. Bull.*, 2006, 41, 1550–1557.

192 A. Demessence and J. R. Long, *Chem. Eur. J.*, 2010, 16, 5902–5908.

193 J.-Z. Gu, W.-G. Lu, L. Jiang, H.-C. Zhou, and T.-B. Lu, *Inorg. Chem.*, 2007, 46, 5835–5837.

194 M. Plabst, L. B. McCusker, and T. Bein, *J. Am. Chem. Soc.*, 2009, 131, 18112–18118.

195 K. L. Gurunatha and T. K. Maji, *Eur. J. Inorg. Chem.*, 2009, 2009, 1592–1599.

196 A. Aijaz, E. Barea, and P. K. Bharadwaj, *Cryst. Growth Des.*, 2009, 9, 4480–4486.

197 R. M. P. Colodrero, A. Cabeza, P. Olivera-Pastor, A. Infantes-Molina, E. Barouda, K. D. Demadis, and M. A. G. Aranda, *Chem. - A Eur. J.*, 2009, 15, 6612–6618.

198 M. Gustafsson, A. Bartoszewicz, B. Martín-Matute, J. Sun, J. Grins, T. Zhao, Z. Li, G. Zhu, and X. Zou, *Chem. Mater.*, 2010, 22, 3316–3322.

199 R. Grünker, I. Senkovska, R. Biedermann, N. Klein, M. R. Lohe, P. Müller, and S. Kaskel, *Chem. Commun.*, 2011, 47, 490–492.

200 M. Gustafsson, J. Su, H. Yue, Q. Yao, and X. Zou, *Cryst. Growth Des.*, 2012, 12, 3243–3249.

201 B. Mu, F. Li, Y. Huang, and K. S. Walton, *J. Mater. Chem.*, 2012, 22, 10172-10178.

202 F. Salles, G. Maurin, C. Serre, P. L. Llewellyn, C. Knöfel, H. J. Choi, Y. Filinchuk, L. Oliviero, A. Vimont, J. R. Long, and G. Férey, *J. Am. Chem. Soc.*, 2010, 132, 13782–13788.

203 Z.-Q. Jiang, G.-Y. Jiang, F. Wang, Z. Zhao, and J. Zhang, *Chem. Eur. J.*, 2012, 18, 10525–10529.

204 O. Fabelo, L. Cañadillas-Delgado, J. Pasán, P. Díaz-Gallifa, A. Labrador, and C. Ruiz-Pérez, *CrystEngComm*, 2012, 14, 765–767.

205 R. M. P. Colodrero, P. Olivera-Pastor, E. R. Losilla, M. a. G. Aranda, L. Leon-Reina, M. Papadaki, A. C. McKinlay, R. E. Morris, K. D. Demadis, and A. Cabeza, *Dalton. Trans.*, 2012, 41, 4045-4051.

206 W. Yang, A. J. Davies, X. Lin, M. Suyetin, R. Matsuda, A. J. Blake, C. Wilson, W. Lewis, J. E. Parker, C. C. Tang, M. W. George, P. Hubberstey, S. Kitagawa, H. Sakamoto, E. Bichoutskaia, N. R. Champness, S. Yang, and M. Schröder, *Chem. Sci.*, 2012, 3, 2993-2999.

207 J. Xiao, Y. Wu, M. Li, B. Y. Liu, X. C. Huang, and D. Li, *Chem. Eur. J.*, 2013, 19, 1891–1895.

208 Y.-Y. Liu, S. Couck, M. Vandichel, M. Grzywa, K. Leus, S. Biswas, D. Volkmer, J. Gascon, F. Kapteijn, J. F. M. Denayer, M. Waroquier, V. Van Speybroeck, and P. Van Der Voort, *Inorg. Chem.*, 2013, 52, 113–120.

209 Y. Liu, Y.-P. Chen, T.-F. Liu, A. a. Yakovenko, A. M. Raiff, and H.-C. Zhou, *CrystEngComm*, 2013, 15, 9688-9693.

210 A. Husain, M. Ellwart, S. a. Bourne, L. Öhrström, and C. L. Oliver, *Cryst. Growth Des.*, 2013, 13, 1526–1534.

211 M. Mazaj, G. Mali, M. Rangus, E. Žunkovič, V. Kaučič, and N. Zabukovec Logar, *J. Phys. Chem. C*, 2013, 117, 7552–7564.

212 T. Birsa Čelič, M. Mazaj, N. Guillou, E. Elkaïm, M. El Roz, F. Thibault-Starzyk, G. Mali, M. Rangus, T. Čendak, V. Kaučič, and N. Zabukovec Logar, *J. Phys. Chem. C*, 2013, 117, 14608–14617.

213 M. Taddei, F. Costantino, A. Ienco, A. Comotti, P. V Dau, and S. M. Cohen, *Chem. Commun.*, 2013, 49, 1315-1317.

214 H. Leclerc, T. Devic, S. Devautour-Vinot, P. Bazin, N. Audebrand, G. Férey, M. Daturi, A. Vimont, and G. Clet, *J. Phys. Chem. C*, 2011, 115, 19828–19840.

215 W. M. Bloch, C. J. Doonan, and C. J. Sumby, *CrystEngComm*, 2013, 15, 9663.-9671

216 J. Wang, J. Luo, J. Zhao, D.-S. Li, G. Li, Q. Huo, and Y. Liu, *Cryst. Growth Des.*, 2014, 14, 2375–2380.

217 D. Fröhlich, S. K. Henninger, and C. Janiak, *Dalton. Trans.*, 2014, 43, 15300–15304.

218 M. Lange, M. Kobalz, J. Bergmann, D. Lässig, J. Lincke, J. Möllmer, A. Möller, J. Hofmann, H. Krautscheid, R. Staudt, and R. Gläser, *J. Mater. Chem. A*, 2014, 2, 8075-8085.

219 S. Kumar and S. Mandal, *CrystEngComm*, 2015, DOI:10.1039/c5ce01116g

220 S. Mukherjee, B. Joarder, A. V. Desai, B. Manna, R. Krishna, and S. K. Ghosh, *Inorg. Chem.*, 2015, 54, 4403–4408.

221 H.-R. Fu and J. Zhang, *Cryst. Growth Des.*, 2015, 15, 1210–1213.

222 H.-R. Fu and J. Zhang, *Chem. Eur. J.*, 2015, 21, 5700–5703.

223 D. N. Dybtsev, H. Chun, and K. Kim, *Angew. Chem. Int. Ed.*, 2004, 43, 5033–5036.

224 K. Uemura, Y. Yamasaki, Y. Komagawa, K. Tanaka, and H. Kita, *Angew. Chem. Int. Ed.*, 2007,

46, 6662–6665.

225 Z. Wang and S. M. Cohen, *J. Am. Chem. Soc.*, 2009, 131, 16675–16677.

226 S. Henke, R. Schmid, J.-D. Grunwaldt, and R. A. Fischer, *Chem. Eur. J.*, 2010, 16, 14296–14306.

227 S. Henke, D. C. Florian Wieland, M. Meilikhov, M. Paulus, C. Sternemann, K. Yusenko, and R. A. Fischer, *CrystEngComm*, 2011, 13, 6399-6404.

228 S. Henke, A. Schneemann, A. Wütscher, and R. A Fischer, *J. Am. Chem. Soc.*, 2012, 134, 9464–9474.

229 R. K. Motkuri, P. K. Thallapally, S. K. Nune, C. A Fernandez, B. P. McGrail, and J. L. Atwood, *Chem. Commun.*, 2011, 47, 7077-7079.

230 A. Aijaz, P. Lama, and P. K. Bharadwaj, *Eur. J. Inorg. Chem.*, 2010, 24, 3829–3834.

231 S. Bureekaew, H. Sato, R. Matsuda, Y. Kubota, R. Hirose, J. Kim, K. Kato, M. Takata, and S. Kitagawa, *Angew. Chem. Int. Ed.*, 2010, 49, 7660–7664.

232 N. Klein, C. Herzog, M. Sabo, I. Senkovska, J. Getzschmann, S. Paasch, M. R. Lohe, E. Brunner, and S. Kaskel, *Phys. Chem. Chem. Phys.*, 2010, 12, 11778-11784.

233 H. C. Hoffmann, B. Assfour, F. Epperlein, N. Klein, S. Paasch, I. Senkovska, S. Kaskel, G. Seifert, and E. Brunner, *J. Am. Chem. Soc.*, 2011, 133, 8681–8690.

234 N. Klein, H. C. Hoffmann, A. Cadiau, J. Getzschmann, M. R. Lohe, S. Paasch, T. Heydenreich, K. Adil, I. Senkovska, E. Brunner, and S. Kaskel, *J. Mater. Chem.*, 2012, 22, 10303-10312.

235 V. Bon, N. Klein, I. Senkovska, A. Heerwig, J. Getzschmann, D. Wallacher, I. Zizak, M. Brzhezinskaya, U. Mueller, and S. Kaskel, *Phys. Chem. Chem. Phys.*, 2015, 17, 17471–17479.

236 Y. Sakata, S. Furukawa, M. Kondo, K. Hirai, N. Horike, Y. Takashima, H. Uehara, N. Louvain, M. Meilikhov, T. Tsuruoka, S. Isoda, W. Kosaka, O. Sakata, and S. Kitagawa, *Science.*, 2013, 339, 193–196.

237 J. Seo, R. Matsuda, H. Sakamoto, C. Bonneau, and S. Kitagawa, *J. Am. Chem. Soc.*, 2009, 131, 12792–12800.

238 S. A. Moggach, T. D. Bennett, and A. K. Cheetham, *Angew. Chem. Int. Ed.*, 2009, 48, 7087–7089.

239 A. L. Spek, *Acta Crystallogr. Sect. C Struct. Chem.*, 2015, 71, 9–18.

240 D. Fairen-Jimenez, S. A Moggach, M. T. Wharmby, P. A Wright, S. Parsons, and T. Düren, *J. Am. Chem. Soc.*, 2011, 133, 8900–8902.

241 S. Aguado, G. Bergeret, M. P. Titus, V. Moizan, C. Nieto-Draghi, N. Bats, and D. Farrusseng, *New J. Chem.*, 2011, 35, 546–550.

242 D. L. Chen, N. Wang, F. F. Wang, J. Xie, Y. Zhong, W. Zhu, J. K. Johnson, and R. Krishna, *J. Phys. Chem. C*, 2014, 118, 17831–17837.

243 M. T. Wharmby, S. Henke, T. D. Bennett, S. R. Bajpe, I. Schwedler, S. P. Thompson, F. Gozzo, P. Simoncic, C. Mellot-Draznieks, H. Tao, Y. Yue, and A. K. Cheetham, *Angew. Chem.*, 2015, 127, 6547–6551.

244 X.-L. Li, G.-Z. Liu, L.-Y. Xin, and L.-Y. Wang, *CrystEngComm*, 2012, 14, 5757-5760.

245 C. R. Murdock, Z. Lu, and D. M. Jenkins, *Inorg. Chem.*, 2013, 52, 2182–2187.

246 I.-H. Park, S. S. Lee, and J. J. Vittal, *Chem. - A Eur. J.*, 2013, 19, 2695–2702.

247 S. Sen, S. Neogi, K. Rissanen, and P. K. Bharadwaj, *Chem. Commun.*, 2015, 51, 3173–3176.

248 R. Kitaura, K. Seki, G. Akiyama, and S. Kitagawa, *Angew. Chem. Int. Ed.*, 2003, 42, 428–431.

249 J.-H. Wang, M. Li, and D. Li, *Chem. Sci.*, 2013, 4, 1793-1801.

250 S. Yang, X. Lin, W. Lewis, M. Suyetin, E. Bichoutskaia, J. E. Parker, C. C. Tang, D. R. Allan, P. J. Rizkallah, P. Hubberstey, N. R. Champness, K. M. Thomas, A. J. Blake, and M. Schröder, *Nat. Mater.*, 2012, 11, 710–716.

251 B. Manna, A. V. Desai, N. Kumar, A. Karmakar, and S. K. Ghosh, *CrystEngComm*, 2015, 17, 1166–1169.

252 A. Kondo, H. Noguchi, S. Ohnishi, H. Kajiro, A. Tohdoh, Y. Hattori, W.-C. Xu, H. Tanaka, H. Kanoh, and K. Kaneko, *Nano Lett.*, 2006, 6, 2581–2584.

253 Y. Cheng, A. Kondo, H. Noguchi, H. Kajiro, K. Urita, T. Ohba, K. Kaneko, and H. Kanoh, *Langmuir*, 2009, 25, 4510–4513.

254 V. Bon, I. Senkovska, D. Wallacher, A. Heerwig, N. Klein, I. Zizak, R. Feyerherm, E. Dudzik, and S. Kaskel, *Microporous Mesoporous Mater.*, 2014, 188, 190–195.

255 W. M. Bloch and C. J. Sumby, *Chem. Commun.*, 2012, 48, 2534-2536.

256 J. Seo, C. Bonneau, R. Matsuda, M. Takata, and S. Kitagawa, *J. Am. Chem. Soc.*, 2011, 133, 9005–9013.

257 P. D. C. Dietzel, R. E. Johnsen, R. Blom, and H. Fjellvåg, *Chem. Eur. J.*, 2008, 14, 2389–2397.

258 Y. Chen, J. Zhang, J. Li, and J. V. Lockard, *J. Phys. Chem. C*, 2013, 117, 20068–20077.

259 C. Yang, X. Wang, and M. a Omary, *J. Am. Chem. Soc.*, 2007, 129, 15454–15455.

260 C. Yang, X. Wang, and M. a. Omary, *Angew. Chem. Int. Ed.*, 2009, 48, 2500–2505.

261 M.-H. Zeng, X.-L. Feng, and X.-M. Chen, *Dalton. Trans.*, 2004, 2217-2223.

262 M.-H. Zeng, X.-L. Feng, W.-X. Zhang, and X.-M. Chen, *Dalton. Trans.*, 2006, 5294-5303.

263 M.-H. Zeng, S. Hu, Q. Chen, G. Xie, Q. Shuai, S.-L. Gao, and L.-Y. Tang, *Inorg. Chem.*, 2009, 48, 7070–7079.

264 R. Medishetty, D. Jung, X. Song, D. Kim, S. S. Lee, M. S. Lah, and J. J. Vittal, *Inorg. Chem.*, 2013, 52, 2951–2957.

265 A. P. Nelson, D. a. Parrish, L. R. Cambrea, L. C. Baldwin, N. J. Trivedi, K. L. Mulfort, O. K. Farha, and J. T. Hupp, *Cryst. Growth Des.*, 2009, 9, 4588–4591.

266 Y. He, J. Yang, Y. Liu, and J. Ma, *Inorg. Chem.*, 2014, 53, 7527–7533.

267 Y. Takashima, V. M. Martínez, S. Furukawa, M. Kondo, S. Shimomura, H. Uehara, M. Nakahama, K. Sugimoto, and S. Kitagawa, *Nat. Commun.*, 2011, 2, 168.

268 G. Férey and C. Serre, *Chem. Soc. Rev.*, 2009, 38, 1380–1399.

269 Y.-S. Wei, K.-J. Chen, P.-Q. Liao, B.-Y. Zhu, R.-B. Lin, H.-L. Zhou, B.-Y. Wang, W. Xue, J.-P. Zhang, and X.-M. Chen, *Chem. Sci.*, 2013, 4, 1539-1546.

270 Y.-X. Tan, F. Wang, Y. Kang, and J. Zhang, *Chem. Commun.*, 2011, 47, 770–772.

271 C. Mellot-Draznieks, C. Serre, S. Surblé, N. Audebrand, and G. Férey, *J. Am. Chem. Soc.*, 2005, 127, 16273–16278.

272 C. Serre, C. Mellot-Draznieks, S. Surble, N. Audebrand, Y. Filinchuk, and G. Ferey, *Science.*, 2007, 315, 1828–1831.

273 F. Carson, J. Su, A. E. Platero-Prats, W. Wan, Y. Yun, L. Samain, and X. Zou, *Cryst. Growth Des.*, 2013, 13, 5036–5044.

274 P. Horcajada, F. Salles, S. Wuttke, T. Devic, D. Heurtaux, G. Maurin, A. Vimont, M. Daturi, O. David, E. Magnier, N. Stock, Y. Filinchuk, D. Popov, C. Riekel, G. Férey, and C. Serre, *J. Am. Chem. Soc.*, 2011, 133, 17839–17847.

275 I. Senkovska, F. Hoffmann, M. Fröba, J. Getzschmann, W. Böhlmann, and S. Kaskel, *Microporous Mesoporous Mater.*, 2009, 122, 93–98.